Molecular Recognition and Regioselective Functionalization of Carbohydrates by Synthetic Host Molecules

Takuya Kurahashi

2000

Preface

The studies presented in this thesis have been carried out under the direction of Professor Hisanobu Ogoshi (now, President of Fukui National College of Technology) and Professor Jun-ichi Yoshida during 1995 to 2000 at the department of Synthetic Chemistry and Biological Chemistry at Kyoto University. The studies are concerned with new artificial receptors for precise molecular recognition of carbohydrates, and new nucleophilic catalysts for regioselective functionalization of carbohydrates.

The author wishes to express his supreme gratitude to Professor Jun-ich Yoshida for his valuable discussion and warm encouragement. The author also wishes to express his supreme gratitude to Professor Hisanobu Ogoshi for his kind guidance and encouragement.

The author wishes to express his sincere gratitude to Associate Professor Tadashi Mizutani for his constant advice, valuable discussion, and hearty encouragement throughout this work.

The author is deeply grateful to Associate Professor Shigeru Yamago, Dr. Seiji Suga, and Dr. Kenichiro Itami for their valuable comments and warm encouragement. The author is also indebted to Professor Yasuhisa Kuroda at Kyoto Institute of Technology and Associate Professor Takashi Hayashi at Kyushu University for their helpful suggestions and warm encouragement.

The author wishes to thank Mr. Tadao Kobatake for measurement of mass spectra. The author also wishes to thank Mr. Haruo Fujita for his valuable suggestion on NMR measurement. The author is thankful to the staff at the Microanalysis Center of Kyoto University for the elemental analysis.

The author expresses his hearty thanks to Dr. Masanobu Sugawara, Ms. Yuki Makino, Messrs. Mitsuru Watanabe, Takao Manabe, Koichi Mitsudo, Masayuki Asai, Toru Koike, Toshiki Nokami, Toshiyuki Kamei, and all the other members of Yoshida's group for their friendship and kind help. The author also expresses his hearty thanks to Mses. Makiko Ueda (Murakami), Miho Nishitani for doing office work.

The author is fortunate to have the great assistance of Messrs. Thomas Jörg and Takuma Sakai. The author is thankful to Dr. Yusuke Kato and Mr. Takeshi Murakami for their fruitful discussion and valuable suggestion. The author is also thankful to all the other members of Ogoshi's group for their friendship and kind help. The author is also thankful to Mses. Yoko Watanabe Ohmizu, Tae Arai, and Fumiko Ohwatari for doing office work.

The author acknowledges Japan Society for the Promotion of Science for financial support (JSPS Research Fellowships for Young Scientists).

Finally, the author expresses his deep appreciation to his parents, Mr. Namio Kurahashi and Mrs. Fumie Kurahashi for their constant assistance and encouragement.

Takuya Kurahashi

Department of Synthetic Chemistry
and Biological Chemistry
Graduate School of Engineering
Kyoto University

2000

Contents

General Introduction

Carbohydrates in Nature. Carbohydrates are ubiquitous in Nature. They are produced from water and carbon dioxide continuously in a large scale by photosynthesis. Plants utilize D-glucose, a major carbohydrate produced by photosynthesis, to build polymers such as cellulose and starch. Cellulose is a structural component of plants, and starch serves as energy source for both plants and animals. Other than these polymers, carbohydrate molecules are widely distributed in Nature. They are found as building units of virtually all forms of natural products such as proteins, nucleic acids, lipids, steroids, alkaloids, *etc.* Some of them are important natural antibiotics. Numerous studies have revealed the ubiquity of complex oligosaccharides attached at cell surfaces. The function of these oligosaccharides is cell–cell communication such as inflammation, immune response, and bacterial and viral infections.

Considering diversed utilizations and functions in Nature, carbohydrate molecules are highly promising as drugs and materials. However, molecular design and preparation of carbohydrate derivatives pose challenging problems. At the beginning of this Chapter, the author would like to make the points clear in connection with supramolecular chemistry, which is explosively expanding its area from life science to material science.

Carbohydrates as Building Blocks for Supramolecular Assemblies. Carbohydrate molecules possess attractive chemical structures for the construction of supramolecular assemblies. Due to multiple hydroxy groups appended on chiral five or six-membered rings, relatively a small number of monosaccharides are derivatized to a wide array of complex derivatives through regiospecific introduction of various substituents. The remaining hydroxy groups could form intra- and intermolecular hydrogen bonding to give highly diversed three-dimensional structures.

One of fascinating examples in Nature is commelinin, a blue-colored anthocyanin isolated from deep blue flower petals of *commelina communis* (tsuyukusa). It consists of 6 molecules each of malonylawobanin (M) and flavocommelin (F), and 2 atoms of magnesium in the form of $[M_6F_6Mg_2]^{6-}$.[1a] The highly associated structure of commelinin was revealed by X-ray crystallography as Cd complex in 1992 (Figure 1).[1b] Carbohydrates surround a core hydrophobic region and possibly stabilize or fine-tune the central stacking interactions of the aromatic nucleus via hydrogen-bonding. It is interesting to note that attached acyl groups are essential for formation of a commelinin-

like structure.

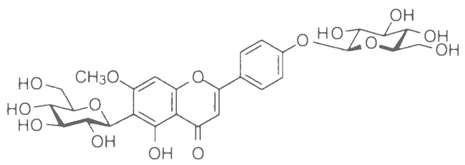

Flavocommelin (F)

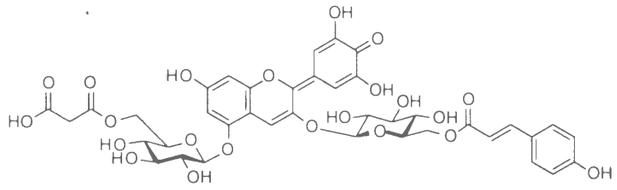

Malonylawobanin (M)

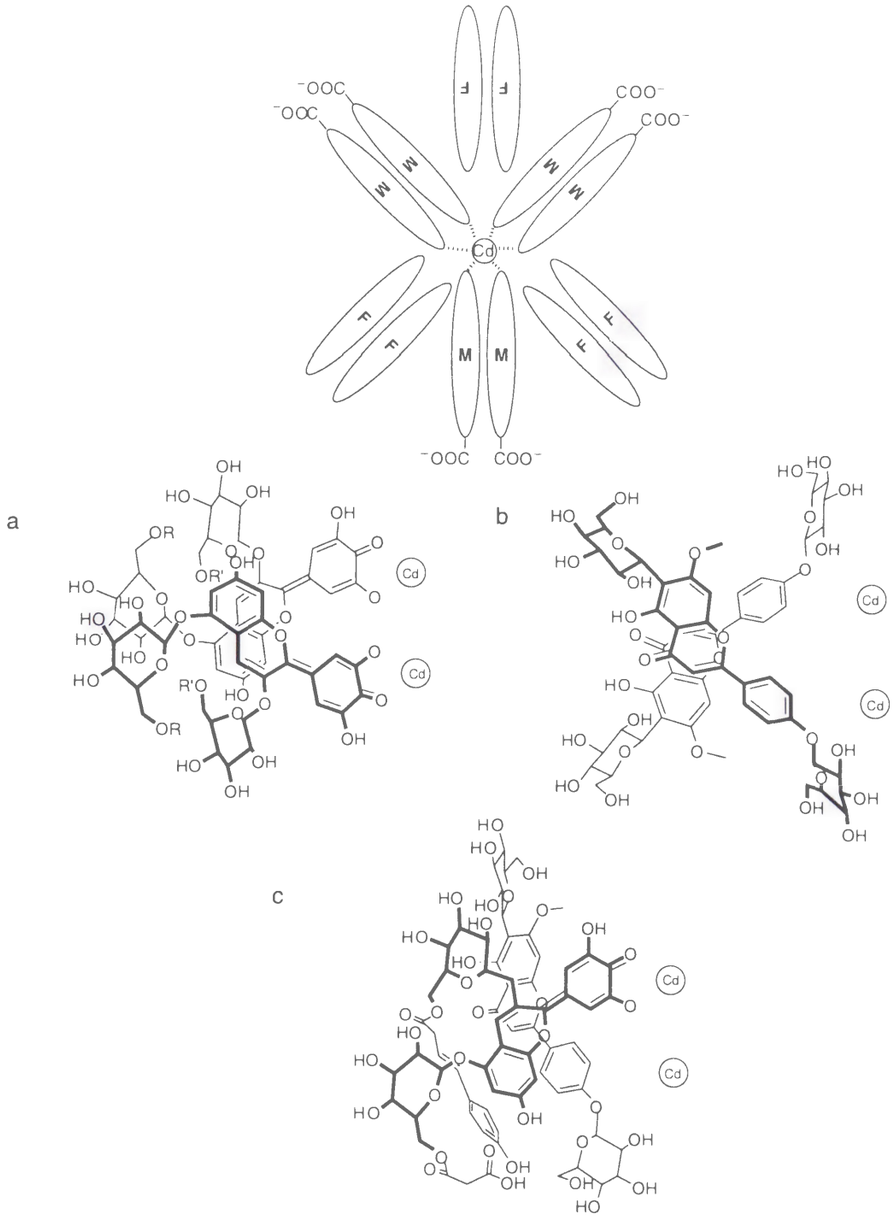

Figure 1. Gross structure of Cd-commelinin and the stacking arrangement of (a) M and M, (b) F and F, (c) M and F in Cd-commelinin.

Such splendid supramolecular assemblies in Nature have been stimulating synthetic chemists. One of the prominent achievements in recent years is self-assembling peptide nanotubes reported by M. R. Ghadiri *et. al.* (Figure 2).[2a] They designed cyclic peptides with an even number of alternating D- and L-amino acids, expecting that these cyclic

peptides adopt a flat conformation in which all amide functionalities lie perpendicular to the structure. The complementary proton donor-proton acceptor arrangement will result in well-defined intermolecular interaction. The designed cyclic peptide, synthesized by the well-established solid phase method, was found to form the desired hollow tubular structure and exhibited efficient ion and glucose transport activity when combined with lipid bilayer system.[2b,c]

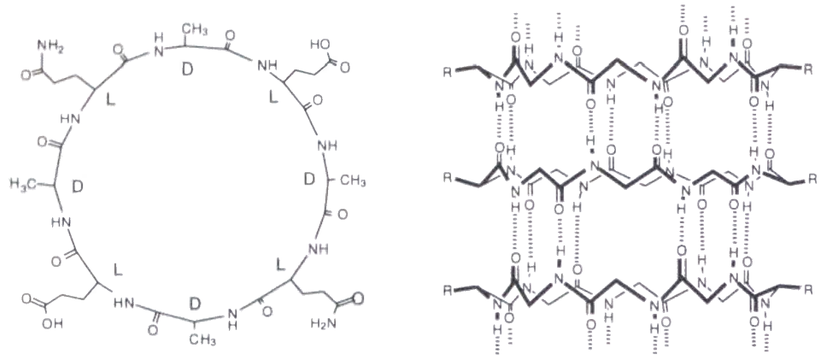

Figure 2. Self-assembling peptide nanotube reported by M. R. Ghadiri.

Utilization of carbohydrates as building blocks for supramolecular architectures, however, has been severely limited.[3] One reason is lack of general strategies for the design of intermolecular interactions in carbohydrate-based supramolecular architectures. Figure 3 illustrates the difficulties of precise molecular recognition of carbohydrates in comparison with the well-known nucleobase paring in which alternating proton donors and acceptors fixed on the planar aromatic rings interact with each other. In molecular recognition of carbohydrates, two questions emerge:

Hydroxy functionality of carbohydrates should be considered as hydrogen donors or acceptors?

In which direction is directed a hydroxy group having a rotatable C-O bond?

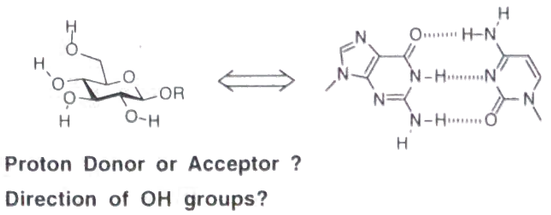

Figure 3. Carbohydrate recognition in comparison with the nucleobase pairing.

Secondary, we can not underestimate synthetic difficulties to prepare carbohydrate derivatives. In synthetic carbohydrate chemistry, stereocontrolled glycosidic bond formation and regioselective introduction of substituents have long been major problems. For our purpose, particularly indispensable is efficient regioselective transformation of carbohydrates to produce a wide variety of derivatives. But at present, tedious protection-deprotection steps are required to control regiochemistry.

Clearly, it is important to tackle the following subjects for the development of supramolecular carbohydrate chemistry.

(1) How to design specific interactions for carbohydrates.

(2) How to introduce substituents regioselectively to a particular OH group.

In the next sections, an overview concerning the above two issues is given.

Molecular Recognition of Carbohydrates by Artificial Receptors: How to Design Specific Interactions for Carbohydrates. Precise molecular recognition of carbohydrates by a synthetic receptor is a challenging goal in artificial receptor chemistry.[4] Considerable efforts have been done to construct model receptors of sugars, including resorcinol-aldehyde cyclotetramer,[5] tetrahydroxycholaphane,[6] C_3 macrocyclic receptor,[7] boronic acid-based receptors,[8] polyaza-cleft,[9] aminocyclodextrins,[10] phosphonates,[11, 17] capped porphyrin,[12] molecular clefts,[13] glycophane,[14] polypyridine-macrocycle,[15] and tricyclic polyamide receptor.[16] These studies focused on diverse aspects of carbohydrate recognition such as diastereo-selectivity, enantio-selectivity, binding in polar solvents, and facile detection of the binding events, particularly by taking advantage of the chirality of carbohydrates.

Among these studies, receptors that recognize carbohydrate via directional non-covalent interactions like hydrogen bonding are shown in Figure 4. These receptors bind monosaccharides with moderate to high affinity in non-polar solvent. But due to the multitude of possible binding modes, detailed complex structures and the origins of high affinity are scarcely discussed.

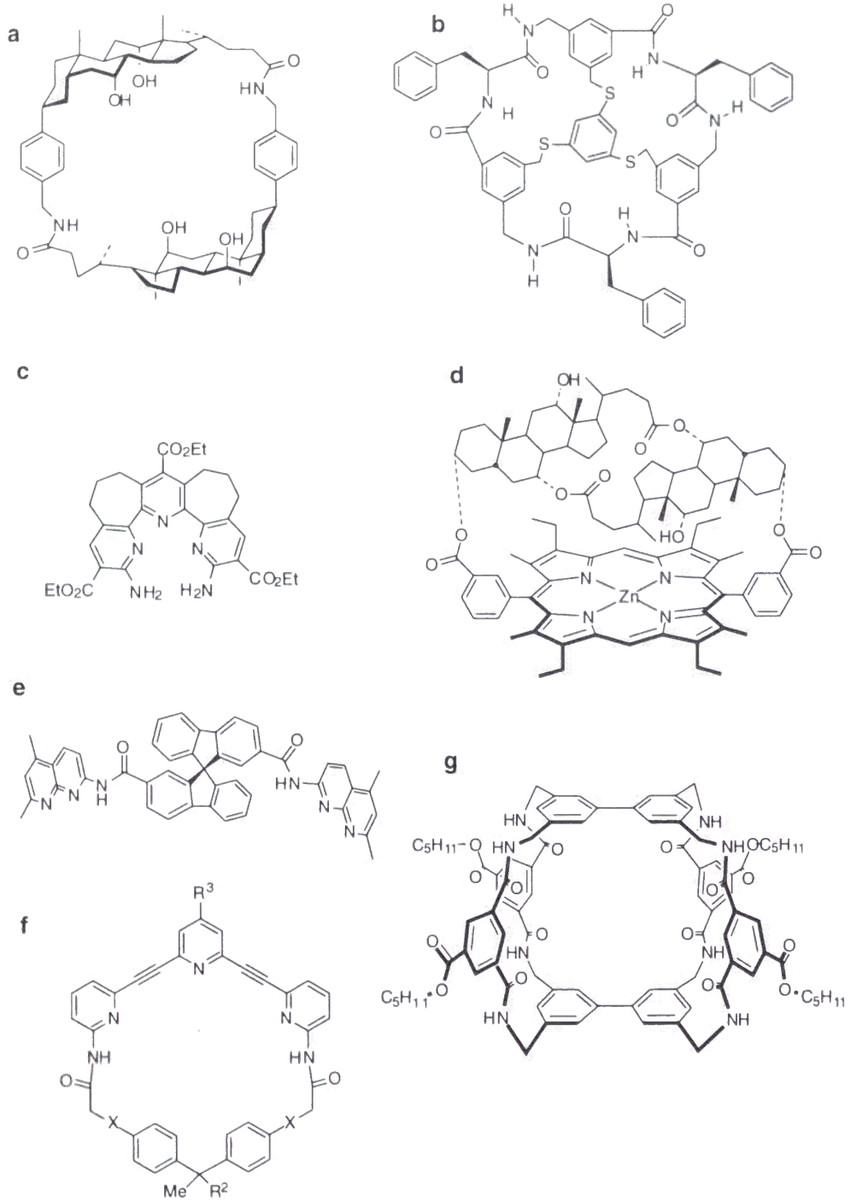

Figure 4. Artificial receptors for monosaccharides. a. tetrahydroxycholaphane reported by A. P. Davis.[6] b. *C*3 macrocyclic receptor reported by W. C. Still.[7] c. polyaza-cleft reported by E. V. Anslyn.[9] d. capped porphyrin reported by R. P. Bonar-Law and J. K. M. Sanders.[12] e. molecular clefts reported by F. Diederich.[13] f. polypyridine-macrocycle reported by M. Iouye.[15] g. tricyclic polyamide receptor reported by A. P. Davis.[16]

Regioselective Functionalization of Unprotected Carbohydrates: How to Introduce Substituents Regioselectively to a Particular OH Group. Regioselective transformation of carbohydrates has long been a fundamental problem in carbohydrate chemistry.[18] This usually requires protection of all hydroxy groups except for the modified OH group. Appropriately protected carbohydrates are mostly prepared according to the well-established procedures as follows.

(1) Direct protection of the primary OH group over secondary hydroxy groups. Large substituents such as *tert*-butyldiphenylsilyl group can be selectively introduced to the primary OH group in the presence of other secondary OH groups in excellent yields (eq 1[19]).

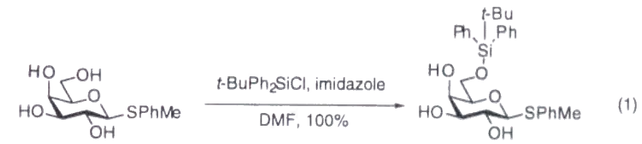

(2) Formation of cyclic acetals and regioselective cleavage of *O*-benzyliden acetals to benzyl ethers (eq 2,[20] eq 3,[21] eq 4[21]).

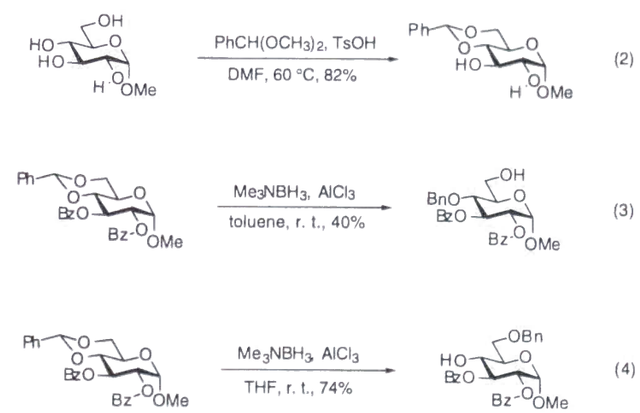

(3) Utilization of stannylene acetals and stannyl ethers (eq 5[22]). Other than organotin derivatives, organoboron derivatives are successfully utilized for regiocontrol, recently.[23]

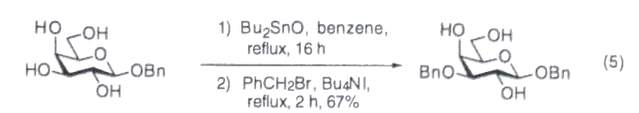

A protection-deprotection strategy in synthetic carbohydrate chemistry was highlighted in the preparation of oligosaccharide libraries from one monosaccharide unit as a core.[19] Difficulties arising from similar reactivities of OH groups were overcome by using a designed building block containing four selectively removable protecting groups as acceptors for glycosidation (Figure 5).

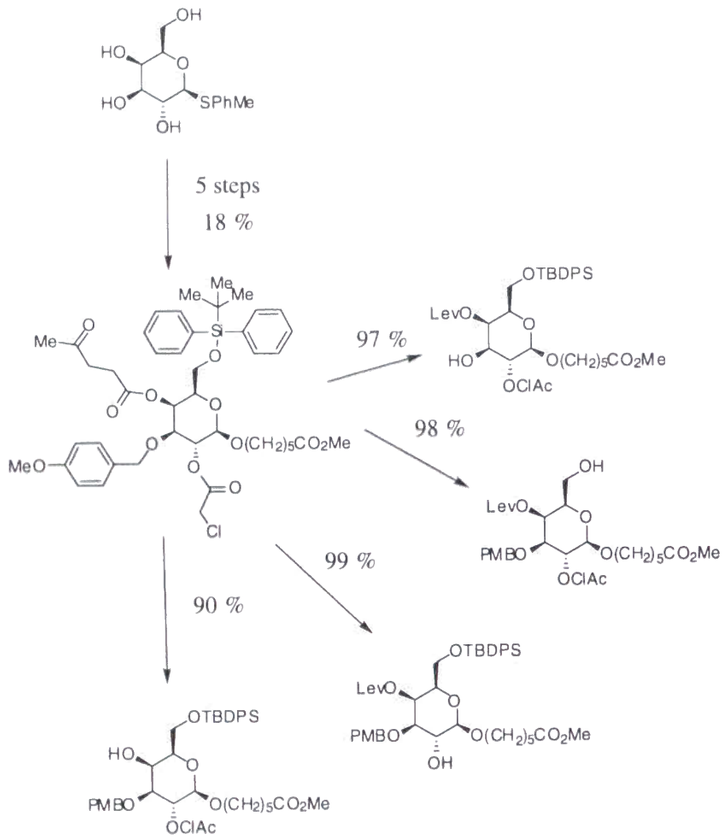

Figure 5. A designed building block for an efficient orthogonal protection–deprotection strategy.

Enzymes, on the other hand, have enabled regioselective transformation without protecting groups. For example, β1,4-galactosyltransferase catalyzes the transfer of galactose from UDP-Gal to the 4-position of GlcNAc residues to produce the Galβ1,4GlcNAc substructure both stereoselectively and regioselectively (Figure 6). These enzymes have been successfully utilized in the synthesis of numerous complex oligosaccharides.

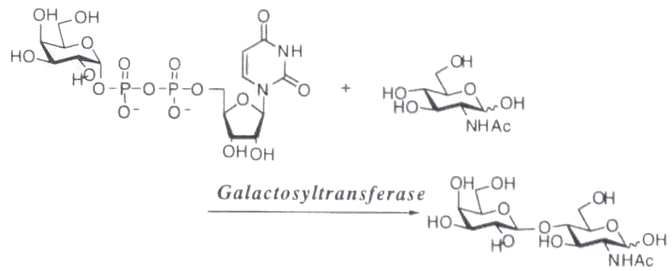

Figure 6. Regioselective glycosidation catalyzed by β1,4-galactosyltransferase.

Survey of This Thesis. Chapters 1 and 2 clarified one of the important aspects in carbohydrate recognition by taking advantage of the characteristic porphyrin chromophore and offered solid foundation for the design of specific interactions for carbohydrates. In Chapters 3 – 5, enzyme-like regioselective transformation of unprotected carbohydrates were explored. New nucleophilic catalysts for regioselective acylation of unprotected carbohydrates were developed.

Chapter 1 describes a preparation of a series of porphyrin-based artificial receptors intended to recognize monosaccharides (Figure 7). Among these receptors, receptor **1** showed marked affinity for octyl glucoside and mannoside in $CHCl_3$. On the other hand, octyl galactosides and octyl 2-*O*-methyl-α-mannoside were found to be poor ligands for **1**. Addition of alcohols to $CHCl_3$ suppressed the binding by **1**, while addition of polar additives such as water, alcohols, phenols, and ethers assisted the binding by **3** and **4** in a low concentration range (0–1.5 mol%).

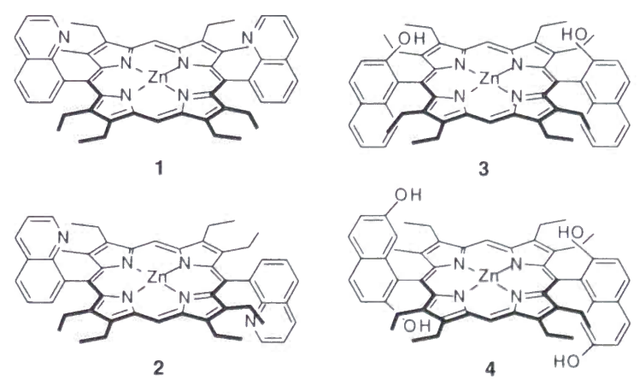

Figure 7. Porphyrin-based artificial receptors for monosaccharides.

Chapter 2 describes a detailed spectroscopic investigation on receptor-

monosaccharide complexes. Analysis of the complexation-induced shifts (CIS) of the carbohydrate OH protons in the ^{1}H NMR revealed that receptor **1** bound the 4-OH group of mannoside and glucoside by coordination to the zinc and the 6-OH and 3-OH groups by hydrogen bonding to the quinolyl nitrogen atoms (Figure 8). These NMR results and comparison of binding affinity with reference receptors and ligands indicated that receptor **1** recognized the trans, trans-1,2-dihydroxy-3-(hydroxymethyl) moiety of carbohydrates by the combination of Lewis acid (zinc) and Lewis bases (quinolyl nitrogens). Poor affinities of **1** to octyl galactosides and octyl 2-*O*-methyl-α-mannoside were ascribed to neighboring group effects, where a neighboring group in ligands not directly involved in the receptor-ligand interactions had considerable influence on the affinity through destabilizing the hydrogen bonding network(s) in the receptor-ligand complex. The circular dichroism induced in the porphyrin Soret band by complexation with the carbohydrates displayed characteristic patterns, which parallel the patterns of the complexation-induced shifts in the ^{1}H NMR. The CD patterns sensitively reflected the receptor-ligand interaction modes, particularly ligand orientation and fluctuation in the complex. Variable-temperature CD revealed that glucoside was fluctuating on **1** while mannoside was rigidly fixed on **1** at room temperature.

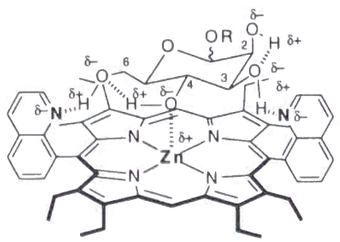

Figure 8. Schematic representation of hydrogen-bonding-networks of the receptor **1**-Man complex based on the ^{1}H NMR CIS values.

Chapter 3 describes a systematic investigation of DMAP-catalyzed acetylation of unprotected monosaccharides in $CHCl_3$. The reaction conditions in eq 6 gave a mixture of regioisomeric monoacetyl sugars, which was readily analyzed by ^{1}H NMR. Unexpectedly, secondary OH groups of octyl glucosides were found to be preferentially acetylated in the presence of the primary OH group at position 6. Systematic acetylation experiments of glucose, mannose, and galactose revealed the decisive role of intramolecular hydrogen-bonding networks among carbohydrate OH groups. The relative reactivities in the DMAP-catalyzed acetylation were successfully correlated with the calculated proton affinity of each OH group in carbohydrates.

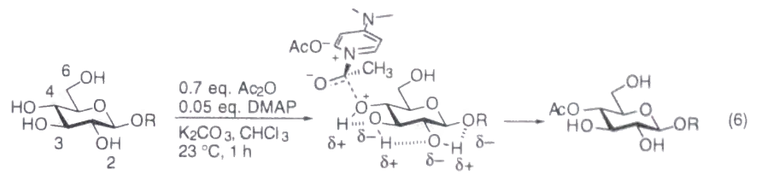

(6)

Chapter 4 describes new nucleophilic catalysts for regioselective acylation of unprotected carbohydrates. Among new nucleophilic catalysts developed, catalyst **1** was found to acetylate 1-*O*-octyl glucopyranosides and 1-*O*-octyl galactopyranosides highly regioselectively at position 6 in $CHCl_3$, although it gave nearly 1:1 mixtures of 4- and 6-monoacetates in the case of mannopyranosides. Catalyst **1** was proposed to regulate the proton transfer of esterification reactions and strictly recognize the primary over secondary OH groups without loss of catalytic activity (Figure 9).

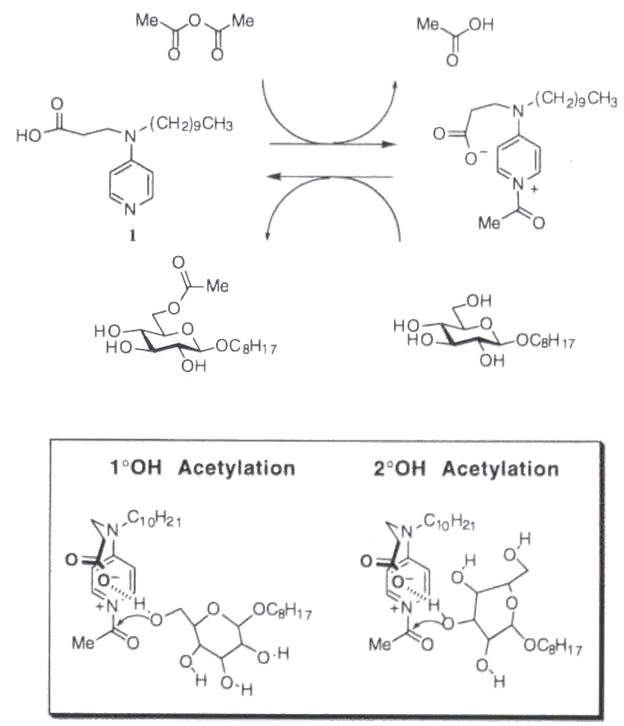

Figure 9. Proposed mechanism for regioselective acylation of carbohydrates catalyzed by **1**.

Chapter 5 describes regioselective acylation of polyhydroxy compounds catalyzed

by newly developed nucleophilic catalysts in polar solvent. Polyhydroxy compounds of natural origin such as oligosaccharides are notoriously insoluble in most organic solvents. Thus, polar solvents which dissolve unprotected monosaccharides were explored. Among polar solvents tested, *tert*-amyl alcohol was found to be suitable solvent in our catalytic system. Several polyhydroxy compounds were regioselectively acetylated in relatively high yield (eq 7).

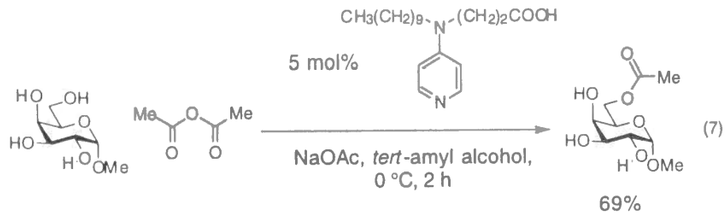

69% (7)

References and Notes

1. (a) Tamura, H.; Kondo, T.; Goto, T. *Tetrahedron Lett.* **1986**, *27*, 1801. (b) Kondo, T.; Yoshida, K.; Nakagawa, A.; Kawai, T.; Tamura, H.; Goto, T. *Nature* **1992**, *358*, 515.
2. (a) Ghadiri, M. R.; Granja, J. R.; Milligan, R. A.; McRee, D. E.; Khazanovich, N. *Nature* **1993**, *366*, 324. (b) Ghadiri, M. R.; Granja, J. R.; Buehler L. K. *Nature* **1994**, *369*, 301. (c) Granja, J. R.; Ghadiri, M. R. *J. Am. Chem. Soc.* **1994**, *116*, 10785.
3. Very few examples of supramolecules are based on non-amidic hydrogen bonding. However, the possibility of generating self-assembling supramolecular structures based on intermolecular hydrogen bonding of OH groups has been demonstrated, recently: (a) Hanessian, S.; Simard, M.; Roelens, S. *J. Am. Chem. Soc.* **1995**, *117*, 7630. (b) Ung, A. T.; Gizachew, D.; Bishop, R.; Scudder, M. L.; Dance, I. G. Craig, D. C. *J. Am. Chem. Soc.* **1995**, *117*, 8745.
4. Review: Davis, A. P.; Wareham, R. S. *Angew. Chem., Int. Ed. Engl.* **1999**, *38*, 2978.
5. (a) Aoyama, Y.; Tanaka, Y.; Sugahara, S. *J. Am. Chem. Soc.* **1989**, *111*, 5397. (b) Kurihara, K.; Ohto, K.; Tanaka, Y.; Aoyama, Y.; Kunitake, T. *J. Am. Chem. Soc.* **1991**, *113*, 444.
6. Bhattarai, K. M.; Bonar-Law, R. P.; Davis, A. P.; Murray, B. A. *J. Chem. Soc., Chem. Commun.* **1992**, 752.
7. Liu, R.; Still, W. C. *Tetrahedron Lett.* **1993**, *34*, 2573.
8. (a) Murakami, H.; Nagasaki, T.; Hamachi, I.; Shinkai, S. *Tetrahedron Lett.* **1993**, *34*, 6273. (b) James, T. D.; Sandanayake, K. R. A. S.; Shinkai, S. *Nature* **1995**, *374*, 345. (c) James, T. D.; Sandanayake, K. R. A. S.; Iguchi, R.; Shinkai, S. *J. Am. Chem. Soc.* **1995**, *117*, 8982. (d) Takeuchi, M.; Imada, T.; Shinkai, S. *J. Am. Chem. Soc.* **1996**, *118*, 10658.
9. (a) Huang, C.-Y.; Cabell, L. A.; Anslyn, E. V. *J. Am. Chem. Soc.* **1994**, *116*, 2778. (b) Bell, D. A.; Dfaz, S. G.; Lynch, V. M.; Anslyn, E. V. *Tetrahedron Lett.* **1995**, *36*, 4155.
10. Eliseev, A. V.; Schneider, H.-J. *J. Am. Chem. Soc.* **1994**, *116*, 6081.
11. Das, G.; Hamilton, A. D. *J. Am. Chem. Soc.* **1994**, *116*, 11139.
12. Bonar-Law, R. P.; Sanders, J. K. M. *J. Am. Chem. Soc.* **1995**, *117*, 259.
13. Cuntze, J.; Owens, L.; Alcázar, V.; Seiler, P.; Diederich, F. *Helv. Chim. Acta*

1995, *78*, 367.

14 Jimenez-Barbero, J.; Junquera, E.; Martin-Pastor, M.; Sharma, S.; Vicent, C.; Penades, S. *J. Am. Chem. Soc.* **1995**, *117*, 11198.

15 (a) Inouye, M.; Miyake, T.; Furusyo, M.; Nakazumi, H. *J. Am. Chem. Soc.* **1995**, *117*, 12416. (b) Inouye, M.; Takahashi, K.; Nakazumi, H. *J. Am. Chem. Soc.* **1999**, *121*, 341.

16 Davis, A. P.; Wareham, R. S. *Angew. Chem., Int. Ed. Engl.* **1998**, *37*, 2270.

17 Schrader, T. *J. Am. Chem. Soc.* **1998**, *120*, 11816.

18 Reviews: (a) Sugihara, J. M. *Adv. Carbohydr. Chem. Biochem.* **1953**, *8*, 1. (b) Haines, A. H. *Adv. Carbohydr. Chem. Biochem.* **1976**, *33*, 11. (c) Haines, A. H. *Adv. Carbohydr. Chem. Biochem.* **1981**, *39*, 13. See, also: *Preparative Carbohydrate Chemistry*; Hanessian, S., Ed.; Dekker: New York, 1996.

19 Wong, C.-H.; Ye X.-S.; Zhang, Z *J. Am. Chem. Soc.* **1998**, *120*, 7137.

20 Evans, M. E. *Carbohydr. Res.* **1972**, *21*, 473.

21 Ek, M.; Garegg, P. J.; Hultberg, H.; Oscarson S. *J. Carbohydr. Chem.* **1983**, *2*, 305.

22 David, S.; Thieffry, A.; Veyrières, A. *J. Chem. Soc., Perkin Trans. 1* **1981**, 1796.

23 (a) Oshima, K.; Kitazono, E.; Aoyama, Y. *Tetrahedron Lett.* **1997**, *38*, 5001.
(b) Oshima, K.; Aoyama, Y. *J. Am. Chem. Soc.* **1999**, *121*, 2315.

Chapter 1

Zinc Porphyrins as Artificial Receptors for Carbohydrates

Abstract

A series of porphyrin-based artificial receptors were prepared for molecular recognition of carbohydrates. Among these receptors, receptor **1** ([*cis*-5,15-bis(8-quinolyl)-2,3,7,8,12,13,17,18-octaethylporphyrinato]zinc(II)) showed marked affinity for octyl glucoside and mannoside in $CHCl_3$. On the other hand, octyl galactosides and octyl 2-*O*-methyl-α-mannoside were found to be poor ligands for **1**. Addition of alcohols to $CHCl_3$ suppressed the binding by **1**, while addition of polar additives such as water, alcohols, phenols, and ethers assisted the binding by **3** ([*cis*-5,15-bis(2-hydroxy-1-naphthyl)-2,3,7,8,12,13,17,18-octaethylporphyrinato]zinc(II)) and **4** ([*trans*-5,15-bis(2,7-dihydroxy-1-naphthyl)-2,3,7,8,12,13,17,18-octaethylporphyrinato]zinc(II)) in a low concentration range (0 – 1.5 mol%).

Introduction

Porphyrins provide a powerful framework for artificial receptors and catalysts, which has been repeatedly demonstrated so far.[1] To construct artificial receptors for carbohydrates, the following features of porphyrins are especially useful.

(1) Several distinct functionalization sites. Many interaction sites are required for artificial receptors for carbohydrates having many OH groups. A porphyrin has the meso position and β-position for functionalization sites (Figure 1).

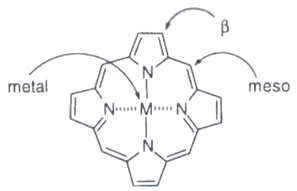

Figure 1. Porphyrin and its functionalization sites.

(2) Central metals of porphyrins. Metal porphyrins may be seen as a model for the metal centers found in certain carbohydrate binding proteins such as mannose-binding protein (Figure 2).[2]

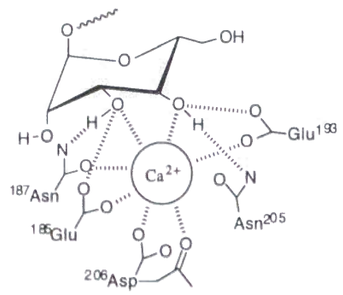

Figure 2. X-ray crystal structure of the carbohydrate-recognition domain of rat mannose-binding protein complexed with mannose.

(3) Chromophores for detecting subtle changes in interactions between porphyrin and surrounding molecules. UV-vis, circular dichroism, fluorescence, resonance Raman, and ^{1}H NMR spectroscopy have been successfully used to probe the intermolecular interactions. Among these spectroscopic methods, UV-vis and circular dichroism spectroscopy can be readily utilized to probe the carbohydrate–receptor interactions. ^{1}H

NMR spectroscopy is also useful owing to the profound ring current effects on the chemical shifts of the protons close to the porphyrin plane.

In this chapter, the author reports the preparation of functionalized zinc porphyrins as an artificial receptor for carbohydrates.

Results

Functionalized Zinc Porphyrins for Carbohydrate Recognition. Five zinc porphyrins were prepared and their affinities for carbohydrate derivatives were investigated. Receptor **1** has two quinolyl groups fixed at 5- and 15-positions of porphyrin with cis configuration, receptor **3** has two 2-hydroxynaphthyl groups with cis configuration, and receptor **4** has two 2,7-dihydroxynaphthyl groups with trans configuration. All these porphyrins have one Lewis acid site and two hydrogen bonding sites arranged in a similar manner to form a recognition pocket above the porphyrin plane. Receptor **2** is the trans isomer of receptor **1**, serving one Lewis acid site and one hydrogen bonding site for carbohydrate binding. Receptor **5**, ZnTPP (TPP = 5,10,15,20-tetraphenylporphyrinato anion), has only one Lewis acid site. Receptor **2** and receptor **5** were used in control experiments to reveal the influence of the quinolyl hydrogen bonding sites.

1

3

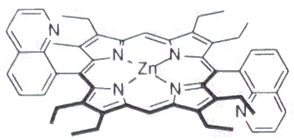

2

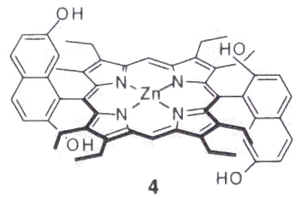

4

Chloroform was used as a solvent for the binding studies to mimic the relatively non-polar environment of the binding pocket of sugar-binding proteins. The effects of polar additives were examined by adding them to the chloroform. To solubilize the carbohydrates in organic solvents, octyl pyranosides were prepared according to reported procedures. Four octyl glycopyranosides, namely, α- and β-octyl galactopyranoside (α- and β-Gal), α- and β-octyl mannopyranoside (α- and β-Man) thus prepared, and commercially available two octyl pyranoside, α- and β-octyl glucopyranoside (α- and β-Glc), were used as ligands. As reference ligands, octyl 2-*O*-α-D-methylmannopyranoside (2-*O*-Me-α-Man), octyl 6-*O*-β-D-acetylglucopyranoside (6-*O*-Ac-β-Glc), and octyl 6-*O*-β-D-benzoylglucopyranoside (6-*O*-Bz-β-Glc) were prepared.

Binding Constants Determinations by UV-vis Titration. The binding constants were determined by UV-vis titration, in which the absorbance changes in the Soret band owing to the increased ligand concentration were monitored and analyzed by least-square curve fitting, assuming a 1:1 complex formation. In all cases, the Soret peak maxima were red-shifted by *ca.* 5 nm, and the difference spectra showed isosbestic points. The curve fitting to 1:1 complexation was satisfactory (standard deviations for the binding constants were *ca.* 5%).

The binding constants of octyl pyranosides and those of the reference ligands, **6**–**13**, are listed in Tables 1 and 2, respectively. Among the receptors investigated, receptor **1** showed the highest affinity for the ligands, especially for β-Man and β-Glc. A similar trend was found for the affinity of **2**, even though the affinity was reduced for all the ligands compared to that of **1**. Binding by receptor **4** was moderate and that by receptor **3** was weak. Comparison of the binding constants of α-Man with those of 2-*O*-Me-α-Man indicated that the 2-*O*-methyl group of 2-*O*-Me-α-Man markedly inhibited the binding by receptors **1** and **2** while it hardly influenced that by receptors **3** and **4**.

Table 1. Binding Constants (K) and Free Energy Changes ($\Delta G°$) of Receptor–Carbohydrate Complex Formation in Chloroform at 15 °C.[a]

	K/M^{-1} ($-\Delta G°$/kcal·mol^{-1})			
Ligand	receptor **1**	receptor **2**	receptor **3**	receptor **4**	receptor **5**
α-Glc	7 570 (5.11)	2 530 (4.49)	320 (3.30)	3 670 (4.70)	< 10 (<1.3)
β-Glc	41 400 (6.09)	6 360 (5.01)	570 (3.63)	2 090 (4.38)	440 (3.49)
α-Gal	1 870 (4.31)	1 030 (3.97)	650 (3.70)	2 240 (4.42)	14 (1.51)
β-Gal	3 840 (4.73)	1 620 (4.23)	690 (3.74)	1 710 (4.26)	< 10 (<1.3)
α-Man	15 500 (5.52)	8 220 (5.16)	810 (3.83)	3 860 (4.73)	695 (3.75)
β-Man	61 700 (6.31)	23 300 (5.76)	250 (3.16)	2 970 (4.58)	78 (2.49)
2-*O*-Me-α-Man	380 (3.40)	250 (3.16)	400 (3.43)	2 550 (4.49)	b
6*O*-Ac-β-Glc	6800 (5.05)	2060 (4.37)	530 (3.59)	b	b
6*O*-Bz-β-Glc	7300 (5.09)	b	600 (3.66)	b	b

[a] Standard deviations in K are about 5 – 10%. [b] not determined.

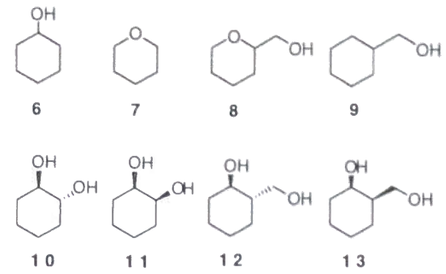

Table 2. Binding Constants (K) and Free Energy Changes ($\Delta G°$) for Complexation of Porphyrin Receptors **1** (or **3**) with Reference Ligands in Chloroform at 15 °C.[a]

	K/M^{-1} ($-\Delta G°$/(kcal·mol^{-1}))	
Ligand	Receptor **1**	Receptor **3**
6	3 (0.63)	3 (0.63)
7	3 (0.63)	19 (1.68)
8	5 (0.92)	17 (1.62)
9	7 (1.11)	5 (0.92)
10	210 (3.05)	140 (2.80)
11	60 (2.32)	43 (2.15)
12	2600 (4.50)	320 (3.29)
13	560 (3.62)	88 (2.56)

[a] In amylene-containing $CHCl_3$. [**1**] = 5.4×10^{-6} M to 7.4×10^{-6} M, [**3**] = 4.6×10^{-6} M to 5.8×10^{-6} M, [**6**–**9**] = 0 – 3.4×10^{-1} M, [**10**–**13**] = 0 – 9.6×10^{-3} M.

Solvent Effects on the Binding. Sanders *et al.*[3] reported that the addition of water and methanol to the chloroform solution assists the binding of carbohydrate derivatives by the capped zinc porphyrin. The author also examined the effects of polar additives on the binding of carbohydrates. The free energy changes of binding of β-Glc, $-\Delta G°$, are plotted against the mole fractions of added alcohols in Figures 3 and 4. For receptor **1**, the binding was simply inhibited as the concentration of alcohols in $CHCl_3$ was higher. On the other hand, for receptor **4**, the values of $-\Delta G°$ increased in the range of the low alcohol concentration and decreased upon further addition of alcohol. In Figure 5, the similar plots are shown for complexation of β-Glc

to **3** for the various additives, such as water, phenol, *p*-nitrophenol, *p*-methoxyphenol, *p*-dimethoxybenzene, and pyridine. Water showed very distinct effects: the binding constant increased rapidly in the low concentration range of water until chloroform was saturated with it. *p*-Dimethoxybenzene and *p*-methoxyphenol also showed distinct effects in the low concentration range. Other phenols showed moderate effects. In contrast, addition of pyridine simply suppressed the binding.

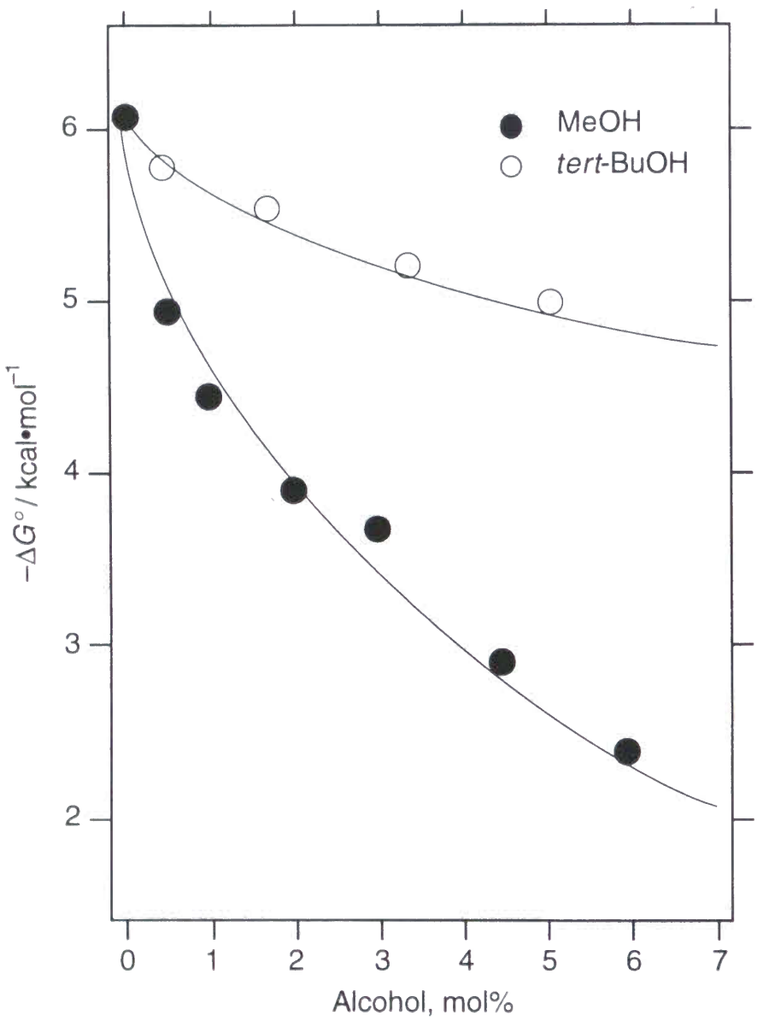

Figure 3. Plot of the free energy changes for complexation between receptor **1** and β-Glc in $CHCl_3$ at 15 °C ($-\Delta G°$) against alcohol concentrations.

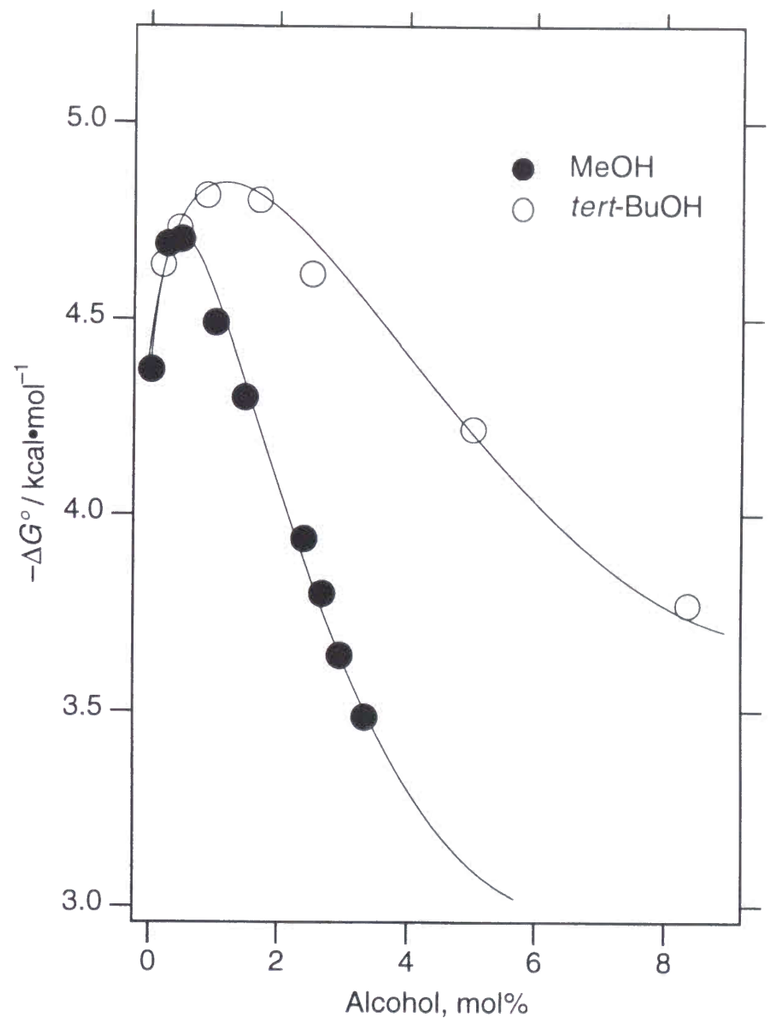

Figure 4. Plot of the free energy changes for complexation between receptor **4** and β-Glc in $CHCl_3$ at 15 °C ($-\Delta G°$) against alcohol concentrations.

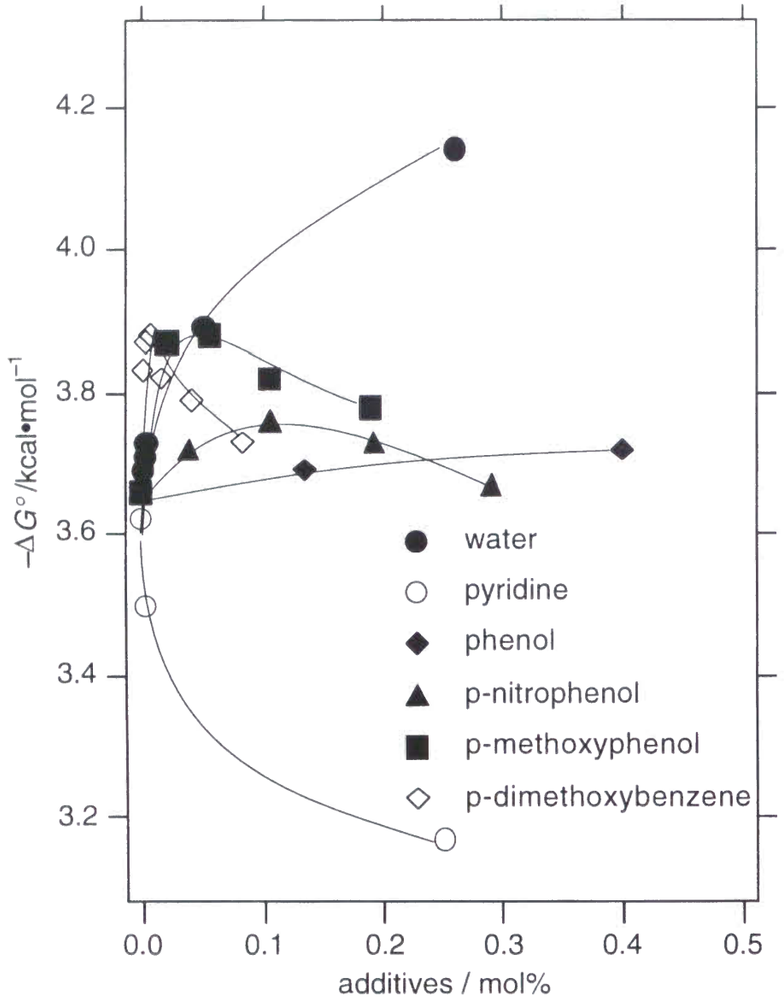

Figure 5. Plot of the free energy changes for complexation between receptor **3** and β-Glc in $CHCl_3$ at 15 °C ($-\Delta G°$) against concentrations of water, phenol, *p*-nitrophenol, *p*-methoxyphenol, *p*-dimethoxybenzene, and pyridine.

Thermodynamics of Carbohydrates Binding by Receptor 1. The results of variable-temperature UV-vis titration in $CHCl_3$ from 5 °C to 35 °C are shown in Figure 6. In all the cases investigated, plotting of $R\ln K$ against $1/T$ resulted in a curve. Bent van't Hoff plots are generally interpreted as evidence of that initial and final states have different heat capacities. Bonar-Law and Sanders found the slightly bent van't Hoff plots for steroid-capped porphyrin–mannoside complexation in a mixture of tetrachloromethane–methanol.[3] Hayashi and Ogoshi encountered a large negative $\Delta C_p°$ in their studies of molecular recognition of ubiquinone analogues in toluene–ethanol

solution and investigated the origin in detail.[4] As already pointed out by Wilcox,[5] a small amount of water in chloroform might cause bent van't Hoff plots in our model system.[6]

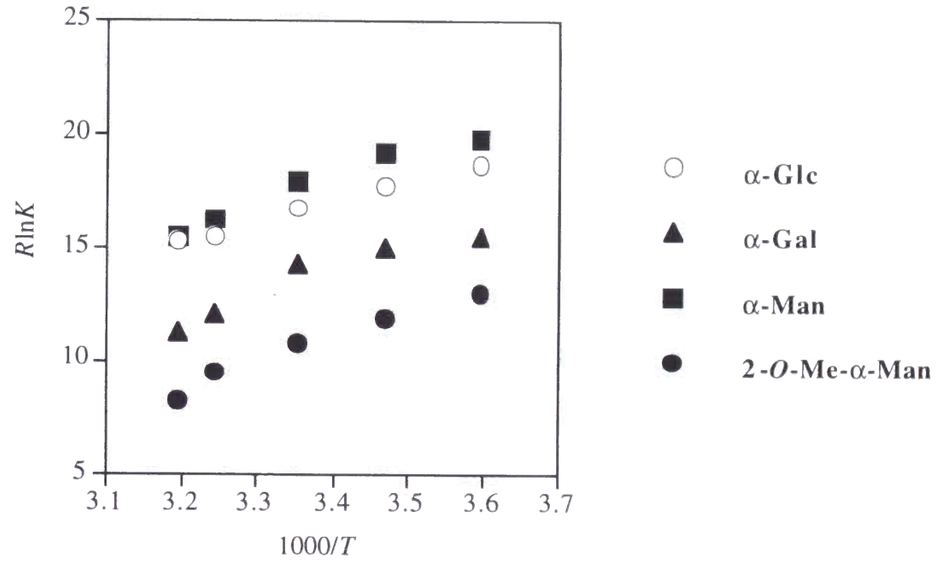

Figure 6. van't Hoff plots for the complexation between **1** and carbohydrates in $CHCl_3$.

Discussion

Receptor Design. Receptors **1**, **3** and **4** all have three interaction sites for carbohydrates, one Lewis acid site (Zn) in common, and two hydrogen bonding sites, namely, hydrogen acceptors (N) in **1** and hydrogen donors (OH) in **3** and **4**. Mizutani and Ogoshi reported previously that **3** and **4** selectively bound amino acid esters with a polar side chain, dimethyl aspartate and dimethyl glutamate.[7] For carbohydrates, however, receptors **1** and **2** showed better affinity and selectivity than **3** and **4**, showing the importance of the hydrogen acceptor/donor combinations for carbohydrate recognition. The Lewis base-Lewis acid-Lewis base combination in **1** formed a better binding site than the Lewis acid-Lewis acid-Lewis acid combination in **3** and **4**. For comparison of selectivity, the differences in $-\Delta G^{\circ}$ between the most strongly bound pyranoside ligand and the most weakly bound ligand are 2.9 for **1**, 0.6 for **3**, and 0.4 kcal/mol for **4**, confirming that the selectivity is highest for receptor **1**. Receptor **2**, the trans isomer of **1**, showed a similar pattern of binding affinity but weaker in magnitude. Therefore, the two quinolyl groups with the cis configuration in **1** cooperatively assisted the binding of the ligands. When the zinc of receptor **1** was replaced with two protons, the free base of **1** showed much reduced affinity for carbohydrates. For instance, the binding constant for β-Glc was *ca.* 600 M^{-1}.[8] This confirms the important role of the zinc. Both the Lewis acid site and the Lewis base sites are needed to bind carbohydrates strongly.

Carbohydrate Selectivity of Receptors 1 and 2. Receptor **1** showed high affinity for both mannosides and glucosides rather than galactosides. The stereochemical arrangement of C-5, C-4, and C-3 of Glc is the same as that of Man, and this arrangement was particularly well recognized by receptor **1**. Gal, the epimer of Glc at C4, was weakly bound, indicating that the stereochemistry at C4 was crucial. In contrast, the stereochemistry at C2 was less important. For the stereochemistry at C1, β-anomers were bound more strongly to receptor **1** than the corresponding α-anomers of Man, Glc, and Gal. The trend of these affinities suggests that, in the **1**–Man complex and the **1**–Glc complex, the 4-OH group was directly involved in the receptor-ligand interaction, while the 2-OH group was not.

As simpler analogs of carbohydrates, the affinities for cyclohexanediols **10**–**13** were determined (Table 2). Comparison of the binding constant between **10** and that of **11** indicates that the trans vicinal dihydroxy configuration was favored over the cis configuration by receptor **1**. Similarly, comparison of the binding constant between **12** and **13** indicates that the trans vicinal hydroxy hydroxymethyl configuration was favored over the cis configuration.

Effects of Polar Additives on the Binding. In the binding pocket of lectins, water often participates in the hydrogen bonding network to stabilize the sugar-receptor complex. Role of a water molecule in the hydrophobic environment in thermodynamics of the interaction is thus an interesting problem.[9] In our model systems, polar additives showed different effects on the complex formation depending on whether receptors have basic recognition sites (**1**) or acidic recognition sites (**3** and **4**). Only inhibition of binding was observed for receptor **1**, while promoting effects of binding by water, alcohols, phenols, and ethers were observed for receptor **3** and receptor **4**.

To elucidate the effects of the steric factors and acidity of the OH group of the additives on the binding constants, the free energy changes in binding ($-\Delta G^{\circ}$) in the presence of water, methyl alcohol, *tert*-butyl alcohol, phenol, *p*-nitrophenol, *p*-methoxyphenol, and *p*-dimethoxybenzene were compared (Figures 3–5). Both of methyl alcohol and *tert*-butyl alcohol showed the promoting effects on the binding, suggesting that steric demand was not severe. Stronger effects of *p*-methoxyphenol than *p*-nitrophenol and phenol indicate that acidity of the OH group is not the major factor for the present effects. Distinct effects of *p*-methoxyphenol and *p*-dimethoxybenzene strongly suggest that the ether group assists the binding. Here again, acid/base combination seems to play important roles. The assistance by the methoxy group of the additives implies that, for the host with three Lewis acidic sites, the Lewis basic methoxy group accepts hydrogen from the complex to form hydrogen bonding network among the receptor, the ligand, and the additive (Figure 7).

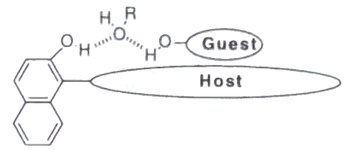

Figure 7. Proposed mechanism for the binding assistance by the additives.

Conclusions

The binding affinities of a series of receptors determined by UV-vis titration experiments indicated that, for diastereo-selective recognition of carbohydrates, the binding pocket of receptor **1** consisting of Lewis base-Lewis acid-Lewis base was found to be effective. The comparison of the affinity for a series of receptors and ligands suggested that receptor **1** with this binding pocket recognized the trans, trans-1,2-dihydroxy-3-(hydroxymethyl) moiety of carbohydrate. Addition of alcohols and ethers simply suppressed the binding by **1** while it assisted the binding by **3** and **4**. In the complex between acidic receptors (**3** and **4**) and the ligands, Lewis basic ethers would assist the formation of hydrogen bonding networks.

Experimental Section

Instrumentation. ^{1}H NMR and ^{13}C NMR spectra were recorded using a JEOL A-500 spectrometer in chloroform-*d* and DMSO-d_6, respectively. ^{1}H NMR chemical shifts in $CDCl_3$ were referenced to $CHCl_3$ (7.24 ppm) and ^{13}C NMR chemical shifts in DMSO-d_6 were reported relative to DMSO (39.5 ppm). UV–vis spectra were recorded on a Hewlett-Packard 8452 diode array spectrometer equipped with a thermostatted cell compartment. Mass spectra were obtained using a JEOL JMS SX-102A mass spectrometer.

Materials. Ether and THF were distilled from sodium benzophenone ketyl radical. Pyridine, DMF, toluene, DMSO, and CH_2Cl_2 were distilled from CaH_2. Benzoyl chloride was distilled from $CaCl_2$. Acetyl chloride was distilled from P_2O_5. Methanol and ethanol were dried by refluxing with, and distilling from magnesium. Octanol was distilled from sodium. Cyclohexene was distilled just before use. Acetic acid was dried by refluxing with acetic anhydride in the presence of 0.2% of 2-naphthalenesulfonic acid as a catalyst and was then fractionally distilled. Acetic anhydride was refluxed with and distilled from magnesium. *cis*- and *trans*-(2-Hydroxymethyl)cyclohexanol were prepared according to the reported procedure.[11] Materials for spectroscopic studies were obtained as follows. $CHCl_3$ containing amylenes as a stabilizer was purchased from Aldrich (A.C.S. HPLC grade, 99.9%, stabilized with amylenes) and was used as received. HPLC-grade water and spectrophotometric-grade methyl alcohol were used as received. *tert*-Butyl alcohol was dried by refluxing with, and distilling from sodium. *p*-Nitrophenol, phenol, *p*-methoxyphenol, and *p*-dimethoxybenzene were completely dried under reduced pressure just before use and their purity was checked by elemental analysis to avoid the influence by water contamination. Unless otherwise noted, other materials were obtained from commercial sources and used without further purification.

Receptors and Carbohydrates. [*cis*-5,15-Bis(2-hydroxy-1-naphthyl)-2,3,7,8,12,13,17,18-octaethylporphyrinato]zinc(II) (**3**) and [*trans*-5,15-bis(2,7-dihydroxy-1-naphthyl)-2,3,7,8,12,13,17,18-octaethylporphyrinato]zinc(II) (**4**) were prepared according to the published procedure.[7] Assignments of ^{1}H NMR signals were done by ^{1}H-^{1}H COSY or ^{1}H-^{1}H PDQF experiments.

Synthesis of [*cis*- and *trans*- 5,15-Bis(8-quinolyl)-

2,3,7,8,12,13,17,18-octaethylporphyrinato]zinc(II). It was synthesized according to the reported procedure.[12]

8-Formylquinoline. 8-Methylquinoline (1.46 g, 10 mmol) and selenium dioxide (1.3 g, 12 mmol) were mixed and the suspension was stirred for 2 h at 160 °C. After cooled to room temperature, the reaction mixture was poured to saturated $NaHCO_3$ aq. and extracted with dichloromethane. The organic layer was dried over K_2CO_3 and evaporated. The residue was recrystallized from ethanol to obtain 8-formylquinoline (367 mg, 23 %): ^{1}H NMR (500 MHz, $CDCl_3$) δ 11.46 (d, J = 0.9 Hz, 1H), 9.07 (dd, J = 4.3, 1.5 Hz, 1H), 8.35 (dd, J = 7.3, 1.5 Hz, 1H), 8.26 (dd, J = 8.3, 1.5 Hz, 1H), 8.11 (dd, J = 8.3, 1.5 Hz, 1H), 7.70 (dd, J = 7.3, 7.3 Hz, 1H), 7.53 (dd, J = 8.6, 4.3 Hz, 1H).

***cis*- and *trans*- 5,15-Bis(8-quinolyl)-2,3,7,8,12,13,17,18-octaethylporphyrin.** To a solution of 3,3',4,4'-tetraethyl-2,2'-dipyrrylmethene hydrobromide (326 mg, 0.967 mmol)[7] in ethanol (10 mL) was added under N_2 a solution of $NaBH_4$ (39.7 mg, 1.65 mmol) in ethanol (3 mL) until the reaction mixture turned from dark brown to pale brown. After stirring for 1.5 h at room temperature, the solvent was evaporated, and ether (20 mL) was added to the residue. The precipitate was filtered off and the filtrate was evaporated to yield 3,3',4,4'-tetraethyl-2,2'-dipyrrylmethane (246 mg, 0.954 mmol). 3,3',4,4'-Tetraethyl-2,2'-dipyrrylmethane (246 mg, 0.954 mmol) and 8-formylquinoline (157 mg, 1.00 mmol) were dissolved in methanol (11.5 mL, degassed by N_2 bubbling for 1 h) and a solution of *p*-toluenesulfonic acid monohydrate (59 mg, 0.31 mmol) in methanol (4 mL, degassed) was added dropwise. The reaction mixture was then stirred for 20 h in the dark. After the solvent was evaporated, the residue was dissolved in THF (27.6 mL), followed by the addition of a solution of chloranil (345 mg, 1.4 mmol) in THF (2.8 mL). The solution was stirred for 1.2 h. After the solvent was evaporated, the residue was purified by silica gel column chromatography ($CHCl_3$:acetone = 25:1) to separate the trans and cis isomer. The cis isomer was recrystallized from $CHCl_3$-hexane: UV-vis ($CHCl_3$ containing amylenes) λ_{max} (log ε) 416 nm (5.26), 512 nm (4.16), 546 nm (3.63), 579 nm (3.79), 631 nm (3.08); ^{1}H NMR (500 MHz, $CDCl_3$) δ 10.10 (s, 2H), 8.72 (dd, J = 3.7, 1.6 Hz, 2H), 8.47 (dd, J = 8.6, 1.8 Hz, 2H), 8.34 (dd, J = 6.4, 0.9 Hz, 2H), 8.28 (dd, J = 8.5, 1.2 Hz, 2H), 7.84 (dd, J = 8.3, 7.1 Hz, 2H), 7.46 (dd, J = 8.5, 4.0 Hz, 2H), 3.96–3.87 (m, 8H), 2.57–2.50 (m, 4H), 2.43–2.35 (m, 4H), 1.79 (t, J = 7.7 Hz, 12H), 0.76 (t, J = 7.3 Hz, 12H), –1.68 (br, 2H); HRMS calcd. for $C_{54}H_{56}N_6$ *m/z* 788.4566, found 788.4597.

[*cis*- and *trans*- 5,15-Bis(8-quinolyl)-2,3,7,8,12,13,17,18-octaethylporphyrinato]zinc(II). To the free base porphyrin (11.1 mg, 14.4 μmol)

dissolved in $CHCl_3$ (20 mL) was added methanol saturated with zinc acetate (1.5 mL), and the solution was refluxed for 30 min. The reaction mixture was poured to water and the resultant mixture was extracted with $CHCl_3$. The organic layer was washed with water, dried over Na_2SO_4, and evaporated.

[*cis*-5,15-Bis(8-quinolyl)-2,3,7,8,12,13,17,18-octaethylporphyrinato]zinc(II) (1). Cis-isomer was separated via silica gel column chromatography using 17% EtOAc in $CHCl_3$ as an eluent and further purified by recrystallization from $CHCl_3$-hexane. Pure **1** was dried in vacuo at room temperature for over 50 h: UV-vis ($CHCl_3$ containing amylenes) λ_{max} (log ε) 417 nm (5.43), 543 nm (4.23), 579 nm (3.97); ^{1}H NMR (500 MHz, $CDCl_3$) δ 10.11 (s, 2H), 8.59 (dd, J = 4.9, 1.5 Hz, 2H), 8.46 (m, 4H), 8.29 (dd, J = 8.2, 1.5 Hz, 2H), 7.85 (dd, J = 7.0, 8.2 Hz, 2H), 7.41 (dd, J = 8.5, 4.0 Hz, 2H), 3.95–3.83 (m, 8H), 2.51–2.44 (m, 4H), 2.29–2.22 (m, 4H), 1.79 (t, J = 7.6 Hz, 12H), 0.73 (t, J = 7.3 Hz, 12H); HRMS calcd for $C_{54}H_{54}N_6Zn$ *m/z* 850.3702, found 850.3710.

[*trans*-5,15-Bis(8-quinolyl)-2,3,7,8,12,13,17,18-octaethylporphyrinato]zinc(II) (2). Trans-isomer was separated by passing through triethylamine pre-treated silica gel column using 5% EtOAc in $CHCl_3$ as an eluent, and further purified by recrystallization from $CHCl_3$-hexane. Pure **2** was dried in vacuo at room temperature for over 50 h: UV-vis ($CHCl_3$ containing amylenes) λ_{max} (log ε) 417 nm (5.45), 543 nm (4.18), 579 nm (3.93); ^{1}H NMR (500 MHz, $CDCl_3$) δ 10.10 (s, 2H), 8.57 (dd, J = 4.0, 1.8 Hz, 2H), 8.55 (dd, J = 6.7, 1.5 Hz, 2H), 8.44 (dd, J = 8.2, 1.8 Hz, 2H), 8.29 (dd, J = 8.2, 1.5 Hz, 2H), 7.88 (dd, J = 8.2, 6.7 Hz, 2H), 7.38 (dd, J = 8.6, 4.0 Hz, 2H), 3.89 (q, J = 7.6 Hz, 8H), 2.48–2.41 (m, 4H), 2.32–2.25 (m, 4H), 1.76 (t, J = 7.6 Hz, 12H), 0.71 (t, J = 7.6 Hz, 12H); HRMS calcd for $C_{54}H_{54}N_6Zn$ *m/z* 850.3702, found 850.3717.

Octyl β-D-glucopyranoside. (Dojindo laboratories, used as received): ^{1}H NMR (500 MHz, 1.7 mM in $CDCl_3$ at 25 °C) δ 4.29 (d, J = 7.6 Hz, 1H, 1-H), 3.93–3.78 (m, 2H), 3.88 (dt, J = 9.5, 6.7 Hz, 1H, CH_3-$(CH_2)_6$-$\underline{CH_2}$O-), 3.61–3.48 (m, 2H), 3.51 (dt, J = 9.5, 7.0 Hz, 1H, CH_3-$(CH_2)_6$-$\underline{CH_2}$O-), 3.41–3.32 (m, 2H), 2.62 (d, J = 2.1 Hz, 1H, 3-OH), 2.50 (d, J = 2.8 Hz, 1H, 4-OH), 2.37 (d, J = 2.1 Hz, 1H, 2-OH), 1.96 (t, J = 7.0 Hz, 1H, 6-OH), 1.61 (m, 2H, CH_3-$(CH_2)_5\underline{CH_2}$-CH_2O-), 1.26 (m, 10H, CH_3-$(\underline{CH_2})_5CH_2$-CH_2O-), 0.86(t, J = 7.0 Hz, 3H, $\underline{CH_3}$-$(CH_2)_6$-CH_2O-).

Octyl α-D-glucopyranoside. (Sigma, used as received): ^{1}H NMR (500 MHz, 1.9 mM in $CDCl_3$ at 25 °C) δ 4.85 (d, J = 4.0 Hz, 1H, 1-H), 3.87–3.78 (m, 2H), 3.74–3.62 (m, 2H), 3.71 (dt, J = 9.5, 6.5 Hz, 1H, CH_3-$(CH_2)_6$-$\underline{CH_2}$O-), 3.57–

3.53 (m, 1H), 3.48–3.40 (m, 1H), 3.43 (dt, J = 9.0, 7.0 Hz, 1H, CH_3-$(CH_2)_6$-$\underline{CH_2}$O-), 2.55 (d, J = 2.1 Hz, 1H, 3-OH), 2.47 (d, J = 2.8 Hz, 1H, 4-OH), 1.97 (d, J = 10.7 Hz, 1H, 2-OH), 1.89 (dd, J = 7.0, 5.5 Hz, 1H, 6-OH), 1.58 (m, 2H, CH_3-$(CH_2)_5\underline{CH_2}$-CH_2O-), 1.26 (m, 10H, CH_3-$(\underline{CH_2})_5CH_2$-CH_2O-), 0.87 (t, J = 7.0 Hz, 3H, $\underline{CH_3}$-$(CH_2)_6$-CH_2O-).

Octyl β-D-galactopyranoside. It was synthesized by the literature procedure.[13] Obtained crude product was purified via silica gel column chromatography (EtOAc:MeOH = 6:1). Further purification was done by recrystallizing from EtOH-hexane. The crystals were completely dried at 60 °C under reduced pressure for 100 h: ^{1}H NMR (500 MHz, 2.5 mM in $CDCl_3$ at 25 °C) δ 4.24 (d, J = 7.3 Hz, 1H, 1-H), 4.01–3.95 (m, 2H), 3.93–3.85 (m, 2H), 3.66–3.58 (m, 2H), 3.55–3.48 (m, 2H), 2.78 (d, J = 2.4 Hz, 1H, 4-OH), 2.61 (d, J = 4.6 Hz, 1H, 3-OH), 2.38 (d, J = 1.8 Hz, 1H, 2-OH), 2.09 (dd, J = 7.9, 4.9 Hz, 1H, 6-OH), 1.62 (m, 2H, CH_3-$(CH_2)_5\underline{CH_2}$-CH_2O-), 1.27 (m, 10H, CH_3-$(\underline{CH_2})_5CH_2$-CH_2O-), 0.86 (t, J = 7.3 Hz, 3H, $\underline{CH_3}$-$(CH_2)_6$-CH_2O-); ^{13}C NMR (125.65 MHz, DMSO-d_6) δ 103.47 (1-C), 75.09, 73.51, 70.56, 68.47, 68.13, 60.40, 31.29, 29.37, 28.91, 28.73, 25.57, 22.11, 13.95; Anal. Calcd for $C_{14}H_{28}O_6$: C, 57.51; H, 9.65. Found: C, 57.30; H, 9.88.

Octyl α-D-galactopyranoside. It was obtained as a complex mixture by the literature procedure.[14] The crude product was then passed through a Dowex 1×2 (OH form, Dow Chemical Co.) chromatographic column (EtOH:MeOH = 1:1) to give the pure α-anomer, which was completely dried at 60 °C under reduced pressure for 100 h: ^{1}H NMR (500 MHz, 2.3 mM in $CDCl_3$ at 25 °C) δ 4.94 (d, J = 3.7 Hz, 1H, 1-H), 4.08 (m, 1H, 4-H), 3.98–3.94 (m, 1H, 5-H), 3.87–3.69 (m, 4H), 3.71 (dt, J = 9.8, 6.7 Hz, 1H, CH_3-$(CH_2)_6$-$\underline{CH_2}$O-), 3.44 (dt, J = 9.5, 6.7 Hz, 1H, CH_3-$(CH_2)_6$-$\underline{CH_2}$O-), 2.80 (d, J = 0.6 Hz, 1H, 4-OH), 2.53 (d, J = 3.7 Hz, 1H, 3-OH), 2.20 (dd, J = 7.9, 4.6 Hz, 1H, 6-OH), 1.88 (d, J = 10.4 Hz, 1H, 2-OH), 1.59 (m, 2H, CH_3-$(CH_2)_5\underline{CH_2}$-CH_2O-), 1.27 (m, 10H, CH_3-$(\underline{CH_2})_5CH_2$-CH_2O-), 0.86 (t, J = 7.3 Hz, 3H, $\underline{CH_3}$-$(CH_2)_6$-CH_2O-); ^{13}C NMR (125.65 MHz, DMSO-d_6) δ 98.84 (1-C), 71.14, 69.58, 68.84, 68.37, 66.88, 60.57, 31.25, 29.11, 28.84, 28.68, 25.71, 22.07, 13.94; Anal. Calcd for $C_{14}H_{28}O_6$: C, 57.51; H, 9.65. Found: C, 57.21; H, 9.48.

Octyl β-D-mannopyranoside. It was synthesized by the literature procedure.[15] The obtained product was further purified by a Dowex 1×2 (OH form, Dow Chemical Co.) chromatographic column (EtOH:MeOH = 2:1). The product was completely dried at 60 °C under reduced pressure for 100 h: ^{1}H NMR (500 MHz, 0.6 mM in $CDCl_3$ at 25 °C) δ 4.52 (d, J = 1.2 Hz, 1H, 1-H), 3.99 (m, 1H), 3.95–3.87 (m, 2H), 3.85–3.80 (m, 1H), 3.76–3.72 (m, 1H), 3.55–3.47 (m, 2H), 3.30–3.26 (m, 1H),

2.47 (d, J = 9.5 Hz, 1H, 3-OH), 2.42 (d, J = 2.8 Hz, 1H, 4-OH), 2.36 (d, J = 2.4 Hz, 1H, 2-OH), 2.04 (t, J = 6.7 Hz, 1H, 6-OH), 1.60 (m, 2H, CH_3-$(CH_2)_5\underline{CH_2}$-CH_2O-), 1.26 (m, 10H, CH_3-$(\underline{CH_2})_5CH_2$-CH_2O-), 0.86 (t, J = 7.0 Hz, 3H, $\underline{CH_3}$-$(CH_2)_6$-CH_2O-); ^{13}C NMR (125.65 MHz, DMSO-d_6) δ 100.22 (1-C), 77.49, 73.71, 70.56, 68.36, 67.17, 61.37, 31.23, 29.18, 28.86, 28.68, 25.58, 22.06, 13.94; Anal. Calcd for $C_{14}H_{28}O_6$: C, 57.51; H, 9.65. Found: C, 57.24; H, 9.81.

Octyl α-D-mannopyranoside. It was obtained as a complex mixture by the literature procedure.[14] The crude product was then passed through a Dowex 1×2 (OH form, Dow Chemical Co.) chromatographic column (EtOH:MeOH = 2:1) to give the pure α-anomer, which was completely dried at 60 °C under reduced pressure for 100 h: ^{1}H NMR (500 MHz, 0.3 mM in $CDCl_3$ at 25 °C) δ 4.82 (d, J = 1.5 Hz, 1H, 1-H), 3.93 (m, 1H), 3.89–3.77 (m, 4H), 3.68–3.61 (m, 1H), 3.66 (dt, J = 9.5, 6.7 Hz, 1H, CH_3-$(CH_2)_6$-$\underline{CH_2}$O-), 3.39 (dt, J = 9.5, 6.4 Hz, 1H, CH_3-$(CH_2)_6$-$\underline{CH_2}$O-), 2.37 (d, J = 5.5 Hz, 1H, 3-OH), 2.34 (d, J = 3.1 Hz, 1H, 4-OH), 2.19 (d, J = 4.6 Hz, 1H, 2-OH), 1.99 (t, J = 6.7 Hz, 1H, 6-OH), 1.55 (m, 2H, CH_3-$(CH_2)_5\underline{CH_2}$-CH_2O-), 1.25 (m, 10H, CH_3-$(\underline{CH_2})_5CH_2$-CH_2O-), 0.87 (t, J = 7.3 Hz, 3H, $\underline{CH_3}$-$(CH_2)_6$-CH_2O-); ^{13}C NMR (125.65 MHz, DMSO-d_6) δ 99.70 (1-C), 73.91, 71.00, 70.39, 66.97, 66.17, 61.26, 31.23, 28.97, 28.77, 28.66, 25.73, 22.05, 13.93; Anal. Calcd for $C_{14}H_{28}O_6$: C, 57.51; H, 9.65. Found: C, 57.27; H, 9.82.

Octyl 6-*O*-benzoyl-β-D-glucopyranoside. To a solution of octyl β-D-glucopyranoside (155 mg, 0.52 mmol) and pyridine (3.7 mL) in dichloromethane (3.0 mL) was added benzoyl chloride (144 mg, 1.03 mmol) in dichloromethane (6.0 mL) dropwise over 6 h at –40 °C. After the reaction mixture was allowed to warm to room temperature over 12 h, excess benzoyl chloride was decomposed by the addition of MeOH. The solvent was evaporated, and the residue was purified by column chromatography on silica gel (ether:acetone = 4:1) to obtain octyl 6-*O*-benzoyl-β-D-glucopyranoside (43.9 mg, 0.11 mmol, 22%): ^{1}H NMR (500 MHz, $CDCl_3$) δ 8.07–7.43 (m, 5H, benzoyl-H), 4.75 (dd, J = 12.2, 4.6 Hz, 1H, 6-H), 4.53 (dd, J = 12.2, 2.2 Hz, 1H, 6-H), 4.30 (d, J = 7.7 Hz, 1H, 1-H), 3.89 (dt, J = 9.4, 7.7 Hz, 1H, CH_3-$(CH_2)_6$-$\underline{CH_2}$O-), 3.61 (t, J = 9.1 Hz, 1H, 3-H), 3.57 (m, 1H, 5-H), 3.52 (dt, J = 9.6, 7.0 Hz, 1H, CH_3-$(CH_2)_6$-$\underline{CH_2}$O-), 3.48 (m, 1H, 4-H), 3.38 (dd, J = 9.5, 8.0 Hz, 1H, 2-H), 3.14 (s, 1H, 4-OH), 2.81 (s, 1H, 3-OH), 2.46 (s, 1H, 2-OH), 1.64–1.59 (m, 2H, CH_3-$(CH_2)_5\underline{CH_2}$-CH_2O-), 1.28–1.24 (m, 10H, CH_3-$(\underline{CH_2})_5CH_2$-CH_2O-), 0.87 (t, J = 5.5 Hz, 3H, $\underline{CH_3}$-$(CH_2)_6$-CH_2O-); HRMS calcd for $C_{21}H_{33}O_7$ m/z 397.2226, found 397.2237.

Octyl 6-*O*-acetyl-β-D-glucopyranoside. To a solution of octyl β-D-

glucopyranoside (152 mg, 0.51 mmol) and pyridine (3.7 mL) in dichloromethane (3.0 mL) was added acetyl chloride (80 mg, 1.0 mmol) in dichloromethane (6.0 mL) dropwise over 6 h at –40 °C. After the reaction mixture was allowed to warm to room temperature over 12 h, excess acetyl chloride was decomposed by the addition of MeOH. The solvent was evaporated. The residue was purified by column chromatography on silica gel (ether:acetone = 4:1) to obtain octyl 6-*O*-acetyl-β-D-glucopyranoside (52.6 mg, 0.16 mmol, 31%): ^{1}H NMR (500 MHz, $CDCl_3$) δ 4.55–4.51 (dd, J = 12.5, 4.7 Hz, 1H, 6-H), 4.27 (d, J = 7.8 Hz, 1H, 1-H), 4.25 (dd, J = 12.5, 2.5 Hz, 1H, 6-H), 3.90 (dt, J = 24.7, 19.4 Hz, 1H, CH_3-$(CH_2)_6$-$\underline{CH_2}$O-), 3.58 (m, 1H, 3-H), 3.50 (dt, J = 24.7, 19.4 Hz, 1H, CH_3-$(CH_2)_6$-$\underline{CH_2}$O-), 3.44 (m, 1H, 5-H), 3.39 (m, 2H, 2-H and 4-H), 3.02 (s, 1H, 4-OH), 2.78 (s, 1H, 3-OH), 2.43 (s, 1H, 2-OH), 2.21 (s, 3H, CH_3CO_2-) 1.65–1.57 (m, 2H, CH_3-$(CH_2)_5\underline{CH_2}$-CH_2O-), 1.37–1.21 (m, 10H, CH_3-$(\underline{CH_2})_5CH_2$-CH_2O-), 0.87 (t, J = 5.4 Hz, 3H, $\underline{CH_3}$-$(CH_2)_6$-CH_2O-); HRMS calcd for $C_{16}H_{31}O_7$ *m/z* 335.2056, found 335.2063.

Synthesis of Octyl 2-*O*-methyl-α-D-mannopyranoside.

Mannose pentaacetate. It was prepared from mannose and anhydrous sodium acetate in acetic anhydride by the reported procedure.[16] The obtained product was a mixture of α- and β-anomers and a small amount of straight-chain mannose peracetate. Since separation was quite difficult, this mixture was subjected to the next reaction after passing through a silica gel column (hexane:EtOAc = 1:1).

Octyl 2,3,4,6-tetra-*O*-acetyl-α-D-mannopyranoside. It was obtained stereoselectively by a modified procedure of S. Matsumura *et al.*[13], in which 1.2 equivalent of silver trifluoromethanesulfonate was used instead of silver carbonate, and 3.2 equivalent of tetramethylurea was added together with octanol and silver trifluoromethanesulfonate to minimize ortho ester formation. Purification was done by silica gel column chromatography (hexane:EtOAc = 2:1). The yield was 43%: ^{1}H NMR (500 MHz, $CDCl_3$) δ 5.28 (m, 1H), 5.04 (m, 1H), 4.84 (s, 1H), 4.27 (m, 1H), 4.12–3.88 (m, 3H), 3.65 (m, 1H), 3.44 (m, 1H), 2.09–2.00 (m, 12H), 1.55 (m, 2H), 1.24 (m, 10H), 0.87 (t, J = 7.0 Hz, 3H).

Octyl α-D-mannopyranoside. Deacetylation was carried out by the reported procedure.[15] Less than 1% of β-anomer was detected by ^{1}H NMR. The product was passed through a silica gel column (EtOAc:MeOH = 9:1) and was used for the next reaction. The yield was 92%: ^{1}H NMR (500 MHz, 0.3 mM in $CDCl_3$ at 25 °C) δ 4.82 (d, J = 1.5 Hz, 1H, 1-H), 3.93 (m, 1H), 3.89–3.77 (m, 4H), 3.68–3.61 (m, 1H), 3.66 (dt, J = 9.5, 6.7 Hz, 1H, CH_3-$(CH_2)_6$-$\underline{CH_2}$O-), 3.39 (dt, J = 9.5, 6.4 Hz, 1H,

CH_3-$(CH_2)_6$-$\underline{CH_2}$O-), 2.37 (d, J = 5.5 Hz, 1H, 3-OH), 2.34 (d, J = 3.1 Hz, 1H, 4-OH), 2.19 (d, J = 4.6 Hz, 1H, 2-OH), 1.99 (t, J = 6.7 Hz, 1H, 6-OH), 1.55 (m, 2H, CH_3-$(CH_2)_5\underline{CH_2}$-CH_2O-), 1.25 (m, 10H, CH_3-$(\underline{CH_2})_5CH_2$-CH_2O-), 0.87 (t, J = 7.3 Hz, 3H, $\underline{CH_3}$-$(CH_2)_6$-CH_2O-); ^{13}C NMR (125.65 MHz, DMSO-d_6) δ 99.70 (1-C), 73.92, 71.00, 70.40, 66.97, 66.17, 61.26, 31.24, 28.98, 28.78, 28.68, 25.75, 22.07, 13.94.

Octyl 4,6-*O*-benzylidene-α-D-mannopyranoside. Benzylidenation was effected by $PhCH(OMe)_2$-$HBF_4 \cdot OEt_2$.[17] The temperature was kept at –40 °C during the reaction and gradually increased to room temperature. The crude product was purified by silica gel column chromatography (hexane:EtOAc = 8:5) and further purified by recrystallization from hexane-EtOAc. The yield was 67 %: ^{1}H NMR (500 MHz, $CDCl_3$) δ 7.49–7.47 (m, 2H), 7.38–7.34 (m, 3H), 5.56 (s, 1H), 4.85 (d, J = 1.2 Hz, 1H, 1-H), 4.26 (m, 1H), 4.10–4.03 (m, 2H), 3.91 (m, 1H), 3.84–3.79(m, 2H), 3.68 (dt, J = 9.8, 6.7 Hz, 1H), 3.41 (dt, J = 9.5, 6.7 Hz, 1H), 2.54 (d, J = 2.1 Hz, 1H, OH), 2.53 (d, J = 3.4 Hz, 1H, OH), 1.59–1.51 (m, 2H), 1.27 (m, 10H), 0.87 (t, J = 7.0 Hz, 3H).

Octyl 4,6-*O*-benzylidene-3-*O*-benzyl-α-D-mannopyranoside. The procedure reported by Boger *et al.*[18] was used for selective benzylation of the equatorial 3-OH group of octyl 4,6-*O*-benzylidene-α-D-mannopyranoside. The crude product was purified by silica gel column chromatography (hexane:EtOAc = 4:1). The yield was 81%: ^{1}H NMR (500 MHz, $CDCl_3$) δ 7.50–7.47 (m, 2H), 7.37–7.27 (m, 8H), 5.60 (s, 1H, benzylidene-H), 4.85 (d, J = 11.9 Hz, 1H, benzyl-H), 4.84 (d, J = 1.5 Hz, 1H, 1-H), 4.71 (d, J = 11.9 Hz, 1H, benzyl-H), 4.25 (m, 1H), 4.08 (m, 1H), 4.04 (m, 1H, 2-H). 3.92 (dd, J = 9.5, 3.0 Hz, 1H, 3-H), 3.85–3.81 (m, 2H), 3.67 (dt, J = 9.5, 7.0 Hz, 1H, CH_3-$(CH_2)_6$-$\underline{CH_2}$O-), 3.38 (dt, J = 9.5, 7.0 Hz, 1H, CH_3-$(CH_2)_6$-$\underline{CH_2}$O-), 2.63 (d, J = 1.5 Hz, 1-H, 2-OH), 1.55 (m, 2H, CH_3-$(CH_2)_5\underline{CH_2}$-CH_2O-), 1.26 (m, 10H, CH_3-$(\underline{CH_2})_5CH_2$-CH_2O-), 0.87 (t, J = 7.5 Hz, 3H, $\underline{CH_3}$-$(CH_2)_6$-CH_2O-).

Octyl 4,6-*O*-benzylidene-3-*O*-benzyl-2-*O*-methyl-α-D-mannopyranoside. The procedure for methylation of benzyl 3,4,6-tri-*O*-benzyl-β-L-glucopyranoside[19] was found to be effective for methylation of octyl 4,6-*O*-benzylidene-3-*O*-benzyl-α-D-mannopyranoside. The crude product was purified by silica gel column chromatography (hexane:EtOAc = 4:1). The yield was 89%: ^{1}H NMR (500 MHz, $CDCl_3$) δ 7.45–7.42 (m, 2H), 7.32–7.19 (m, 8H), 5.55 (s, 1H), 4.82 (d, J = 12.2 Hz, 1H), 4.76 (d, J = 1.2 Hz, 1H), 4.65 (d, J = 12.2 Hz, 1H), 4.17 (dd, J = 10.1, 4.3 Hz, 1H), 4.08 (dd, J = 9.8, 9.8 Hz, 1H), 3.89 (dd, J = 10.1, 3.4 Hz, 1H), 3.79 (dd, J = 10.1, 10.1 Hz, 1H), 3.71 (dt, J =4.6, 9.5 Hz, 1H), 3.59 (dt, J = 9.5, 7.0 Hz, 1H), 3.52 (dd, J = 3.1, 1.5 Hz, 1H), 3.49 (s, 3H), 3.32 (dt, J = 9.8, 6.7 Hz, 1H), 1.50 (m, 2H),

1.22 (m, 10H), 0.82 (t, J = 7.0 Hz, 3H).

Octyl 2-*O*-methyl-α-D-mannopyranoside. Removal of both the benzyl group and the benzylidene group was done by catalytic transfer hydrogenation reported by Hanessian *et al.*[20] The crude product was purified first by silica gel column chromatography (EtOAc:MeOH = 9:1) and then by passing through a Dowex 1×2 (OH form, Dow Chemical Co.) chromatographic column using methanol as an eluent. The pure product was obtained in a 98% yield as hygroscopic liquid: ^{1}H NMR (500 MHz, $CDCl_3$) δ 4.89 (d, J = 1.2 Hz, 1H, 1-H), 3.87–3.74 (m, 3H), 3.67 (dt, J = 9.8, 6.7 Hz, 1H, CH_3-$(CH_2)_6$-$\underline{CH_2}$O-), 3.65 (m, 1H, 4-H), 3.58 (m, 1H, 5-H), 3.46 (s, 3H, CH_3O-), 3.45 (dd, J = 1.5 Hz, 1H, 2-H), 3.38 (dt, J = 9.5, 6.4 Hz, 1H, CH_3-$(CH_2)_6$-$\underline{CH_2}$O-), 2.45 (d, J = 2.7 Hz, 1H, 4-OH), 2.29 (d, J = 10.4 Hz, 1H, 3-OH), 2.02 (dd, J = 7.0, 5.8 Hz, 1H, 6-OH), 1.56 (m, 2H, CH_3-$(CH_2)_5\underline{CH_2}$-CH_2O-), 1.26 (m, 10H, CH_3-$(\underline{CH_2})_5CH_2$-CH_2O-), 0.87 (t, J = 7.3 Hz, 3H, $\underline{CH_3}$-$(CH_2)_6$-CH_2O-); ^{13}C NMR (125.65 MHz, DMSO-d_6) δ 96.51 (1-C), 80.57, 73.96, 70.88, 67.24, 66.35, 61.15, 58.55, 31.24, 29.00, 28.78, 28.67, 25.74, 22.08, 13.94; Anal. Calcd for $C_{15}H_{30}O_6 \cdot 1/4$ (H_2O): C, 57.95; H, 9.89. Found: C, 58.03; H, 9.82.

UV–Vis Titrations. Binding constants were determined by UV–vis titrations. To avoid the influence by the ethanol added as a stabilizer to chloroform, amylene-containing chloroform was used throughout the study. The water concentration was estimated to be about 0.002% from ^{1}H NMR. The atropisomerization from the cis isomer (**1**) to the trans isomer (**2**) in a $CDCl_3$ solution occurred slowly: 5 % of **1** was isomerized to **2** at room temperature for 100 h although no isomerization was observed in the solid state. Therefore the receptor solution was prepared just before use. Cis to trans isomerization in receptors **3** and **4** was too slow to observe.

The details of the determination of the binding constant are as follows. To *ca.* 5×10^{-6} M of **1**, **2**, **3**, **4**, or **5** in $CHCl_3$ was added a stock solution of carbohydrate ligands in $CHCl_3$ at 15 °C. The changes in absorbance at around 424 nm in the Soret band were monitored at eight different concentrations of carbohydrate, with volume change due to carbohydrate addition being taken into account during analysis. Assuming 1:1 complexation, the binding constants were evaluated by least square parameter estimation based on the Damping Gauss-Newton method. Calculated curves were well fitted to absorbance changes.

It was reported that glycopyranosides aggregate when dissolved in organic solvent at a high concentration.[3] The UV-vis titration experiments of **1** and **2** were performed in the low concentration range of the ligands, where no aggregation occurs.

In the case of the binding of Man by receptors **3** and **4**, at the highest concentration of Man, aggregation occurred. However the standard deviations of binding constants of these receptor-ligand complexes were 6–10 %, comparable to those for other complexes, showing that the errors owing to the ligand aggregation were negligibly small.

References and Notes

1 See, for example: Ogoshi, H.; Mizutani, T. *Acc. Chem. Res.* **1998**, *31*, 81.

2 Weis, W. I.; Drickamer, K.; Hendrickson, W. A. *Nature* **1992**, *360*, 127.

3 Bonar-Law, R. P.; Sanders, J. K. M. *J. Am. Chem. Soc.* **1995**, *117*, 259.

4 Hayashi, T.; Miyahara, T.; Koide, N.; Kato, Y.; Masuda, H.; Ogoshi, H. *J. Am. Chem. Soc.* **1997**, *119*, 7281.

5 Adrian, J., C., Jr.; Wilcox, C., S. *J. Am. Chem. Soc.* **1991**, *113*, 678.

6 The water concentration in chloroform used was estimated to be about 0.002% from ^{1}H NMR.

7 Mizutani, T.; Murakami, T.; Kurahashi, T.; Ogoshi, H. *J. Org. Chem.* **1996**, *61*, 539.

8 Owing to the small changes in absorbance in vis spectra, the precise determination of binding constants was difficult.

9 (a) Miller, D. M., III.; Olson, J. S.; Pflugrath, J. W.; Quiochio, F. A. *J. Biol. Chem.* **1980**, *255*, 2465. (b) Miller, D. M. III.; Olson, J. S.; Pflugrath, J. W.; Quiochio, F. A. *J. Biol. Chem.* **1983**, *258*, 13665. (c) Bourne, Y.; Rouge, P.; Cambillau, C. *J. Biol. Chem.* **1990**, *265*, 18161.

10 To examine how ligand aggregation affects the dependence of K on additive concentration, we compared behaviors between **1** and **3**. Even though the binding constants were determined in the same concentration range of β-Gal, the binding constant between **3** and β-Gal increased while that between **1** and β-Gal simply decreased with increasing *tert*-butyl alcohol concentration, suggesting that the effects of *tert*-butyl alcohol cannot be ascribed to the dissolution of aggregate of β-Gal. The increased CD band by the addition of *tert*-butyl alcohol to the **3**–β-Glc complex also indicates that the effects of additives were due to the interaction between the additive and the complex (See, Chapter 2).

11 Gaunitz, S.; Schwarz, H.; Bohlmann, F. *Tetrahedron* **1975**, *31*, 185.

12 Aoyama, Y.; Kamohara, T.; Yamagishi, A.; Toi, H.; Ogoshi, H.; *Tetrahedron Lett.* **1987**, *28*, 2143.

13 Matsumura, S.; Imai, K.; Yoshikawa, S.; Kawada, K.; Uchibori, T. *J. Am. Oil Chem. Soc.* **1990**, *67*, 996.

14 Konradsson, P.; Roberts, C.; Fraser-Reid, B. *Recl. Trav. Chim. Pays-Bas* **1991**, *110*, 23.

15 Kaur, K. J.; Hindsgaul, O. *Glycoconjugate J.* **1991**, *8*, 90.

16 Rosevear, P.; VanAken, T.; Baxter, J.; Ferguson-Miller, S. *Biochemistry* **1980**, *19*, 4108.

17 Albert, R.; Dax, K.; Pleschko, R.; Stutz, A. E. *Carbohydr. Res.* **1985**, *137*, 282.

18 Boger, D. L.; Honda, T. *J. Am. Chem. Soc.* **1994**, *116*, 5647.

19 Boger, D. L.; Teramoto, S.; Zhou, J. *J. Am. Chem. Soc.* **1995**, *117*, 7344.

20 Hanessian, S.; Liak, T. J.; Vanasse, B. *Synthesis* **1981**, 396.

Chapter 2

^{1}H NMR and Induced Circular Dichroism Study of the Artificial Receptor-Carbohydrate Interaction

Abstract

Receptor-monosaccharide complexes reported in Chapter 1 were investigated in detail with ^{1}H NMR and circular dichroism spectroscopies. Analysis of the complexation-induced shifts (CIS) of the carbohydrate OH protons in the ^{1}H NMR revealed that receptor **1** ([*cis*-5,15-bis(8-quinolyl)-2,3,7,8,12,13,17,18-octaethylporphyrinato]zinc(II)) bound the 4-OH group of mannoside and glucoside by coordination to the zinc and the 6-OH and 3-OH groups by hydrogen bonding to the quinolyl nitrogen atoms. These NMR results and comparison of binding affinity with reference receptors and ligands indicated that receptor **1** recognized the trans, trans-1,2-dihydroxy-3-(hydroxymethyl) moiety of carbohydrates by the combination of Lewis acid (zinc) and Lewis bases (quinolyl nitrogens). Poor affinities of **1** to octyl galactosides and octyl 2-*O*-methyl-α-mannoside were ascribed to neighboring group effects, where a neighboring group in ligands not directly involved in the receptor-ligand interactions had considerable influence on the affinity through destabilizing the hydrogen bonding network(s) in the receptor-ligand complex. The circular dichroism induced in the porphyrin Soret band by complexation with the carbohydrates displayed characteristic patterns, which parallel the patterns of the complexation-induced shifts in the ^{1}H NMR. The CD patterns sensitively reflected the receptor-ligand interaction modes, particularly ligand orientation and fluctuation in the complex. Variable-temperature CD revealed that glucoside was fluctuating on **1** while mannoside was rigidly fixed on **1** at room temperature.

Introduction

Receptor **1** ([*cis*-5,15-bis(8-quinolyl)-2,3,7,8,12,13,17,18-octaethyl-porphyrinato]zinc(II)) was found to bind octyl glucoside and mannoside with high affinity, but octyl galactosides and octyl 2-*O*-methyl-α-mannoside were found to be poor ligands for **1** as reported in Chapter 1. The comparison of the affinity for monosaccharides and a series of reference ligands suggested that receptor **1** recognized the trans, trans-1,2-dihydroxy-3-(hydroxymethyl) moiety of carbohydrate. However, binding mechanism is not necessarily clear. Thus, a detailed spectroscopic investigation was conducted by taking advantage of the characteristic porphyrin chromophore.

^{1}H NMR spectroscopy is a powerful tool to investigate the geometry of the bound carbohydrate on the porphyrin plane. As shown in Figure 1, chemical shifts of the bound substrate were exposed to the profound ring current effects of the porphyrin chromophore.

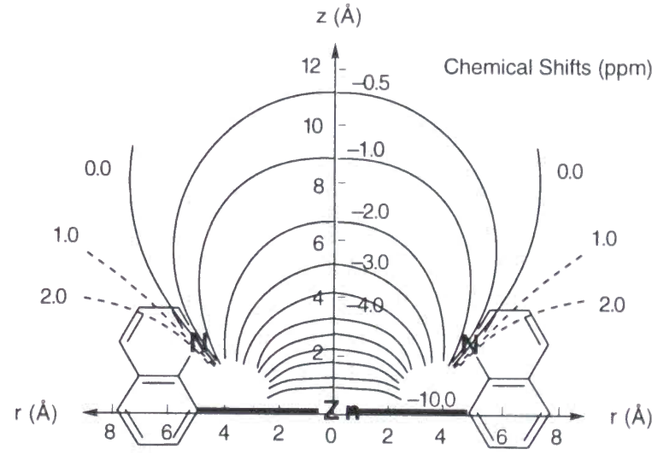

Figure 1. Isoshielding lines of porphyrin on receptor **1** calculated by using Johnson-Bovey equation.[1]

Circular dichroism spectroscopy is also useful to investigate host-guest interaction. Mizutani and Ogoshi reported that aliphatic amino acid esters induce circular dichroism spectra upon complexation with achiral functionalized zinc porphyrins.[2] Their systematic study revealed that multi-point interaction between hosts and guests is indispensable for split-type induced circular dichroism spectra as shown in Figure 2.

Theoretical calculations suggested that the coupling between transition dipole moment of fixed carbonyl chromophore and that of the porphyrin chromophore caused the spectra.

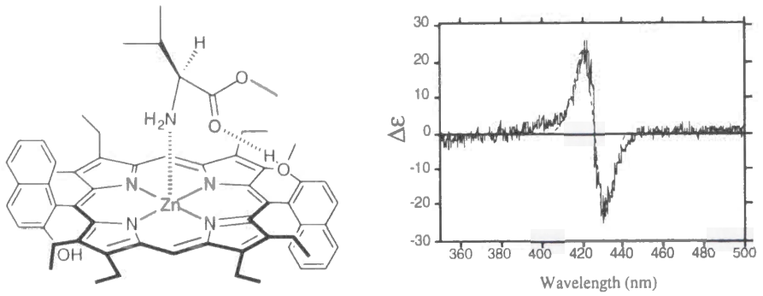

Figure 2. Amino acid ester-zinc porphyrin complex and the induced circular dichroism spectrum.

In this Chapter, the author reports a detailed investigation of artificial receptor-carbohydrate interaction with ^{1}H NMR and circular dichroism spectroscopy.

Results

^{1}H NMR Study of Binding. The complexation-induced shifts (CIS) of the 1-H, 2-OH, 3-OH, 4-OH, and 6-OH resonances of α- and β-anomers of Glc, Man, and Gal were determined in $CDCl_3$ in the low concentration range of receptor **1**. The assignments of the resonances of the four hydroxy protons were made based on the ^{1}H–^{1}H COSY or PDQF experiments. The observed chemical shifts were the average values of the free and the complexed ligand in the limit of fast chemical exchange. Figure 3 shows the ^{1}H NMR spectra of β-Man in the presence of varying amounts of receptor **1** in $CDCl_3$. Upon addition of **1**, the resonance for the 6-OH proton moved downfield and those for the 1-H, 3-OH, and 4-OH protons moved upfield. The signal for the 2-OH proton was hardly influenced at all upon complexation. The spectral changes in the resonances of the β-Glc protons were similar to those of the β-Man protons. For β-Gal, the resonances associated with all these protons were shifted upfield. The values of CIS were linearly increased as the fraction of the ligand complexed with the receptor was increased as shown in Figure 4, and the CIS values for the complex are determined by extrapolation to 100% complexation and listed in Tables 1 and 2 Similarly, the values of CIS of β-Glc, β-Man, and β-Gal by receptor **2** were determined, and are listed in Table 3.

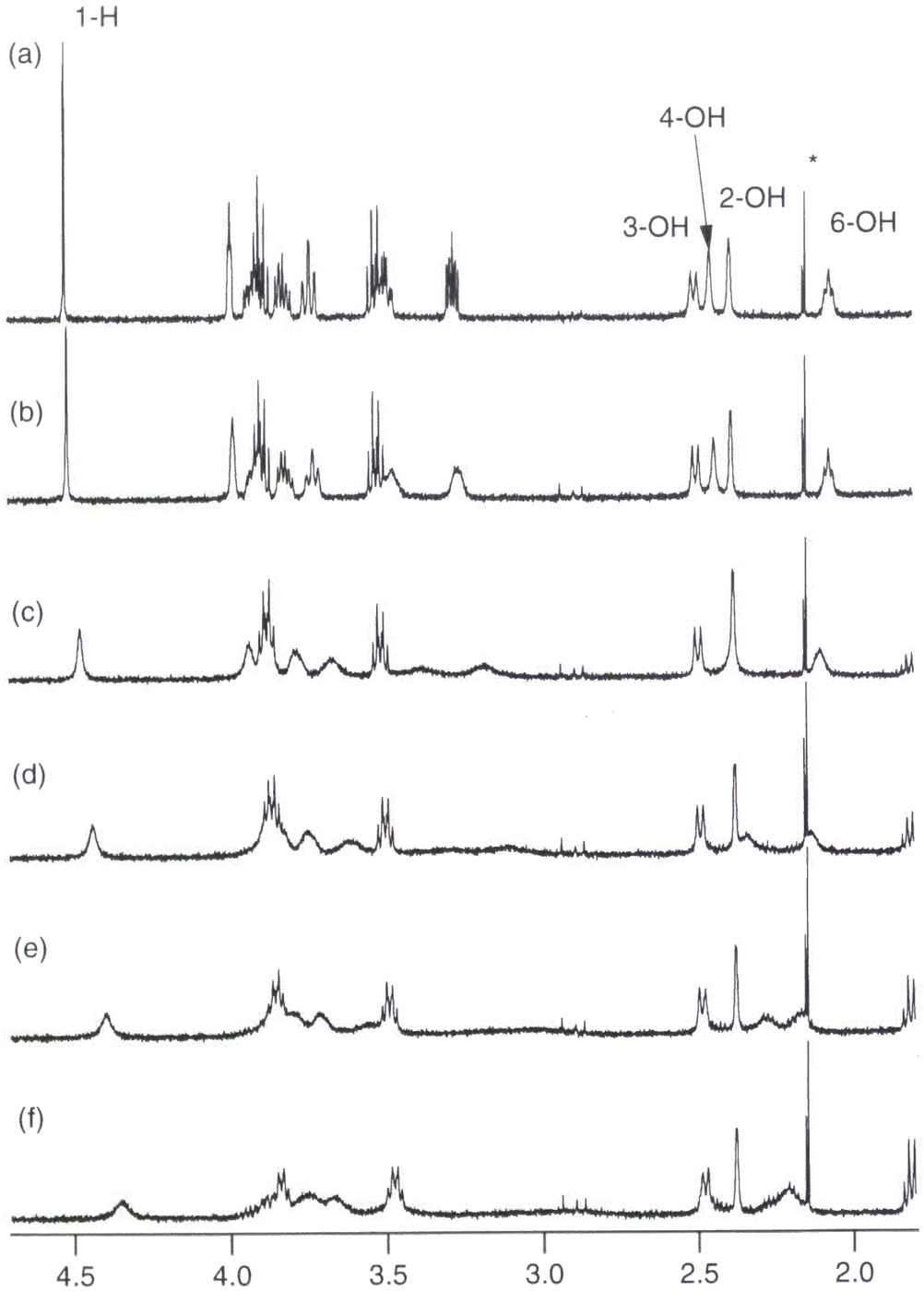

Figure 3. The ^{1}H NMR spectra of $CDCl_3$ solutions of β-Man in the presence of receptor **1** at 25 °C. (a) 0%, (b) 0.4%, (c) 2.5%, (d) 4.7%, (e) 6.8%, and (f) 8.9% of β-Man was complexed with receptor **1**.

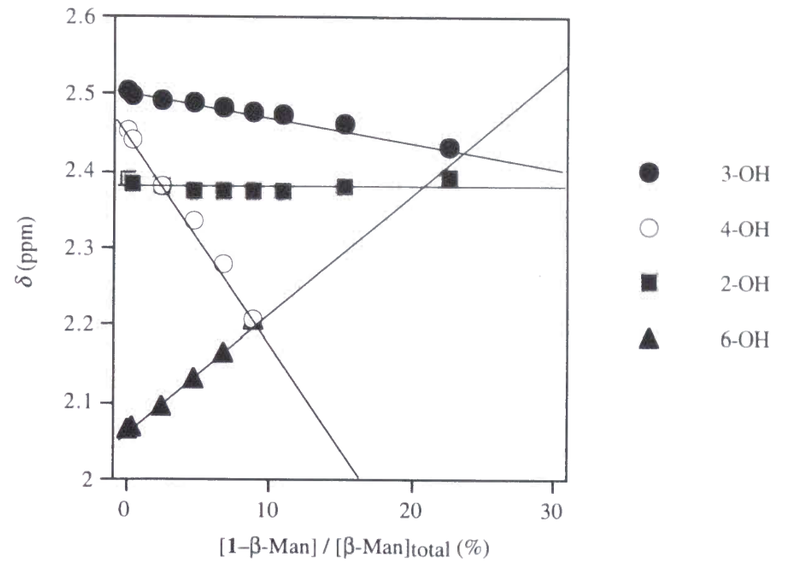

Figure 4. Plot of chemical shifts of β-Man against the fraction of β-Man complexed with receptor **1**.

Table 1. ^{1}H NMR Complexation-Induced Shifts (CIS, $\Delta\delta$/ppm) of β-Man, β-Glc and β-Gal upon Addition of **1** in $CDCl_3$ at 25 °C.[a]

	$\Delta\delta$/ppm (δ of free ligand/ppm)		
	β-Man	β-Glc	β-Gal
1-H	–2.1 (4.53)	–1.8 (4.29)	–3.8 (4.25)
2-OH	0.0 (2.38)	–0.1 (2.38)	–0.9 (2.37)
3-OH	–0.3 (2.50)	–1.5 (2.63)	–2.6 (2.60)
4-OH	–2.7 (2.45)	–2.2 (2.52)	–0.5 (2.76)
6-OH	+1.6 (2.06)	+1.2 (1.97)	–0.5 (2.08)

[a] Extrapolated to 100% complex from the CIS values at 0–25% complexation. Signal assignments were made based on the ^{1}H-^{1}H COSY or PDQF experiments.

Table 2. ^{1}H NMR Complexation-Induced Shifts (CIS, $\Delta\delta$/ppm) of α-Man, α-Glc and α-Gal upon Addition of **1** in $CDCl_3$ at 25 °C.[a]

	$\Delta\delta$/ppm (δ of free ligand/ppm)		
	α-Man	α-Glc	α-Gal
1-H	–1.6 (4.83)	–1.5 (4.85)	–2.2 (4.94)
2-OH	+0.9 (2.20)	+0.3 (1.96)	+0.6 (1.88)
3-OH	–1.8 (2.40)	–2.2 (2.52)	–3.4 (2.52)
4-OH	–2.4 (2.36)	–2.0 (2.44)	–1.7 (2.79)
6-OH	+1.4 (1.99)	+0.4 (1.88)	+0.5 (2.20)

[a] Extrapolated to 100% complex from the CIS values at 0–25% complexation. Signal assignments were made based on the ^{1}H-^{1}H COSY or PDQF experiments.

Table 3. ^{1}H NMR Complexation-Induced Shifts (CIS, $\Delta\delta$/ppm) of β-Man, β-Glc, and β-Gal upon Addition of **2** in $CDCl_3$ at 25 °C.[a]

	$\Delta\delta$/ppm (δ of free ligand/ppm)		
	β-Man	β-Glc	β-Gal
1-H	–1.0 (4.53)	–1.2 (4.29)	–1.5 (4.24)
2-OH	–0.3 (2.38)	–0.4 (2.36)	–1.3 (2.35)
3-OH	–0.3 (2.47)	–1.4 (2.60)	–0.8 (2.58)
4-OH	–2.0 (2.42)	–2.2 (2.48)	–0.6 (2.75)
6-OH	+0.3 (2.03)	+0.2 (1.95)	+0.1 (2.06)

[a] Extrapolated to 100% complex from the CIS values at 0–25% complexation. Signal assignments were made based on the ^{1}H-^{1}H COSY experiments.

Induced Circular Dichroism Study of Binding. Induced circular dichroism was observed in the Soret band of porphyrin receptors for some combinations of receptors and ligands. In Figure 5, the CD spectra of the **1**–β-Man complex and the

1–β-Glc complex are shown. Although both of β-Glc and β-Man were strongly bound to receptor **1**, the two ICD spectra were quite different. The **1**–β-Man complex showed biphasic Cotton effects (Figure 5a) while the **1**–β-Glc complex showed very weak Cotton effects (Figure 5b). Table 4 summarizes the values of $\Delta\varepsilon$ for each complex, where the CD spectra were recorded under the conditions that 30% to 95% of receptor was complexed, and the values of $\Delta\varepsilon$ were corrected for the fractions of complexed porphyrin receptors. The ICD patterns induced in **1**–**3** by α-anomers were similar to those by β-anomers for Glc, Man, and Gal. The signal intensities of the ICD of **1** decrease in the order, Man >> Gal > Glc. High affinity for Glc and the very small Cotton effects induced by it are indications that the intensity of Cotton effects is not related to the binding affinity. The different ICD between Man and Glc indicates that the stereochemistry at C-2 carbon has significant effects on the ICD. In order to further investigate the effects of substituents at C-2 on the ICD, the CD spectrum of the 2-*O*-Me-α-Man was recorded. Interestingly, the Cotton effects were nearly diminished ($|\Delta\varepsilon| < 5$). Although receptors **3** and **4** showed weak affinity for the ligand, some complexes showed Cotton effects with comparable intensity to those of the **1**–Man complex. For instance, the receptor **3**–Glc complex showed distinct Cotton effects even though the binding was weak.

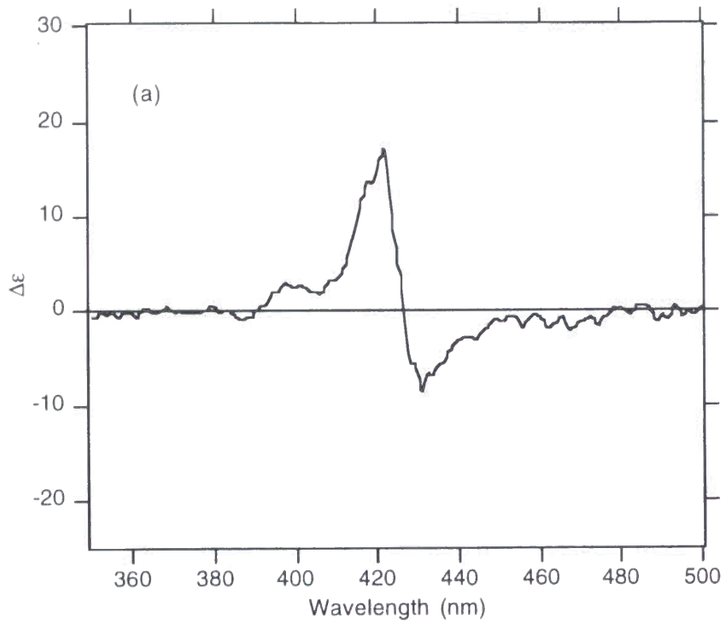

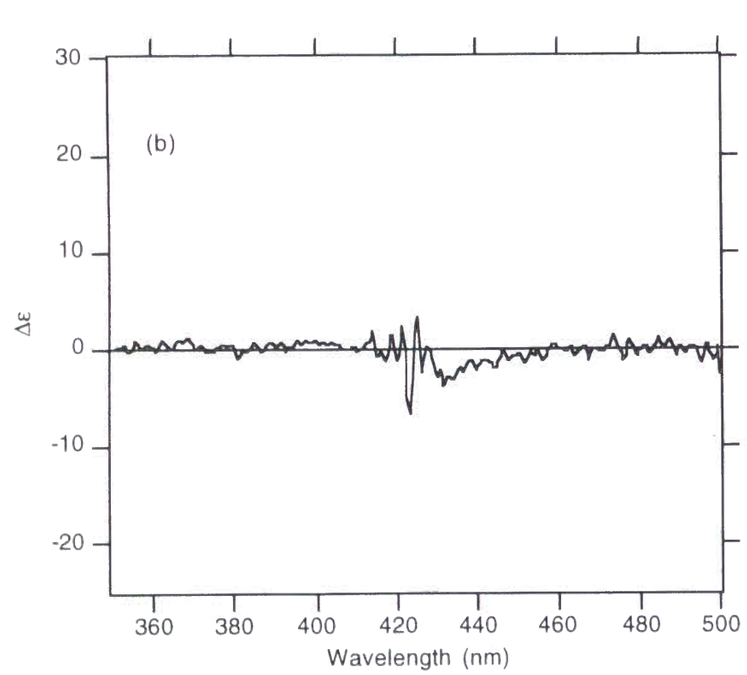

Figure 5. Circular dichroism induced in receptor **1** by (a) β-Man, and (b) β-Glc in $CHCl_3$ at 15 °C. [**1**] = 6.51×10^{-6} M, [β-Man] = 5.36×10^{-3} M, [β-Glc] = 1.22×10^{-2} M.

Table 4. Differential Dichroic Absorption ($\Delta\varepsilon$) of Receptor–Carbohydrate Complexes in Chloroform at 15 °C.

	$\Delta\varepsilon/cm^{-1}M^{-1}$, (wavelength/nm)				
Ligand	receptor **1**	receptor **2**	receptor **3**	receptor **4**	receptor **5**[b]
α-Glc	a	–8 (423)	18 (418)	18 (418)	a
			–18 (428)	–9 (433)	
β-Glc	a	–8 (425)	20 (420)	5 (420)	a
			–10 (430)	–3 (435)	
α-Gal	a	a	a	11 (420)	a
β-Gal	a	a	a	–5 (420)	a
α-Man	22 (420)	6 (416)	18 (418)	–13 (428)	a
	–26 (426)	–13 (427)	–24 (438)		
β-Man	18 (422)	7 (416)	17 (418)	–5 (420)	a
	–6 (432)	–6 (427)	–12 (436)		
2-*O*-Me-α-Man	a	a	–10 (410)	–19 (417)	
			13 (421)		

[a] $|\Delta\varepsilon| < 5$ in 400–450 nm. [b] ZnTPP.

The CD spectra were also recorded for some of the complexes at low temperatures down to –60 °C in $CHCl_3$. The Cotton effects for both the receptor **1**–α-Man complex and the receptor **1**–α-Glc complex were increased with lowering the temperature. The CD spectra for these complexes are shown in Figure 6. The **1**–α-Glc complex exhibited biphasic Cotton effects at –60 °C similar to those of the **1**–α-Man complex. The **1**–β-Glc complex also exhibited similar biphasic ICD at –60 °C (data not shown). Both the **1**–α-Gal complex and the **1**–β-Gal complex showed biphasic Cotton effects at –60 °C with an opposite sign (negative Cotton effects at 414 nm and positive Cotton effects at 421 nm).

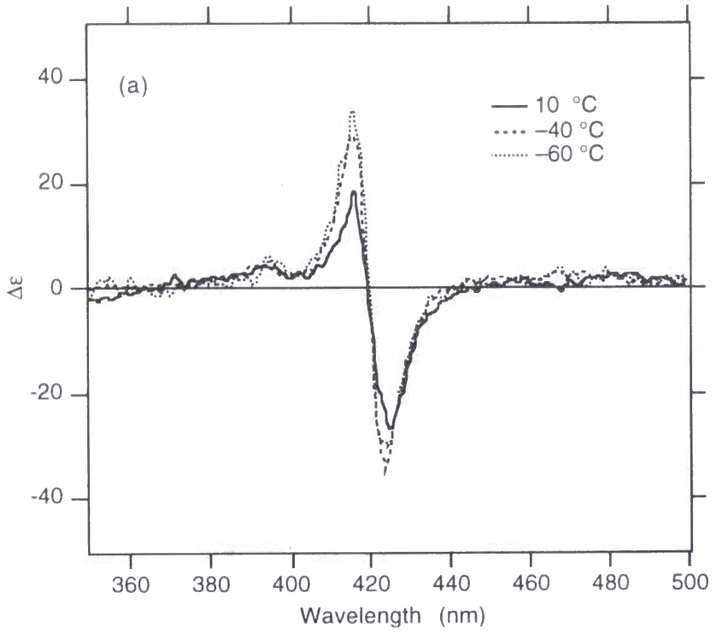

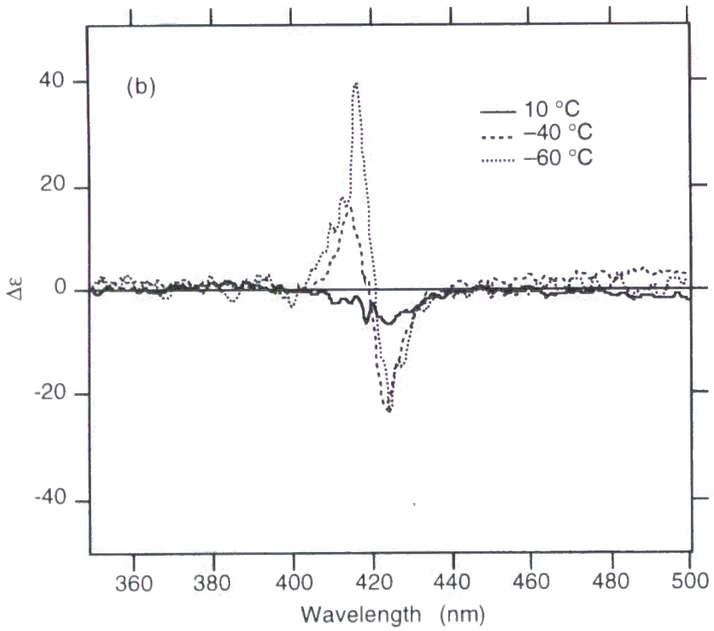

Figure 6. Circular dichroism induced in receptor **1** by (a) α-Man and by (b) β-Glc at 10, –40, and –60 °C in $CHCl_3$. (a) [**1**] = 5.21×10^{-6} M, [α-Man] = 6.31×10^{-3} M, (b) [**1**] = 5.21×10^{-6} M, [α-Glc] = 1.87×10^{-3} M.

The effects of added alcohols on the induced CD of the receptor–ligand complexes were examined. For most of the complexes examined, effects of the additives on the ICD were too small to observe. In the complex between **3** and β-Glc, however, the values of $|\Delta\varepsilon|$ at 427 nm distinctly increased with increasing the *tert*-butyl alcohol concentrations up to 7 mol% (Figure 7). Since the binding constants were decreased beyond 1.5 mol% of *tert*-butyl alcohol, the signal intensity of ICD was increased in the concentration range where the binding constants were decreasing. These results indicate that *tert*-butyl alcohol did interact with the receptor-ligand complex and altered the interaction modes to some extent.

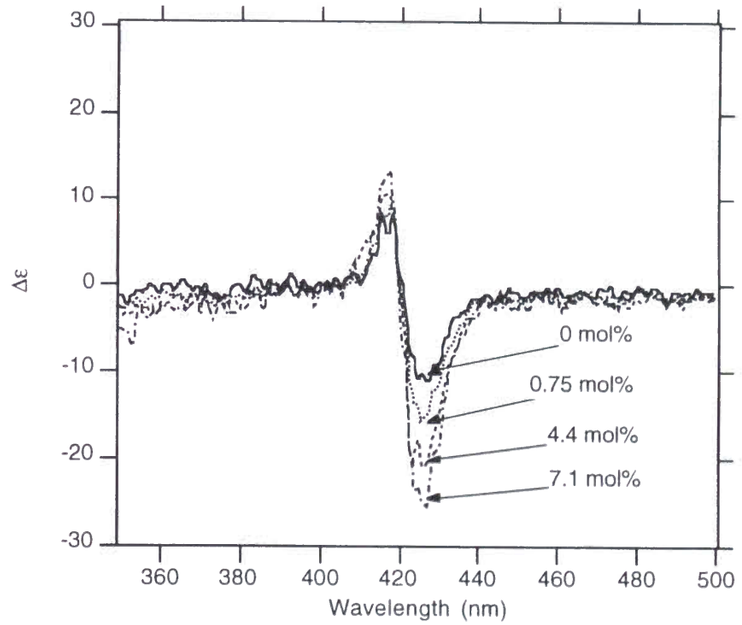

Figure 7. Circular dichroism induced in receptor **3** by β-Glc at 15 °C in $CHCl_3$–*tert*-butyl alcohol solution. [**1**] = 6.21×10^{-6} M, [β-Glc] = 1.15×10^{-2} M.

Discussion

NMR Study for Determination of Interacting Hydroxy Groups. Since receptor **1** has three interaction sites while the pyranoside ligands have four OH groups, it is important to determine which OH groups directly interact with the receptor. The ^{1}H NMR chemical shift displacements for carbohydrate OH protons induced by complexation with porphyrin receptors were found to provide valuable information. Two opposing anisotropic effects should be taken into account to interpret the CIS values of ligand upon complexation with porphyrin receptors: an upfield shift due to the ring current of porphyrin when the ligand proton is located above the porphyrin plane in the center, and a downfield shift of the OH protons upon hydrogen bonding. Effects of the ring current of quinolyl groups were estimated to be small except for the hydrogen bonding protons to the quinolyl nitrogen, based on the isoshielding map.[1]

Table 1 indicates that Man and Glc show similar patterns of the sign of the CIS values, while Gal shows a different trend. The resonance for the 6-OH proton was shifted downfield and that for the 4-OH proton was shifted upfield for both Man and Glc. These CIS values indicate that it is indeed the 4-OH group that is coordinated to the zinc, and the 6-OH group that is hydrogen bonded to the quinolyl nitrogen (see Figure 8). In this hydrogen bonding network, an alternating charge arrangement, Zn(δ+)–4O(δ–)–4*O*-H(δ+)–6O(δ–)–6*O*-H(δ+)–N(δ–), is achieved, which particularly stabilizes the **1**–Man complex and the **1**–Glc complex. The X-ray crystallographic study of Ca^{2+}-dependent lectin showed that mannoside was bound via a hydrogen bonding network involving calcium, glutamate, and aspartate.[3] The binding mode of receptor **1** toward mannoside was thus similar, zinc in place of calcium and quinolyl groups in place of carboxylates.

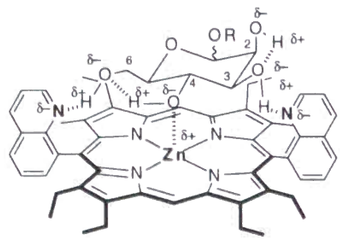

Figure 8. Schematic representation of hydrogen bonding networks of the receptor **1**–Man complex based on the ^{1}H NMR CIS values.

If the receptor **1**–Man (Glc) complexes adopt this bidentate binding mode,

then the 3-OH group is located close to the other quinolyl nitrogen, and can form a hydrogen bond to it. For Man, the 2-OH group can assist the intermolecular hydrogen bonding between the 3-OH group and the quinolyl nitrogen by the intramolecular hydrogen bonding to the 3-OH group as shown in Figure 8. Anslyn *et al.*[4] demonstrated the importance of intramolecular hydrogen bonding in polyols recognition, and pointed out that cis-cyclohexanediol forms stronger intramolecular hydrogen bonding than the trans diol. Therefore, the intramolecular hydrogen bonding between the 2-OH group and the 3-OH group of Man should be stronger than that of Glc. The resonance for the 3-OH proton of Man appeared downfield from that of Glc in the complex (Table 1). This is consistent with the intramolecular hydrogen bonding network shown in Figure 8, because the stronger hydrogen bonding between the 3-OH group of Man and the quinolyl nitrogen should cause greater downfield shift of this proton than the 3-OH proton of Glc. The CD spectroscopic studies at low temperatures also support the above discussion as described later. The higher affinity for Man than Glc can also be accounted for by this intramolecular hydrogen bonding.

The CIS patterns for Gal were different from those of Man and Glc with respect to the signs of CIS of the 6-OH resonance and the magnitude of CIS of the 4-OH resonance. The axial 4-OH in Gal should make the hydrogen bonding network shown in Figure 8 unfeasible. The upfield shift of the 6-OH group of galactose indicates that there was no strong hydrogen bonding between the 6-OH group and the quinolyl nitrogen in the complex. Among the OH protons of Gal, the greatest upfield shift was observed for the resonance of the 3-OH proton, rather than that of the 4-OH proton. This suggests that the 3-OH group was coordinated to the Zn.

Comparison of binding affinities to reference ligands **10**–**13** indicates that trans-1,2-dihydroxy moiety was favored over the cis moiety, and trans-1,2-(hydroxymethyl)hydroxy moiety favored over the cis moiety. The high affinity to Man and Glc with the 4-OH coordination to the zinc of receptor **1**, and the low affinity to Gal with the 3-OH coordination to the zinc are thus consistent with the affinity of **1** to the reference ligands.

Receptor **2**, the trans isomer of **1**, also showed characteristic CIS patterns. For both β-Man and β-Glc, the greatest upfield shifts were observed for the 4-OH resonances, thus suggesting that the 4-OH group was coordinated to the Zn. The difference in the CIS patterns of **2** from those of receptor **1** was that the downfield shifts of the 6-OH resonance were almost diminished, and the shifts of the 2-OH resonance and of the 3-OH resonance remained unchanged. Thus, the quinolyl nitrogen of **2** chose the 3-OH group rather than the 6-OH group of Man and Glc as a hydrogen bond donor.

Lewis Acid/Lewis Base Arrangements in Receptors and Ligands, and Neighboring Group Participation. The binding constants of 2-*O*-Me-α-Man for receptor **1** and receptor **2** were reduced by a factor of 30 to 40 compared to α-Man. The alkylation of the 2-OH group not directly involved in the hydrogen bonding interaction between receptor **1** and Man dramatically suppressed the binding. One can explain, however, this trend by assuming that the methoxy group prevents the original intramolecular hydrogen donation from the 2-OH group to the 3-OH group, and rather the lone-pair electrons of the 2-methoxy group have repulsive interaction with the developing negative charge on the 3-OH group upon hydrogen bonding to the quinolyl nitrogen. In the cases of receptors **3** and **4**, which have acidic OH groups in place of basic quinolyl nitrogen, the binding of 2-*O*-Me-α-Man was reduced only by a factor of at most 2 compared with α-Man. This different behavior of receptor **3** and receptor **4** also supports the above mechanism, that is, for receptor **1**, the combination of basic nitrogen and the 2-methoxy group next to the hydrogen bonding hydroxy group leads to significant destabilization of the complex.

A similar explanation is possible for the low affinity of **1** to galactosides. The ^{1}H NMR study showed that **1** recognized the trans vicinal hydroxy groups of Gal, *i.e.*, the 2-OH and 3-OH groups, by binding the 3-OH group via the zinc and the 2-OH group via the quinolyl nitrogen. Then the 1-octyloxy group comes next to the hydrogen bonding 2-OH group. The repulsion between this alkoxy group and the 2-OH group hydrogen bonded to the quinolyl nitrogen would lead to the low affinity for galactosides. These neighboring group effects are summarized in Figure 9. The OH group α to the hydrogen donating OH group assists the binding by neutralizing the negative charge on the oxygen upon hydrogen bonding, while the alkoxy group at the same position inhibits it by destroying the hydrogen bonding network.

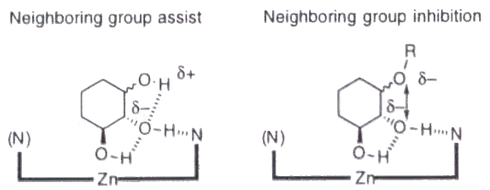

Figure 9. Common structural motif of Man, Gal, and 2-*O*-Me-α-Man interacting receptors **1** and **2**. Left: A neighboring OH group assists the binding by neutralizing the negative charge on the oxygen of the OH group hydrogen bonded to the quinolyl nitrogen. Right: A neighboring alkoxy group inhibits the binding by the negative charge repulsion between the lone pair electrons of the alkoxy group and the hydrogen bonding OH group.

The upfield shift of the 2-OH proton of β-Gal upon addition of **2** indicated that the 2-OH group was coordinated to the Zn. The 2-OH coordination of β-Gal rather than the 3-OH coordination can be ascribed to the neighboring group inhibition shown in Figure 9, where the 3-OH coordination would lead to the unfavorable geometry. These results suggest that Lewis acid/Lewis base combinations of receptors and ligands involving both directly interacting substituents and their neighboring substituents are important for the binding selectivity.

Comparison of Circular Dichroism Induced in Porphyrin Soret Band by Carbohydrates with that by Amino Acid Esters. Mizutani and Ogoshi have reported that chiral amino acid esters induced characteristic biphasic CD in the Soret band of porphyrin receptor upon ditopic binding.[2a] L-Amino acid esters consistently induced biphasic CD in the Soret band with positive Cotton effects at higher energy and negative Cotton effects at lower energy. They also pointed out the importance of the carbonyl chromophore in the induced CD.[2b] The relative orientation of the carbonyl group to porphyrin was suggested to determine the ICD pattern. In contrast to amino acid esters, carbohydrates have five chiral carbons, thus diverse patterns of ICD are expected. It was found that the patterns of the ICD again sensitively reflect receptor-ligand binding modes. The magnitudes of Cotton effects for carbohydrate complexes were comparable or weaker than those for amino acid ester complexes: the values of $|\Delta\varepsilon|$ of the ICD for the complexes between receptors **1**–**5** and carbohydrates were 0–26 $cm^{-1}M^{-1}$, while those for the complexes between trans isomer of **3**, [trans-5,15-bis(2-hydroxy-1-naphthyl)porphyrinato]zinc, and amino acid esters were 10–65 $cm^{-1}M^{-1}$.

Mechanism of Induced CD. The distinct biphasic CD induced in receptor **3** by Glc is contrasting with the weak CD signal induced in receptor **1** by the same ligand. Considering the small binding constant for receptor **3**–Glc complexes, this observation evidently indicates that the ICD reflects the interaction modes such as relative orientations of the ligand to the receptor and the number of stable receptor-ligand configurations, and not the binding affinity.

As shown in Table 4, the ICD patterns of complexes with receptor **2** were similar to those of the corresponding complexes with receptor **1**, although the magnitudes were reduced, showing that combination of zinc and only one quinolyl nitrogen was able to induce the observed ICD pattern, and the second quinolyl nitrogen in **1** had only secondary effects on the ICD. This is in accordance with the ^{1}H NMR CIS patterns, which also indicated that both **1** and **2** bind Glc and Man in a similar fashion via the 4-

HO···Zn coordination and the 3-OH···N hydrogen bonding. Among the zinc porphyrin–amino acid ester complexes, only ditopic binding (Zn···NH_2 and OH···O=C) lead to distinct biphasic ICD. The fact that both **1** and **2** showed similar ICD patterns for Man and Glc indicates that ditopic fixation of the ligand in a similar fashion (4-HO···Zn and 3-OH···N) would determine the ICD patterns.

It is noteworthy that α-Man and β-Man induced biphasic CD in **1**, while α-Glc and β-Glc induced very weak CD at 15 °C, although both carbohydrates were bound strongly to **1**. Thus, the stereochemistry at the C2 position had significant influence on the induced CD pattern and intensity. The ^{1}H NMR studies revealed that the 2-OH group of Man and Glc was not involved in the direct hydrogen bonding with receptors **1** and **2**. The different ICD between Man and Glc can be ascribed to the following two mechanisms: (1) the coupling of the local wavefunction of the 2-OH group with that of porphyrin causes the different ICD, and (2) the 2-OH group indirectly affects the binding mode to lead to the different ICD. One important observation for the mechanism of induced CD is that the receptor **1**–α-Glc complex showed only weak Cotton effects at 15 °C but distinct biphasic Cotton effects at –60 °C (Figure 6b). This ICD pattern was similar to that of the **1**–Man complex. Considering the similar ^{1}H NMR CIS patterns between the **1**–Man complex and the **1**–Glc complex, one can ascribe the weak ICD for the receptor **1**–α-Glc complex at room temperature to the thermal fluctuations. In contrast, the ICD of the **1**–Man complex was less sensitive to temperature (Figure 6a), possibly owing to the stronger 3-OH···N hydrogen bond.

If the hydrogen bonding network in the receptor **1**–Man complex as schematically depicted in Figure 8 is assumed, then the orientation of the O–H bond and the C–O bond would be fixed relative to the porphyrin. Any deviation of the orientation of the transition dipole moments from the 5-15 axis and the 10-20 axis would contribute to the CD and their sum would lead to the observed ICD if each contribution does not cancel each other. Figure 10 displays the geometry of the **1**–Man complex according to the molecular orbital calculations, in which one can see that the directions of these bonds are deviated from the axis. Although prediction of the bond directions is beyond the precision of the calculations, the figure suggests that the complex becomes optically active in terms of the directions of these bonds, provided that the ligand is fixed on the porphyrin plane.

These results evidently demonstrate that ICD is the powerful tool to probe the binding modes in the porphyrin-carbohydrate complexes such as ligand orientation and its fluctuation in the complex. It would be more powerful in investigation of polysaccharide recognition, where its ^{1}H NMR spectra are much more complicated and less useful for

probing receptor–ligand structures.

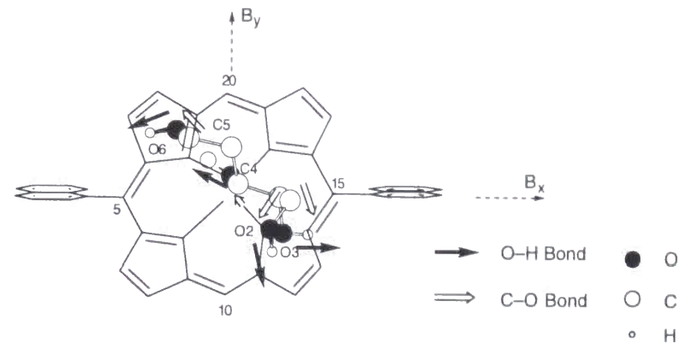

Figure 10. Directions of the C–O bonds and the O–H bonds of the 3-OH, 4-OH, and 6-OH groups for the receptor **1**–β-Man complex. The geometry is based on the PM3 calculations where Zn of receptor **1** is replaced by Al and the ethyl groups by hydrogen. In the figure, hydrogens are omitted for clarity except for the OH protons. C1 and O5 of the ligand are also omitted.

Induced CD Probing Binding Modes. Following examples display that the receptor-ligand interaction modes are deduced from their ICD spectra.

(1) The ICD patterns of α-Man and 2-*O*-Me-α-Man were similar for **4**, while they were different for **1** and **3**. Particularly, the signs of the CD induced in receptor **3** by α-Man were reversed of that induced by 2-*O*-Me-α-Man. Therefore, one can expect that the binding mode of the **3**–α-Man complex is different from that of the **3**–2-*O*-Me-α-Man complex.

(2) It is interesting to note the differences in ICD between α-anomers and β-anomers: the patterns of CD induced by the α-anomers in **1**, **2** and **3** were similar to those induced by the corresponding β-anomers, while those induced by α-anomers in **4** were different from those induced by the corresponding β-anomers. Particularly, the opposite sign of the Cotton effects of **4**–α-Gal to that of **4**–β-Gal indicates that α-Gal and β-Gal were bound to **4** in a different fashion. Therefore, the stereochemistry at C1 did not affect the ICD of **1**–**3**, while it affected the ICD of **4**. Although the binding constants by **4** of α-anomers were similar to those of β-anomers, the binding mode was different, possibly due to the longer distance between the zinc atom and the OH group in **4**.

(3) The ICD signals of **3**–*β*-Glc complex grew with increasing *tert*-butyl alcohol concentrations. This means that *tert*-butyl alcohol did interact with the complex to stabilize it.

Conclusions

The ^{1}H NMR and circular dichroism study, combined with the comparison of the affinity for a series of receptors and ligands, revealed that receptor **1** with an excellent carbohydrate binding pocket recognized the trans, trans-1,2-dihydroxy-3-(hydroxymethyl) moiety of carbohydrate through the zinc site and two quinolyl sites. Receptor **2**, in which only one quinolyl nitrogen and zinc can interact with ligands, the 1,2-trans-dihydroxy moiety was preferentially recognized. The patterns of induced CD parallel those of the CIS in the ^{1}H NMR spectra, suggesting that ICD was a facile probe to elucidate the binding mode. Variable temperature CD study demonstrated that Glc was fluctuating in receptor **1** at 15 °C, while Man was comparatively fixed in the binding pocket of **1** even at 15 °C. Low affinity of **1** for 2-*O*-Me-α-Man, α-Gal, and β-Gal suggests that the neighboring alkoxy group has considerable inhibitory effects on the binding. The intramolecular and intermolecular hydrogen bonding networks formed in the binding pocket markedly affected the selectivity of binding, and their control is the key to the design of receptor for carbohydrates.

Experimental Section

Instrumentation. ^{1}H NMR and ^{13}C NMR spectra were recorded using a JEOL A-500 spectrometer in chloroform-*d* and DMSO-d_6, respectively. ^{1}H NMR chemical shifts in $CDCl_3$ were referenced to $CHCl_3$ (7.24 ppm) and ^{13}C NMR chemical shifts in DMSO-d_6 were reported relative to DMSO (39.5 ppm). UV–vis spectra were recorded on a Hewlett-Packard 8452 diode array spectrometer equipped with a thermostatted cell compartment. Circular dichroism spectra were recorded on either a JASCO J-600 or a JASCO J-720 spectropolarimeter. A cryostat (Oxford, DN1704) was used for CD spectral measurements at low temperatures. Mass spectra were obtained using a JEOL JMS SX-102A mass spectrometer.

Materials. $CHCl_3$ containing amylenes as a stabilizer was purchased from Aldrich (A.C.S. HPLC grade, 99.9%, stabilized with amylenes) and was used as received. HPLC-grade water and spectrophotometric-grade methyl alcohol were used as received. *tert*-Butyl alcohol was dried by refluxing with, and distilling from sodium. *p*-Nitrophenol, phenol, *p*-methoxyphenol, and *p*-dimethoxybenzene were completely dried under reduced pressure just before use and their purity was checked by elemental analysis to avoid the influence by water contamination.

UV–Vis Titrations. Binding constants were determined by UV–vis titrations. To avoid the influence by the ethanol added as a stabilizer to chloroform, amylene-containing chloroform was used throughout the study. The water concentration was estimated to be about 0.002% from ^{1}H NMR. The atropisomerization from the cis isomer (**1**) to the trans isomer (**2**) in a $CDCl_3$ solution occurred slowly: 5 % of **1** was isomerized to **2** at room temperature for 100 h although no isomerization was observed in the solid state. Therefore the receptor solution was prepared just before use. Cis to trans isomerization in receptors **3** and **4** was too slow to observe.

The details of the determination of the binding constant are as follows. To *ca.* 5×10^{-6} M of **1**, **2**, **3**, **4**, or **5** in $CHCl_3$ was added a stock solution of carbohydrate ligands in $CHCl_3$ at 15 °C. The changes in absorbance at around 424 nm in the Soret band were monitored at eight different concentrations of carbohydrate, with volume change due to carbohydrate addition being taken into account during analysis. Assuming 1:1 complexation, the binding constants were evaluated by least square parameter estimation based on the Damping Gauss-Newton method. Calculated curves were well

fitted to absorbance changes.

It was reported that glycopyranosides aggregate when dissolved in organic solvent at a high concentration.[5] The UV-vis titration experiments of **1** and **2** were performed in the low concentration range of the ligands, where no aggregation occurs. In the case of the binding of Man by receptors **3** and **4**, at the highest concentration of Man, aggregation occurred. However the standard deviations of binding constants of these receptor-ligand complexes were 6-10 %, comparable to those for other complexes, showing that the errors owing to the ligand aggregation were negligibly small.

^{1}H NMR Study of Binding. $CDCl_3$ was completely deacidified by passing through alumina (basic, activity super 1, ICN) just before use. To 0.3 – 0.8 mM of carbohydrate in $CDCl_3$ was added a stock solution of **1** or **2** in $CDCl_3$ at 25 °C and the complexation-induced shifts of signals for carbohydrates were recorded. The concentration of **1** or **2** was kept considerably low ($[H\text{-}G] / [G]_{total} < 20\%$) to avoid signal broadening. The CIS values were determined by extrapolating the chemical shift to 100 % complex, based on the concentrations of the complex calculated from K determined by UV-vis titration.

References and Notes

1 Johnson, C. E. J.; Bovey, F. A. *J. Chem. Phys.* **1958**, *29*, 1012.

2 (a) Mizutani, T.; Ema, T.; Yoshida, T.; Kuroda, Y.; Ogoshi, H. *Inorg. Chem.* **1993**, *32*, 2072. (b) Mizutani, T.; Ema, T.; Yoshida, T.; Renné, T.; Ogoshi, H. *Inorg. Chem.* **1994**, *33*, 3558.

3 Weis, W. I.; Drickamer, K.; Hendrickson, W. A. *Nature* **1992**, *360*, 127.

4 Huang, C.-Y.; Cabell, L. A.; Anslyn, E. V. *J. Am. Chem. Soc.* **1994**, *116*, 2778.

5 Bonar-Law, R. P.; Sanders, J. K. M. *J. Am. Chem. Soc.* **1995**, *117*, 259.

Chapter 3

Effect of Intramolecular Hydrogen-Bonding Network on the Relative Reactivities of Carbohydrate OH Groups

Abstract

Toward the development of enzyme-like catalysts for regioselective functionalization of unprotected sugars, DMAP-catalyzed acetylation of unprotected carbohydrates in chloroform was investigated. Product distributions of monoacetylated sugars were determined under kinetic control. To accurately evaluate the relative reactivity of each OH group, reaction conditions were used under which only monoacetylated sugars were obtained and almost no diacetylated sugars were formed as by-products. Systematic acetylation experiments of glucose, mannose, and galactose revealed the decisive role of intramolecular hydrogen-bonding networks among carbohydrate OH groups. The relative reactivities in the DMAP-catalyzed acetylation were successfully correlated with the calculated proton affinity of each OH group in carbohydrates.

Introduction

Biological functions of oligosaccharides depend not only on the sequence of sugar residues but also on the position where the next sugar residue is attached.[1] In order to construct diverse oligosaccharides with biological functions such as cell recognition, Nature has developed enzymes called glycosyltransferases which introduce sugar residues regiospecifically to a particular position. These enzymes have been effectively utilized to prepare complex oligosaccharides in the laboratory.[2] However, exactly how glycosyltransferases activate one particular hydroxy group among many other OHs of similar reactivity is shrouded in mystery. It is one of the big challenges for chemists to understand the chemical nature of this fascinating enzyme reaction.

In the field of synthetic organic chemistry, the efficient synthesis of oligosaccharides is still under active investigation.[3] However, most research projects have mainly focused on the control of the anomer stereochemistry, and the control of regiochemistry is usually achieved by multiple protection–deprotection procedures. A protection–deprotection strategy in synthetic carbohydrate chemistry was highlighted in the preparation of oligosaccharide libraries from one monosaccharide unit as a core.[4] Difficulties arising from similar reactivities of OH groups were overcome by using a designed building block containing four selectively removable protecting groups as acceptors for glycosidation. Another approach to the control of regiochemistry of carbohydrate OH groups is metal-assisted activation of OH groups. For this purpose, organotin derivatives[5a] have been studied for a long time and recently organoboron derivatives[5b] have been utilized.

Without the help of enzymes it is usually extremely difficult to directly functionalize a desired OH group of unprotected carbohydrates except for the primary OH groups. In addition, many studies have shown that OH groups in unprotected carbohydrates often exhibit anomalous reactivity.[6] Especially in the case of oligosaccharides and nucleosides, the electrophile functionalizes exclusively at the secondary hydroxy group instead of the usually more reactive primary one.[6,7] For a complete understanding of unusual reactivities of carbohydrate OH groups, Krepinsky, Csizmadia and co-workers reported a series of studies on reduced reactivities of the primary 5'-OH group of nucleosides, which are generally observed in the reaction with various electrophiles.[8] They pointed out the presence of the strong intramolecular hydrogen bonding between the 5'-OH group and the heteroaromatic system in their simple model system by *ab initio* calculations. They proposed that strong intramolecular

hydrogen bonding might prevent hydrogen abstraction. Brewster *et. al.*[9a] and Houdier and Pérez[9b] reported theoretical investigations of the relative reactivities of oligosaccharide OH groups in compounds such as β-maltose and sucrose. They evaluated the acidities of OH groups by semi-empirical calculations and found a moderate correlation with the increased reactivity of the 2-OH group. They proposed a key role for intramolecular hydrogen bonds of some kind. On the other hand, a systematic survey on the reactivity of simple monosaccharides is quite rare, although each monosaccharide was investigated by different researchers under different reaction conditions and procedures.[6] According to these results, primary 6-OH groups were functionalized far more preferentially than were other, secondary OH groups. The reactivity orders of secondary OH groups were not determined without ambiguity. It is often said that an equatorial OH group in a six-membered ring system can be functionalized preferentially in the presence of secondary axial partners, but it has been repeatedly pointed out that the relative reactivities of monosaccharide OH groups are highly dependent on the reaction conditions employed. To his best knowledge, no intensive effort has been made to clarify the relative reactivities in terms of monosaccharide structures.

The ultimate objective is to construct enzyme-like catalysts which introduce substituents regioselectively to a desired OH group through noncovalent interactions. Recently, chiral nucleophilic catalysts for kinetic resolution of racemic alcohols have been actively studied. In some of these examples, enzyme-like chiral cavities were constructed around DMAP, 4-pyrrolidinopyridine or imidazole to promote enantioselective acylation.[10] This strategy can be applied to regioselective acylation of carbohydrates through noncovalent bonding by providing a carbohydrate recognition site for the nucleophilic catalysts (Figure. 1). In this context, investigation of DMAP-catalyzed acetylation of unprotected carbohydrates was initiated. Unexpectedly, it was found that secondary OH groups of glucose were preferentially acetylated in the presence of the primary OH group at position 6. Sterically unhindered primary OH groups at position 6 are supposed to be acetylated far more readily according to the usual stereochemical analysis. In deed, many reactions are known to derivatize selectively the primary alcohols of carbohydrates.[11]

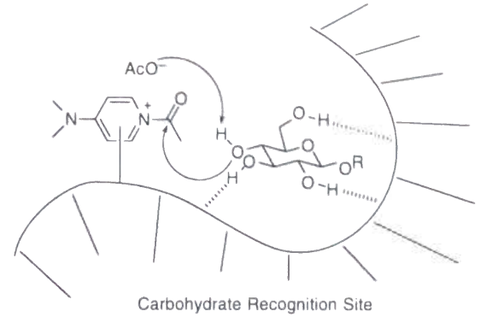

Figure 1. Schematic representation of regioselective acetylation of carbohydrates through noncovalent interactions.

In order to clarify operating forces which determine the selectivity in the DMAP-catalyzed acetylation system, the author conducted systematic acetylation experiments of glucose, mannose, and galactose and discussed structure–reactivity relationships in detail. In Chapter 3, the author addresses the decisive role of an intramolecular hydrogen-bonding network among neighboring OH groups in the relative reactivities of carbohydrate OH groups.

Results

Reaction Conditions for DMAP-Catalyzed Acetylation. The following three points are important to accurately evaluate the relative reactivities of carbohydrate OH groups. (1) Non-hydrogen-bonding, non-polar solvents should be used in which hydrogen bonding is effective. (2) Introduction of more than two acetyl groups should be suppressed because both analysis of reaction mixtures and interpretation of obtained results become markedly difficult. (3) Neutral, mild reaction conditions and a short reaction period should be employed to avoid acetyl-group migration that gives thermodynamically stable regioisomers.

The reaction conditions shown in Scheme 1 were adopted. Chloroform was used as a non-polar solvent that readily dissolves various organic compounds. To solubilize highly hydrophilic carbohydrates in chloroform, a long alkyl chain was introduced onto the anomeric OH group. It is well known that carbohydrates solubilized in non-polar solvents form aggregates at high concentrations.[12] So reactions were carried out tentatively at 2 mM to minimize the effect of aggregation (for a detailed examination of the effect of the monosaccharide concentration, see below). To bind liberated acetic acid, K_2CO_3 was used because soluble bases might disturb hydrogen bonding. By use of 5 mol% of DMAP, acetic anhydride was completely consumed in 1 h.

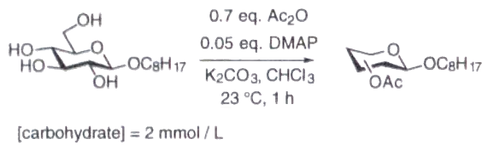

Scheme 1

Determination of the Product Distribution. Regioisomeric mixtures obtained by acetylation were analyzed according to the procedure described below. (1) DMAP was removed by passage through a short silica gel column. (2) The crude product was dried in vacuo at 60 °C for 4 h. (3) The yield of each regioisomer was determined by integration of the corresponding acetyl group at $\delta \sim 2.1$ in the ^{1}H NMR spectrum (Figure 2b). In Figure 2a is shown the ^{1}H NMR spectrum of the reaction mixture before passage through a short silica gel column. Comparison of Figure 2b with Figure 2a indicated that no isomerization took place upon a silica gel short column

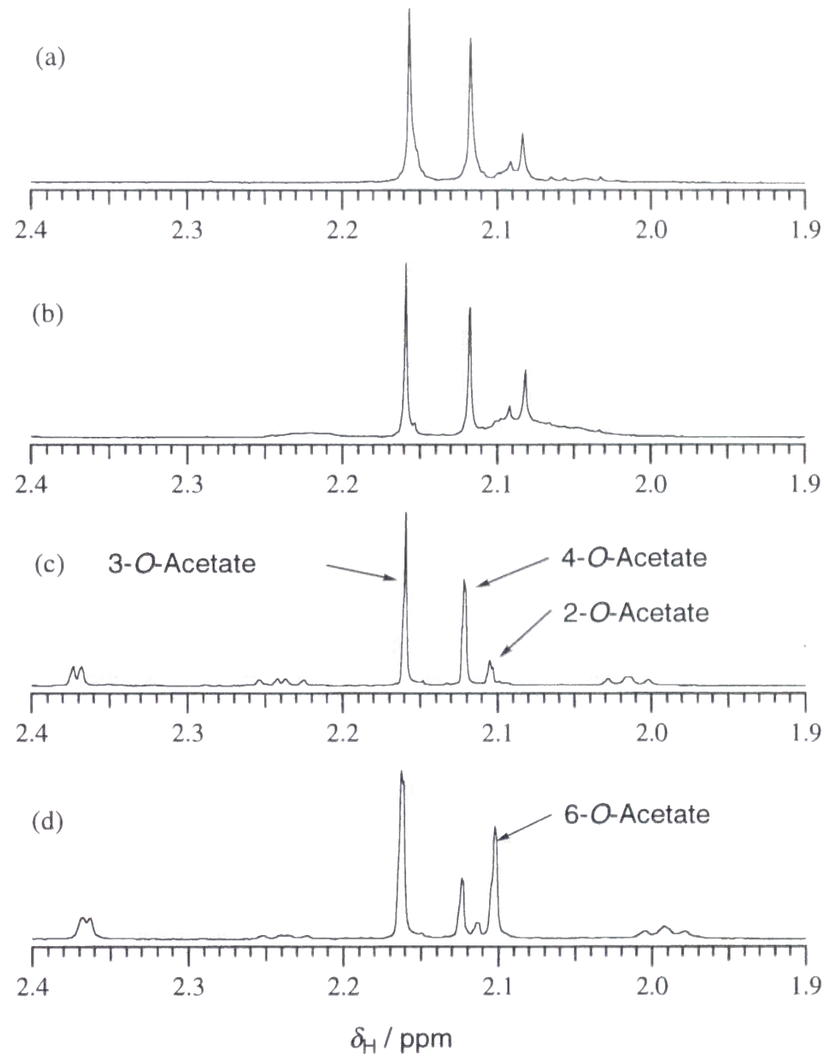

Figure 2. ^{1}H NMR spectra of the reaction mixture and partially purified samples in the DMAP-catalyzed acetylation of octyl β-D-glucopyranoside. (a) Before silica gel short column. (b) After silica gel short column. (c) One of GPC fractions containing octyl 2-, 3- and 4-*O*-acetyl-β-D-glucopyranoside. (d) One of the GPC fractions containing octyl 6-*O*-acetyl-β-D-glucopyranoside.

operation. (4) Next, the crude product was separated into two fractions by gel-permeation chromatography (GPC) to characterize each regioisomer (Figure 2c, 2d). Structural characterization of each regioisomer was done mainly by Double-Quantum Filtered COSY (DQF-COSY). Two major regioisomers formed were identified as the 3- and 4-*O*-acetate as shown in Figure 2. Unexpectedly, 3- and 4-acetylated glucopyranosides were formed in much higher yields in the presence of the primary 6-OH group.

As shown in Figure 2, all major signals at $\delta \sim 2.1$ were assigned to monoacetyl glucopyranosides. It should be noted that no diacetylated product was formed at all.

Relative Reactivities of OH Groups in Glucose, Mannose, and Galactose. The same acetylation conditions were applied to glucose, mannose, and galactose to investigate the stereochemical effect on the relative reactivities of carbohydrate OH groups. Product distributions were determined in exactly the same manner. The results are summarized in Table 1. Every acetylation experiment was repeated twice to confirm the reproducibility.

Intriguing trends were observed. In all cases, 2-OH groups were found to be least reactive, irrespective of the stereochemistry of the 2-OH group and the neighboring anomeric position. The product ratio of 6-*O*-acetylated sugars increased in the order glucose < mannnose < galactose. Total yields of monoacetyl-mannoses and -galactoses were decreased compared with monoacetylglucoses under exactly the same reaction conditions, suggesting that reactivities of secondary OH groups were considerably suppressed in the case of mannose and galactose. The author would like to point out several other interesting observations on the stereochemical effect. Comparison between glucose and mannose showed that the stereochemistry of the 2-OH apparently affected the reactivity of the distant 6-OH group. In the case of glucose, the stereochemistry of the anomeric position affected the relative reactivities of the 3- and 4-OH groups whereas both anomers of mannose and galactose exhibited similar reactivities. The relative reactivity of the 6-OH group in galactose was considerably increased compared with glucose, which was caused by the inversion of the stereochemistry of the 4-OH group.

Table 1 DMAP-Catalyzed Acetylation of Monosaccharides.[a]

Substrate	Product Ratio (Yield of One Regioisomer/Total Yield)				
	2-*O*-Acetate	3-*O*-Acetate	4-*O*-Acetate	6-*O*-Acetate	Total Yield (%)[b]
Octyl β-Glc	0.02	0.42	0.37	0.19	quant.
Octyl α-Glc	c	0.25	0.61	0.14	98
Octyl β-Man	c	0.22	0.46	0.32	72
Octyl α-Man	0.07	0.16	0.40	0.37	75
Octyl β-Gal	c	0.16[d]	0.14[d]	0.70	81
Octyl α-Gal	c	0.14[d]	0.28[d]	0.58	73

[a] Reaction conditions are shown in Scheme 1. [b] NMR yield relative to Ac_2O. [c] Not detected. [d] Product ratio could not be determined accurately due to poor separation of signals.

Possibility of Acetyl Migration. Surprisingly, secondary 3- and 4-OH groups of glucopyranosides were acetylated more readily than were the primary 6-OH groups. One possible explanation for this unexpected result is as follows; An acetyl group was incorporated into the most reactive 6-OH first. The introduced acetyl group migrated intramolecularly to the neighboring 4-OH group and then to the 3-OH group by the action of DMAP. To check this possibility, 6-*O*-acetylated glucopyranoside was prepared independently and exposed to similar reaction conditions as shown in Scheme 2. No acetyl migration was observed and the possibility of acetyl migration was ruled out.

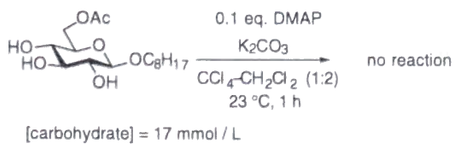

Scheme 2

Detailed Examinations of the Reaction Conditions. The reaction conditions employed in this study were examined thoroughly to find decisive factors for

observed selectivities. First, the concentration of carbohydrates was varied from 0.5 to 10 mM (Table 2). ^{1}H NMR dilution experiments showed that octyl β-D-glucopyranoside formed intermolecular hydrogen bonds with each other at ~ 10 mM in $CDCl_3$ at 22 °C.[12] Although a small amount of diacetylated glucopyranoside was formed at 10 mM, negligibly small differences in the product distribution were observed. So selectivity seems to originate chiefly in intramolecular forces, rather than intermolecular factors like aggregation. Next, the effect of DMAP was investigated (Table 3). In the presence of DMAP, product distributions were identical irrespective of the concentration of DMAP. In contrast, the 6-*O*-acetylated product was the major one in the absence of DMAP although the yield was very low. Interestingly, the product distribution in the absence of DMAP is closely similar to the reported selectivity of glucopyranosides.[6] *N*-Acetylpyridinium acetate, an effective acetylating reagent formed from DMAP and acetic anhydride, seems to be the key to the unique selectivity. The time dependence of the product distribution was next investigated. As shown in Table 4, product distributions did not change as a function of the reaction time. Together with the above consideration of the possibility of acetyl migration of independently prepared 6-*O*-acetylated glucopyranoside, this result suggests that acetyl migration is negligible in this reaction system and that the product distribution is determined under kinetic control. In Table 5 is shown the influence of an added bulky base, 2,6-dimethylpyridine (2,6-lutidine). No appreciable effect was observed for the distribution of each regioisomer. This means acidic elements in the reaction system, such as acetic anhydride or liberated acetic acid, do not participate in determining product distributions. In addition, the above result suggests the deprotonation step in the acetylation reaction does not affect product distributions. It is notable that operating forces are strong enough to maintain the unique selectivity by the addition of a considerable amount of base. Finally, K_2CO_3 was replaced by 2,6-lutidine (Table 6). No change was observed.

As demonstrated from the above investigation, the observed selectivity is not dependent on any element in the reaction conditions when the acetylation is catalyzed by DMAP. In the present reaction system, each regioisomer was kinetically produced irrespective of its thermodynamic stability. It was elucidated that the 3- and 4-OH groups are activated toward *N*-acetylpyridinium acetate compared with the primary 6-OH group without any outside assistance. For further discussion on reactivity–structure relationships it is important to note that intramolecular forces matter most in the present acetylation system. The unique selectivity seems to originate in the monosaccharide structure.

Table 2 Dependence of the Product Distribution on the Concentration of Octyl β-D-glucopyranoside in the DMAP-Catalyzed Acetylation of Octyl β-D-glucopyranoside.

	Product Ratio (Yield of One Regioisomer/Total Yield)				
[β -Glc][a] (mmol/L)	2-*O*- Acetate	3-*O*- Acetate	4-*O*- Acetate	6-*O*- Acetate	Total Yield (%)[b]
0.5	0.04	0.45	0.36	0.15	33
2.0	0.02	0.42	0.37	0.19	quant.
10[c]	0.10	0.37	0.32	0.21	91

[a] Other reaction parameters are shown in Scheme 1. [b] NMR yield relative to Ac_2O. [c] A small amount of diacetylated sugars was formed at this concentration.

Table 3 Dependence of the Product Distribution on the Concentration of DMAP in the DMAP-Catalyzed Acetylation of Octyl β-D-glucopyranoside.

	Product Ratio (Yield of One Regioisomer/Total Yield)				
[DMAP][a] (mol%)	2-*O*- Acetate	3-*O*- Acetate	4-*O*- Acetate	6-*O*- Acetate	Total Yield (%)[b]
0	0.21	0.19	0.14	0.46	4
1	0.06	0.51	0.32	0.11	53
5	0.02	0.42	0.37	0.19	quant.
10	0.09	0.41	0.36	0.14	quant.

[a] Other reaction parameters are shown in Scheme 1. [b] NMR yield relative to Ac_2O.

Table 4 Dependence of the Product Distribution on the Reaction Time in the DMAP-Catalyzed Acetylation of Octyl β-D-glucopyranoside.

	Product Ratio (Yield of One Regioisomer/Total Yield)				
Time[a] (*t*/h)	2-*O*-Acetate	3-*O*-Acetate	4-*O*-Acetate	6-*O*-Acetate	Total Yield (%)[b]
1	0.06	0.51	0.32	0.11	53
6	0.03	0.41	0.39	0.17	quant.
24	0.05	0.47	0.37	0.11	quant.

[a] 1 mol% of DMAP was used. Other reaction parameters are shown in Scheme 1. [b] NMR yield relative to Ac_2O.

Table 5 Effect of Added 2,6-Lutidine on the Product Distribution in the DMAP-Catalyzed Acetylation of Octyl β-D-glucopyranoside.

	Product Ratio (Yield of One Regioisomer/Total Yield)				
[Lutidine][a] (vol%)	2-*O*-Acetate	3-*O*-Acetate	4-*O*-Acetate	6-*O*-Acetate	Total Yield (%)[b]
0	0.02	0.42	0.37	0.19	quant.
2.6	0.04	0.45	0.37	0.14	quant.
11	0.02	0.46	0.36	0.16	56

[a] Other reaction parameters are shown in Scheme 1. [b] NMR yield relative to Ac_2O.

Table 6 Effect of K_2CO_3 on the Product Distribution in the DMAP-Catalyzed Acetylation of Octyl β-D-glucopyranoside.

	Product Ratio (Yield of One Regioisomer/Total Yield)				
Base[a]	2-*O*-Acetate	3-*O*-Acetate	4-*O*-Acetate	6-*O*-Acetate	Total Yield (%)[b]
K_2CO_3	0.02	0.42	0.37	0.19	quant.
2,6-lutidine[c]	0.05	0.44	0.37	0.14	97

[a] Other reaction parameters are shown in Scheme 1. [b] NMR yield relative to Ac_2O. [c] 5 Equiv. of 2,6-lutidine relative to octyl β-D-glucopyranoside was used.

Influence of the Incorporated Acetyl Group on the Second Acetylation. In order to obtain deeper insight into the nature of the unique selectivities, it was investigated how derivatization of one particular hydroxy group affects the rate of acetylation at other positions. Then the author performed a simple experiment in which two acetyl groups were introduced into octyl β-D-glucopyranoside upon treatment with more than 2 equiv. of acetic anhydride (Scheme 3) and the product distribution of diacetyl glucopyranosides was investigated. Figure 3 shows the ^1H NMR spectrum at $\delta \sim 2.1$ for the obtained reaction mixture. Two signals of the same intensity were observed at δ 2.092 and 2.152 together with acetyl-group signals of monoacetylated glucopyranosides. After careful purification, it was found that these two intense signals were coming from diacetylated glucopyranoside with OAc groups at positions 3 and 6. Of five possible regioisomers, the 3,6-di-*O*-acetyl-β-D-glucopyranoside was selectively formed. Formation of other regioisomers seemed to be considerably suppressed, although they were not identified.

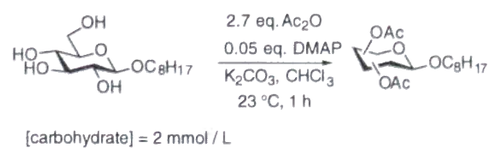

[carbohydrate] = 2 mmol / L

Scheme 3

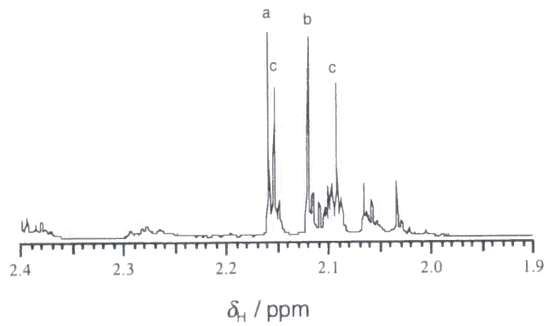

Figure 3. The ^{1}H NMR spectrum of the reaction mixture containing monoacetylated and diacetylated glucoses. [a] Octyl 3-*O*-acetyl-β-D-glucopyranoside. [b] Octyl 4-*O*-acetyl-β-D-glucopyranoside. [c] Octyl 3,6-di-*O*-acetyl-β-D-glucopyranoside.

In the case of monoacetylation, 3-*O*-acetyl- and 4-*O*-acetyl-β-D-glucopyranosides were produced in nearly equal amounts as major products and the formation of 6-*O*-acetyl-β-D-glucopyranoside was remarkably suppressed as described in the previous section. The second acetylation reaction is supposed to proceed through monoacetylated sugars of this product distribution. Therefore the dominant diacetylation pathway is considered as one shown in bold arrows in Scheme 4, *i.e.* the first acetyl group was introduced onto the 3-OH group and then the second onto the 6-OH group. In other words, the acetyl group introduced at position 3 considerably reduced the reactivity of the neighboring 4-OH group, which showed one of the highest reactivities in monoacetylation. On the other hand, the acetyl group at position 4 does not seem to affect the reactivity of the neighboring 3-OH group. Lack of formation of the diacetylated glucopyranoside at positions 4 and 6 suggests that the 3-OH group still has relatively high reactivity after acetylation of the 4-OH group and competes with the primary 6-OH group.

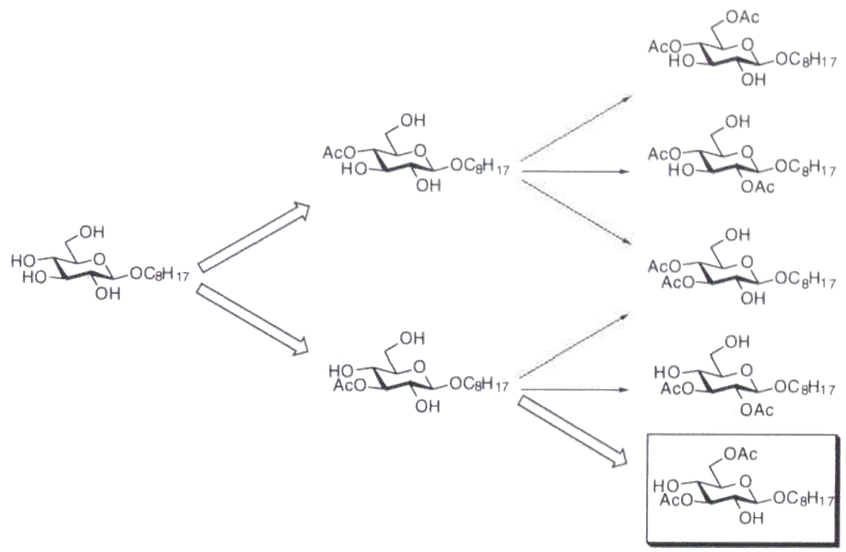

Scheme 4. *Note*: Thick arrows do *not* imply a retrosynthetic scheme (see the Results section).

Discussion

The results reported here are probably the first example of a systematic investigation into the relative reactivities of monosaccharide OH groups. As acetylation experiments were conducted under exactly the same reaction conditions, product distributions can be compared with each other and discussed in detail from the viewpoint of structure–reactivity relationships. In addition, the present DMAP-catalyzed acetylation reaction is superior in the following two points.

To begin with, the author have to point out that reaction conditions were not well controlled in past studies. In those studies, relative reactivities were estimated based on the reaction mixtures consisting of monoacetylated, diacetylated and further acetylated sugars and they failed to take into account the effect that substitution at one hydroxy group might have on the rate of substitution at another.[6] The author have demonstrated that an acetyl group incorporated at a particular position altered the reactivities of the other hydroxy groups dramatically. So the reactivities of OH groups in unprotected monosaccharides must be evaluated from the ratio of monoacetylated sugars without the concomitant formation of more acetylated sugars. As is clearly seen in Figure 2, the present study fulfilled this criteria.

Another problem to note is the possibility of intramolecular acetyl migration. It is well known that an acyl group can easily migrate to a neighboring OH group especially under basic conditions.[13] Considering that partially acetylated sugars were usually obtained by treatment of unprotected sugars with acetic anhydride or acetyl chloride in pyridine in the past, reactivity orders determined under the above conditions reflected to a considerable degree the thermodynamic stability of each regioisomer. On the other hand, the reaction conditions used in the present study were nearly neutral and the acetylation reaction was stopped after a short period. Therefore the product ratios were determined mainly by kinetic factors. This was also supported by the fact that the product ratio was independent of the reaction time. Consequently, the present experiments estimate kinetic factors of acetylation reactions as correctly as possible.

Rate-Determining Step. The author next turned his attention to the rate-determining step of the DMAP-catalyzed acetylation of carbohydrates. Although no detailed mechanistic survey was conducted on DMAP-catalyzed acetylation of carbohydrates, the author obtained an intriguing result to allow him to speculate on the mechanism: the fact that the selectivity was almost reversed in the absence of DMAP as

shown in Table 3. This confusing result led him to the assumption that acetylation of a hydroxy group proceeded in two steps. The first step is an attack of a hydroxy group on a carbonyl group to form an unstable adduct as shown in Figure 4. In the second step, this high-energy intermediate gives the acetylated product after deprotonation and departure of the leaving group. Inspection of the structure of these reaction intermediates suggests that, in the case of the DMAP-catalyzed reaction, the first addition process is rate-determining and the following step proceeds smoothly because pyridinium ion is an excellent leaving group and, in addition, the counter-ion acetate will work effectively as a base. In the absence of DMAP, the second proton-transfer step seems to become rate-determining due to the poor leaving ability of acetate ion. This drastic change of rate-determining step seems to be the origin of the completely reversed selectivity. The theoretical investigation suggests that if the carbonyl carbon has a good leaving group, the concerted process is likely rather than the process via a tetrahedral intermediate,[14] supporting his idea that an attack of a hydroxy group on a carbonyl group is rate-determining in the reaction of *N*-acetylpyridinium acetate with alcohols. Although the assumption presented here seems difficult to verify from detailed mechanistic investigations,[15] this simplified view of the acetylation mechanism is quite useful in allowing him to understand the relative reactivities of carbohydrate OH groups toward various reagents (*vide infra*).

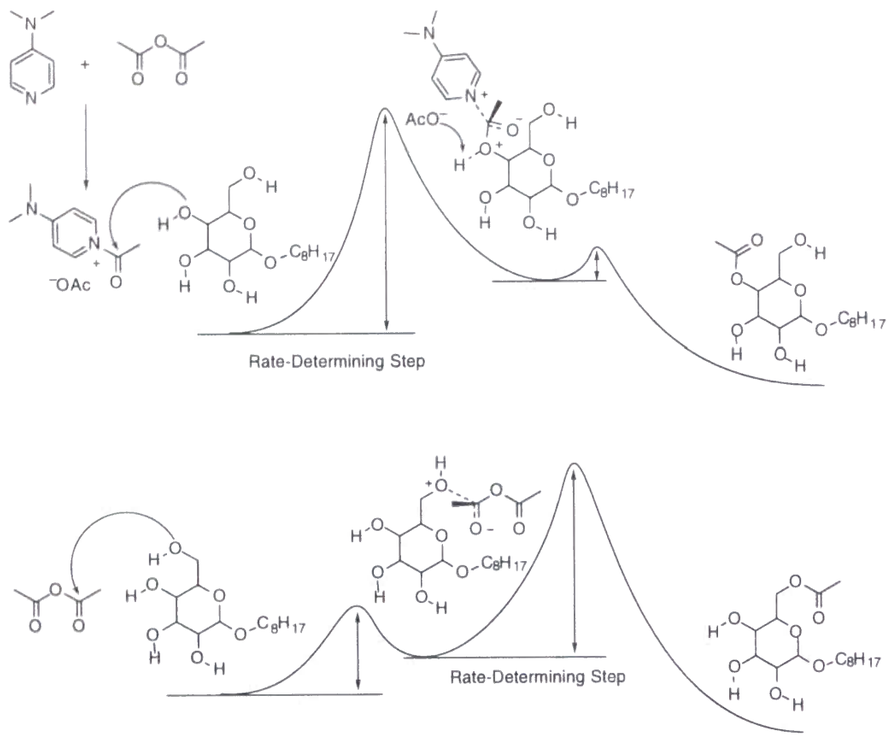

Figure 4. Proposed energy diagrams for the DMAP-catalyzed acetylation (above) and the uncatalyzed acetylation (below) with acetic anhydride.

Delocalization of Positive Charge through Hydrogen-Bonding Networks. The usual steric discussion cannot explain the present results, especially the fact that the secondary 3- and 4- OH groups were more acetylated than the primary 6-OH group in the case of glucose. Clearly, the primary 6-OH group must be preferentially acetylated from the viewpoint of steric factors. There must be some other dominant factors operative in the DMAP-catalyzed acetylation of carbohydrates.

The following three experimental results seem to be important in the elucidation of the mechanism. (1) Among the secondary OH groups, the reactivity of the 2-OH group is considerably reduced in all carbohydrates examined. (2) The effect of stereochemistry on the reactivities of OH groups is complicated. For example, the axial 2-OH group in mannose affects not only the reactivity of the neighboring 3-OH group but also the reactivities of the remote 4-OH and 6-OH groups. The axial 4-OH group in galactose reduces the reactivity of the 3-OH group, but on the other hand increases the reactivity of the 6-OH group. (3) Acetylation of the 3-OH group of glucose reduces the reactivity of the 4-OH group considerably, which is one of the most reactive OH groups. However,

substitution at position 4 does not affect the reactivity of the neighboring 3-OH group so much.

To explain all these results, the author proposes that the formation of hydrogen-bonding networks is mainly responsible for the relative reactivities of OH groups in carbohydrates. As shown in Figure 5, the positive charge in the transition state is delocalized through hydrogen-bonding networks.[16] The extent of delocalization increased in the order of substitution at 2-, 3-, and 4-OH and the transition state is stabilized in the same order. Thus 4-OH groups were acetylated preferentially in all carbohydrates. Compared with secondary OH groups, primary 6-OH groups do not show consistent reactivity trends expected from hydrogen-bonding networks. That is probably due to the high flexibility of primary 6-OH groups.

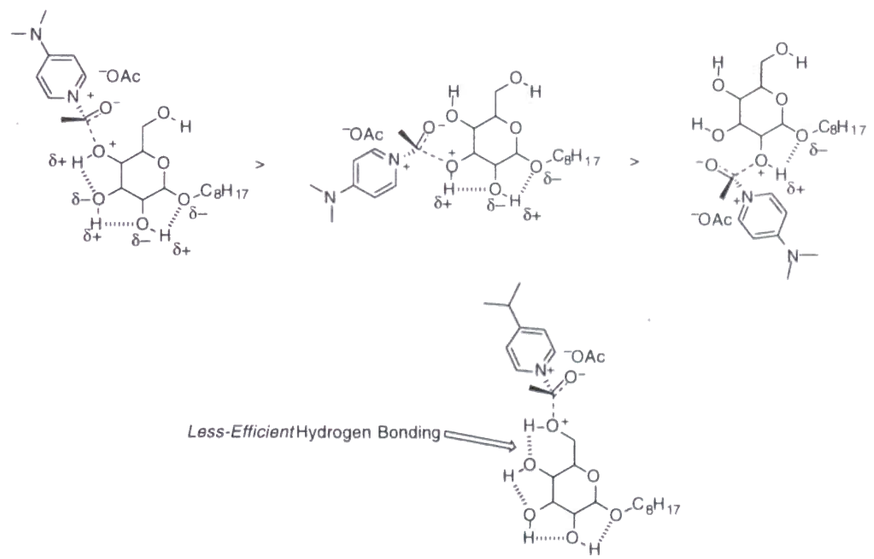

Figure 5. Schematic representation of delocalized positive charge through hydrogen bonding networks.

All three points mentioned above could be easily understood from the viewpoint of hydrogen-bonding networks. First, reduced reactivities of the 2-OH groups in all carbohydrates originate in the smallest stabilization energy. This situation is not dependent on the stereochemistry of the 2-OH group and the anomer position. Therefore both anomers of glucose, mannose, and galactose generally show reduced reactivities for the 2-OH group. Reactivity changes arising from stereochemistry of OH groups can be best understood as a result of the effectiveness of hydrogen-bonding networks. For instance, the axial 2-OH group in mannose diminishes effectiveness of

the hydrogen-bonding network compared with glucose. Thus, the reactivities of all secondary OH groups involved in the hydrogen-bonding network are reduced and the primary 6-OH group which does not effectively participate in the hydrogen-bonding network shows relatively increased reactivity. Considerably reduced yields for acetylation of mannose and galactose are also consistent with this idea. In the case of galactose, the hydrogen-bonding between 6-OH (as a hydrogen donor) and 4-OH (as a hydrogen acceptor) is far more effective than in the case of glucose and mannose probably because the distance between 6-O and 4-O is shorter in galactose. Thus, the primary 6-OH group of galactose is preferentially acetylated. Without considering directional hydrogen-bonding networks, it seems impossible to understand a simultaneous increase and decrease of the reactivities of neighboring OH groups. The result on diacetylation strongly suggests the importance of intramolecular hydrogen-bonding networks. That is, acetylation of the 3-OH group completely destroys the hydrogen-bonding network from the 4-OH group to the anomeric oxygen and then the reactivity of the 4-OH group is considerably reduced. On the other hand, substitution at the 4 position does not affect the reactivity of the 3-OH group because the hydrogen-bonding network from the 3-OH group to the anomeric oxygen still survives.

Calculated Proton Affinity of Each OH Group in Monosaccharides. In order to estimate the effect of hydrogen-bonding networks, the author attempted to utilize the proton affinity of each OH group as a qualitative measure of positive charge delocalization. If positive charge delocalization truly matters most in the DMAP-catalyzed acetylation reaction, good correlation between reactivity trends and proton affinities would be anticipated. Dewar and Dieter calculated proton affinities for simple alcohols with the semi-empirical method (AM1) and they found that experimental trends are accurately reproduced.[17] So the author employed semi-empirical calculations (PM3) to evaluate the proton affinity of each OH group in monosaccharides. At first, the author encountered a serious problem concerning the flexibility of carbohydrate molecules. Orientation of OH groups was found to affect significantly their calculated values. In order to find the best OH group orientation for hydrogen-bonding networks, the author performed Monte Carlo simulations to find the most stable conformer.

Computations were done as follows. First, the author searched for the most stable conformer by employing Monte Carlo conformational searches with the AMBER* force field implemented on MacroModel Version 6.0.[18] Because good parameters for oxonium ion were not available in molecular mechanics, R-OH_2^+ was replaced by R-NH_2. Then the most stable conformer thus obtained was transferred to the SPARTAN platform

and subjected to semi-empirical calculations (PM3) after replacing R-NH_2 by R-OH_2^+. The C- OH_2^+ bond was rotated by 30 degrees and the geometries of 12 conformers thus generated were each optimized with PM3-level[19] calculations. Proton affinities were calculated according to (1),

$$\text{Proton Affinity (R-OH)} = \Delta H_f(\text{H}^+) + \Delta H_f(\text{R-OH}) - \Delta H_f(\text{R-OH}_2^+) \quad (1)$$

in which ΔH_f is the calculated heat of formation. The experimental ΔH_f (H^+)-value of 1536 kJ mol^{-1} was used following Dewar and Dieter. Calculated proton affinities are listed in Table 7. Irrespective of the stereochemistry of OH groups, proton affinities increased in the order of the 2-, 3-, and 4-OH group in all the cases studied. This result supports his proposal on positive charge delocalization through hydrogen-bonding networks. However, the relative reactivities observed in this study were not always strictly parallel to proton affinities. It might be too simplistic to estimate transition state energies by proton affinities. In addition, it should be stressed that the PM3-level semi-empirical method might not be well qualified to calculate cationic species with densely packed, highly polar functionality like carbohydrates.

Table 7 Proton Affinity of Each OH Group in Monosaccharides.

	Proton Affinity / kJ mol^{-1}			
Substrate	2-OH	3-OH	4-OH	6-OH
Methyl β-Glc	713	730	755	747
Methyl β-Man	741	742	749	741
Methyl β-Gal	734	762	785	781

Conclusions

Hydroxy groups in simple monosaccharides showed unique reactivities in the DMAP-catalyzed acetylation reaction. Especially in the case of glucose, secondary OH groups exhibited much higher reactivities than the primary OH group at position 6. To accurately evaluate relative reactivities of carbohydrate OH groups, reaction conditions were employed under which only monoacetylated products were formed and acetyl migration was suppressed to a minimum. The product distributions showed no concentration dependence. Therefore the unique selectivities were confirmed to originate in carbohydrate structures, not in carbohydrate–carbohydrate interaction in non-polar solvents.

Careful comparison of the relative reactivities of hydroxy groups in glucose, mannnose, and galactose implied an important role for intramolecular hydrogen-bonding networks among carbohydrate OH groups. Furthermore, a markedly large effect of the introduced acetyl group at a particular position on the regiochemistry of the second acetylation clearly demonstrated the directional hydrogen-bonding network starting from 4-, 3-, and 2-OH groups to the anomer oxygen as a hydrogen acceptor. Based on these considerations, the author proposed that positive charge delocalization through a hydrogen-bonding network is a dominant factor in determining the relative reactivities of carbohydrate OH groups. As a qualitative measure of positive charge delocalization, the author calculated the proton affinity of each OH group in monosaccharides by the combination of Monte Carlo simulations and semiempirical calculations. The author found a satisfactory correlation between proton affinities and reactivity trends. The methodologies and discussion presented here are not necessarily limited to DMAP-catalyzed acetylation systems. Unusual reactivities of carbohydrate OH groups should be reconsidered in the light of intramolecular hydrogen bonding networks as well as the position of the rate-determining step for a reaction of interest.

In addition to the traditional steric factors, the author demonstrated that hydrogen-bonding networks played a decisive role in the DMAP-catalyzed acetylation of unprotected carbohydrates.

Experimental Section

Instrumentation. ^{1}H and ^{13}C NMR spectra were recorded using a JEOL A-500 spectrometer for samples in chloroform-*d* . ^{1}H and ^{13}C NMR chemical shifts in $CDCl_3$ were referenced to $CHCl_3$ (δ 7.24 and 77.0, respectively). Water content in chloroform was measured by Karl-Fischer equipment (HIRANUMA, AQUACOUNTER AQ-7). GPC was performed on a Recycling Preparative HPLC (LC-908) equipped with a JAIGEL-2H column (Japan Analytical Industry) and a refractive index detector; flow rate, 4.5 mL min^{-1}; mobile phase, chloroform.

Material. Octyl β-D-glucopyranoside and octyl α-D-glucopyranoside were purchased from Wako Pure Chemical Industries and SIGMA, respectively and used as received. Preparations of other octyl glycopyranosides have already been reported.[20] Chloroform stabilized with 2-methylbut-2-ene was purchased from Tokyo Chemical Industry and dried over molecular sieves 3Å. Acetic anhydride was purified by distillation after azeotropic removal of acetic acid with toluene. DMAP was recrystallized from benzene and dried *in vacuo*. K_2CO_3 was dried *in vacuo* over P_2O_5. Column chromatography was carried out with Silica Gel 60N (spherical, neutral, 40–100 μm) from Kanto Chemicals. $CDCl_3$ was completely deacidified by passage through activated alumina just before use.

General Procedure for the DMAP-Catalyzed Acetylation of Unprotected Carbohydrates. In every experiment, it was confirmed that water content of chloroform was less than 5 ppm. Stock solutions of DMAP and acetic anhydride were prepared beforehand by dissolving DMAP (12.0 mg, 98 μmol) in chloroform (2 mL), and acetic anhydride (101.7 mg, 1 mmol) in chloroform (1 mL, 1.45 g), respectively.

Octyl β-D-glucopyranoside (11.8 mg, 40.4 μmol) was dissolved in chloroform (20 mL) under Ar. K_2CO_3 (54 mg) was added to the solution. Then the DMAP stock solution (41 mL, 2 μmol) was added to the solution via microsyringe. The solution was stirred well with a magnetic stirrer. The temperature was kept at 23 °C during the acetylation reaction. Finally, the acetic anhydride stock solution (44.3 mg, 28.4 μmol) was added to initiate the acetylation reaction. After being stirred for 1 h, the reaction mixture was passed through a silica gel short column (1 g) to remove DMAP. The reaction flask was washed well with chloroform and the washings were also passed

through the column. Monoacetylated sugars, together with remaining unprotected sugar, were eluted by ethyl acetate–methanol solvent (4:1; 15 mL). The solvent was evaporated off and the product was dried *in vacuo*. The product was taken up in chloroform (2 mL) and passed through a polypropylene filter to remove traces of silica gel. The chloroform was then evaporated off. The sample was completely dried by heating *in vacuo* at 60 °C for 4 h and subjected to NMR analysis.

Determination of the Product Distribution. The sample was dissolved in deacidified $CDCl_3$ and the ^1H NMR spectrum was measured. In order to get reproducible results, the temperature was always kept at 30 °C during measurement. The yield of each regioisomer was determined by integration of acetyl group signals at δ ~ 2.1 relative to added bromoform as an internal standard (for assignment of each signal, see below). For accurate integration, a curve-fitting computer program was utilized, in which Lorentzian function was fitted to experimental curves. The ^{13}C NMR spectrum was also measured and the number of signals for anomeric carbons was counted. In every case, consistent results were obtained.

Assignment of Partially Acetylated Sugars. GPC was used for purification. Remaining unprotected sugars were separated completely. Monoacetylated sugars could not be separated from each other, so characterization was done at this stage. Exactly the same procedure was applied for the diacetylation experiment.

Structural characterization relied mainly on the assignment of OH signals and α-proton signals based on the phase-sensitive DQF-COSY measurement in $CDCl_3$ (For structural characterization of the diacetylated glucopyranoside, CD_3CN was used for better separation of C-H signals). Each acetyl group signal was assigned to the corresponding regioisomer and results are summarized in Table 8. Structures of regioisomers were further confirmed by analysis of coupling constants. As shown in Figure 6, two informative regions were separated well from the complicated C-H region in chloroform-*d*. One is the hydroxy proton region, in which one can distinguish the presence of primary 6-OH groups. Second, upon introduction of an acetyl group, the alpha proton moved downfield and analysis of coupling patterns became possible. In the case of mannose and galactose, the position where the acetyl group was introduced can be sometimes determined unambiguously from analysis of coupling constants between neighboring C-H protons.

Table 8. Chemical Shifts of Acetyl Groups in Monoacetylated Carbohydrates.

Substrate	Chemical Shift (δ)			
	2-*O*-Acetate	3-*O*-Acetate	4-*O*-Acetate	6-*O*-Acetate
Octyl β-Glc	2.091	2.159	2.117	2.081
Octyl α-Glc	a	2.151	2.123	2.093
Octyl β-Man	a	2.158	2.109	2.080
Octyl α-Man	2.113	2.143	2.122	2.092
Octyl β-Gal	a	2.154[b]	2.156[b]	2.064
Octyl α-Gal	a	2.149[b]	2.153[b]	2.056

[a] Not determined. [b] The assignment of pairs of resonances may be reversed.

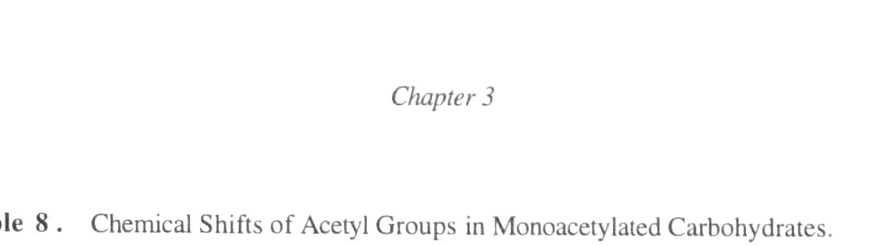

Figure 6. The ^1H NMR spectrum of one of the GPC fractions containing octyl 3- and 4-*O*-acetyl-β-D-glucopyranoside.

Estimation of the Proton Affinity of Each OH Group in Carbohydrates. Monte Carlo simulations were performed on a Silicon Graphics O2 workstation with MacroModel Version 6.0.[18] 5000 randomly generated structures were minimized using the AMBER* force field in the gas phase. Among the 100–500 obtained structures, the most stable conformer was subjected to semi-empirical MO calculations. Close examination of conformers around global minima revealed the existence of several local minima at a similar energy level, which only differ in the direction of the 6-OH group. Considering the flexibility of the 6-OH group, two or three of these conformers were arbitrarily selected and subjected to semi-empirical calculations. Semi-empirical calculations were performed on an IBM RS6000

workstation with SPARTAN Version 4.0. C-OH_2^+ bonds were systematically rotated in 30° steps and the heats of formation of 12 obtained conformers were calculated at the PM3 level[19] after geometry optimization. In the case of primary hydroxy groups at position 6, there are two rotatable bonds and so a systematic survey of 144 conformers was conducted. During the estimation of proton affinities, largely distorted conformers were excluded.

Structural Characterization of Partially Acetylated Carbohydrates. The structural characterization relied mainly on the assignment of OH signals and α-proton signals based on the phase-sensitive DQF-COSY or COSY measurement. Cross-peaks are followed starting from characteristic doublet signals of anomer protons except for 3- and 4-*O*-acetyl-β-D-glucopyranosides, in which cross-peaks are followed from 6-H signals as shown in Figure 7. In some cases, analysis of coupling constants between neighboring C-H protons offers unambiguous information on the position of an introduced acetyl group. The following part provides spectral information together with brief explanations for the judgments.

2-*O*-Acetyl-glycopyranosides are readily characterized as shown in Figure 7 and 17 because there is no overlapped cross-peak. The characterization of 6-*O*-acetyl-glycopyranosides is also relatively straightforward. As shown in Figure 8, 10, 12, 14, 16, and 18, two mutually coupled signals moved downfield which correspond to two inequivalent 6-H protons. In the case of 3- and 4-*O*-acetyl-glycopyranosides, analysis of cross-peaks becomes increasingly difficult due to overlaps. However, analysis of coupling patterns of alpha protons offers clear distinction between position 3 and 4 of galactopyranosides or mannopyranosides as shown in Figure 11, 13, 15, and 17. For glucopyranosides, H_α coupling patterns of 3- and 4-*O*-acetate are exactly the same. Difference of signal intensities of 3-H_b and 4-H_a is used for the distinction between 3- and 4-*O*-acetate of α-D-glucopyranosides as shown in Figure 9.

Structural Characterization of 2-, 3-, and 4-*O*-Acetyl-β-D-glucopyranosides.

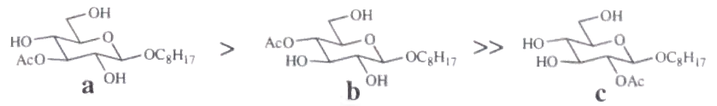

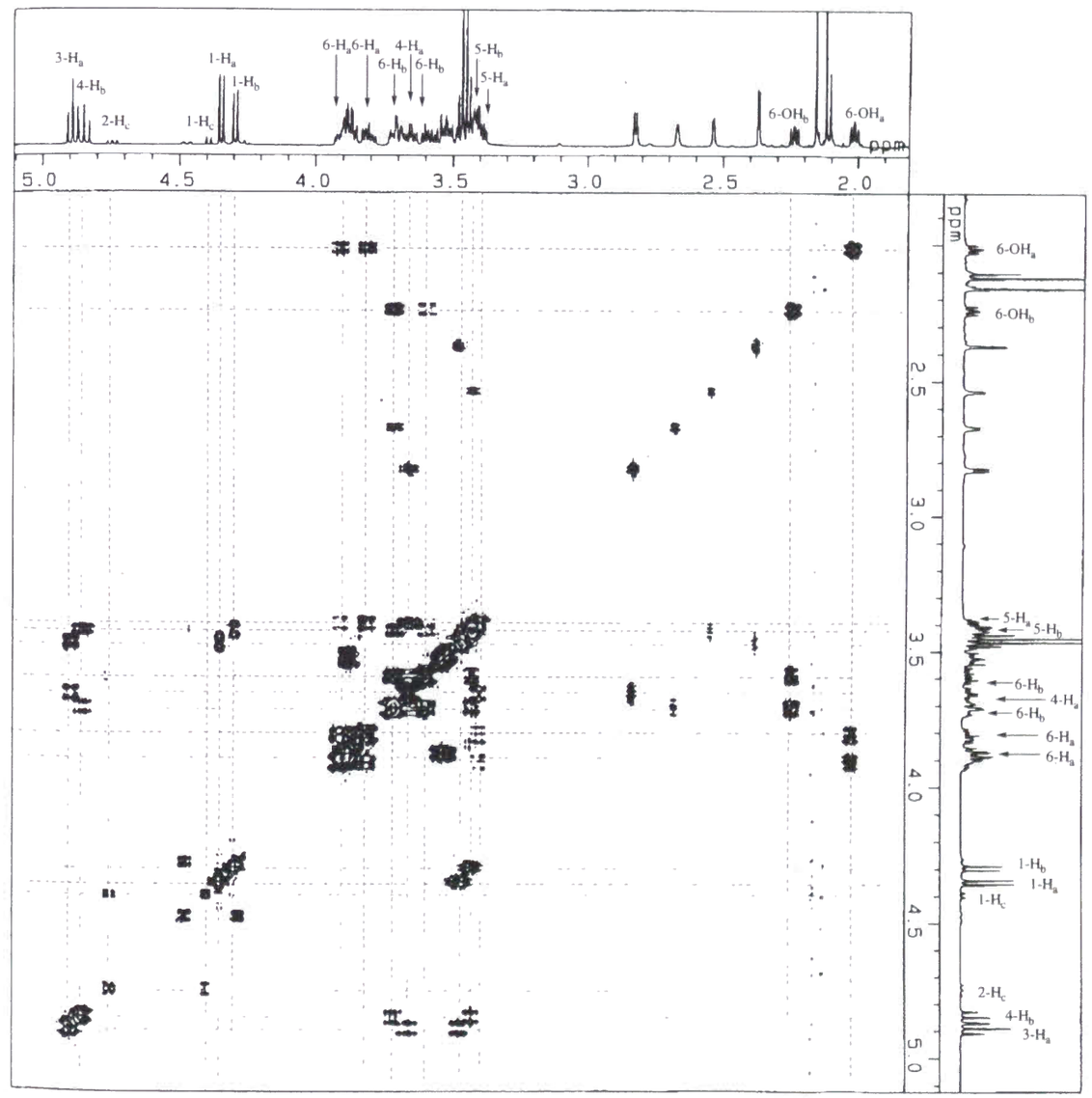

Figure 7. The DQF-COSY spectrum of the mixture of 2-, 3-, and 4-*O*-acetyl-β-D-glucopyranosides in $CDCl_3$

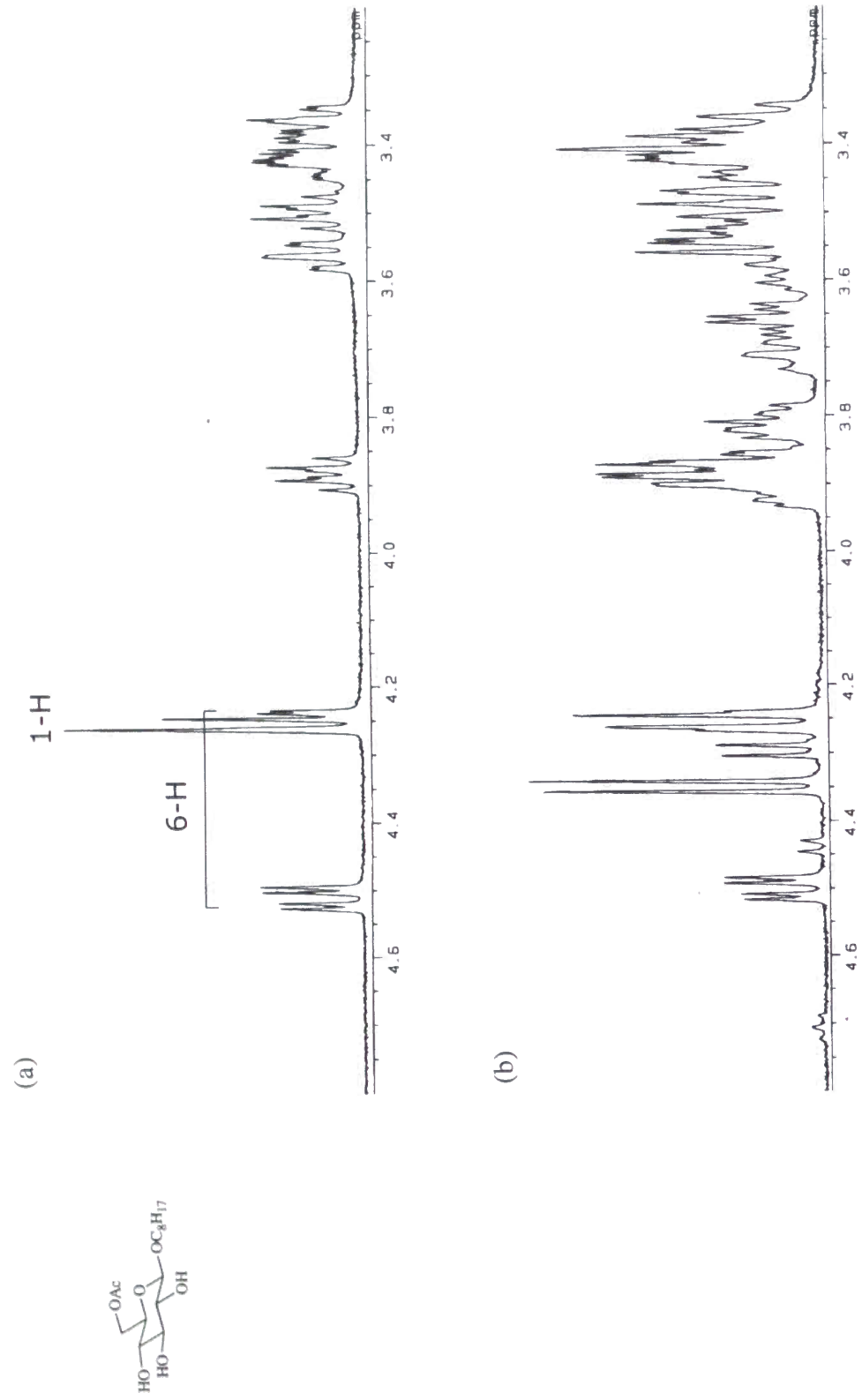

Figure 8. The ^{1}H NMR spectra of (a) octyl 6-*O*-acetyl-β-D-glucopyranoside[20] and (b) one of GPC fractions containing octyl 6-*O*-acetyl-β-D-glucopyranoside in Figure 2 (d).

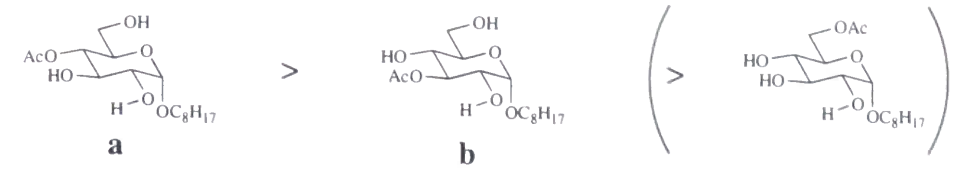

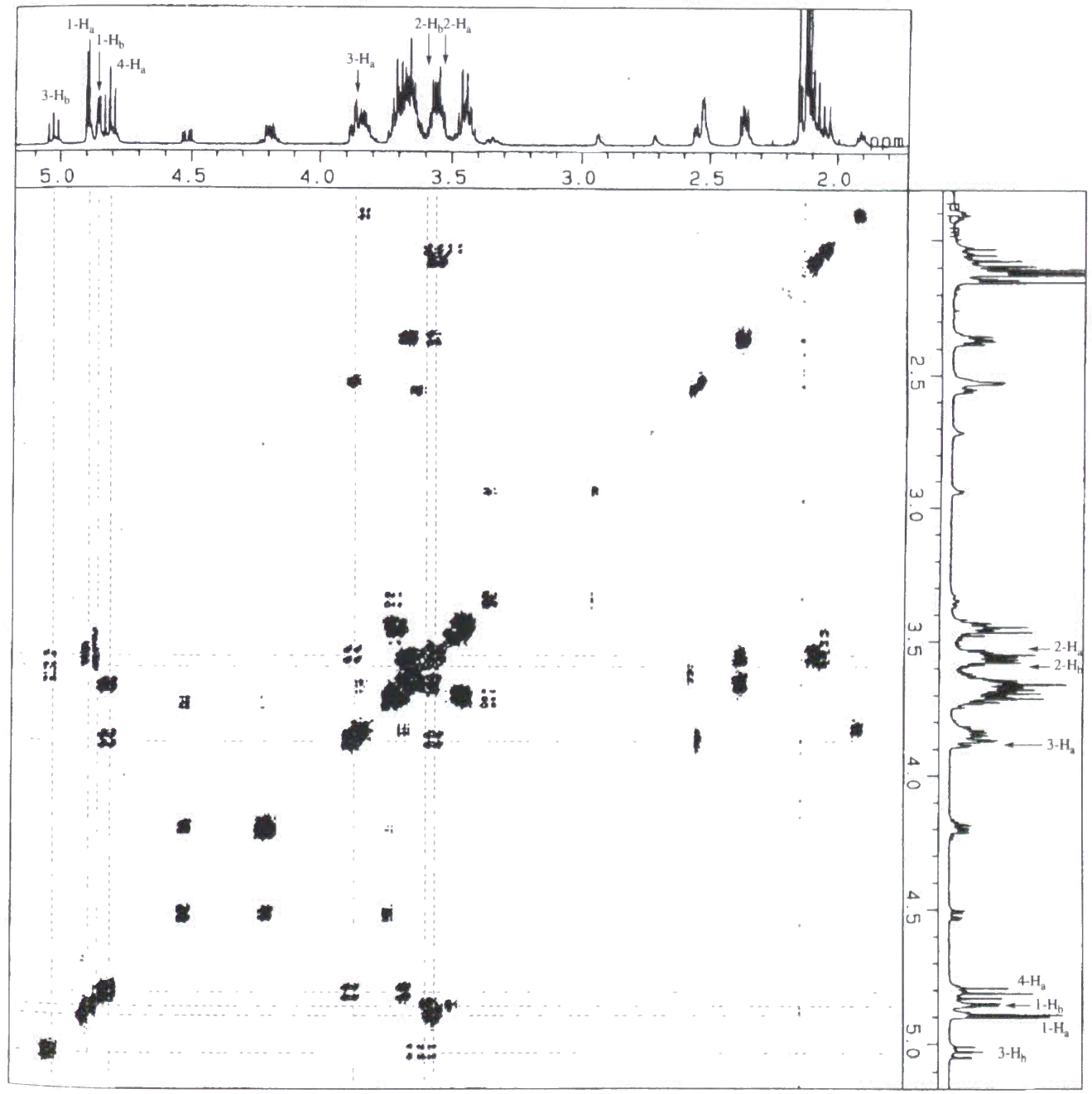

Figure 9. The DQF-COSY spectrum of the mixture of octyl 3- ,4-, and 6-*O*-acetyl-α-D-glucopyranosides in $CDCl_3$.

Structural Characterization of Octyl 6-*O*-Acetyl-α-D-glucopyranoside

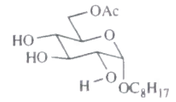

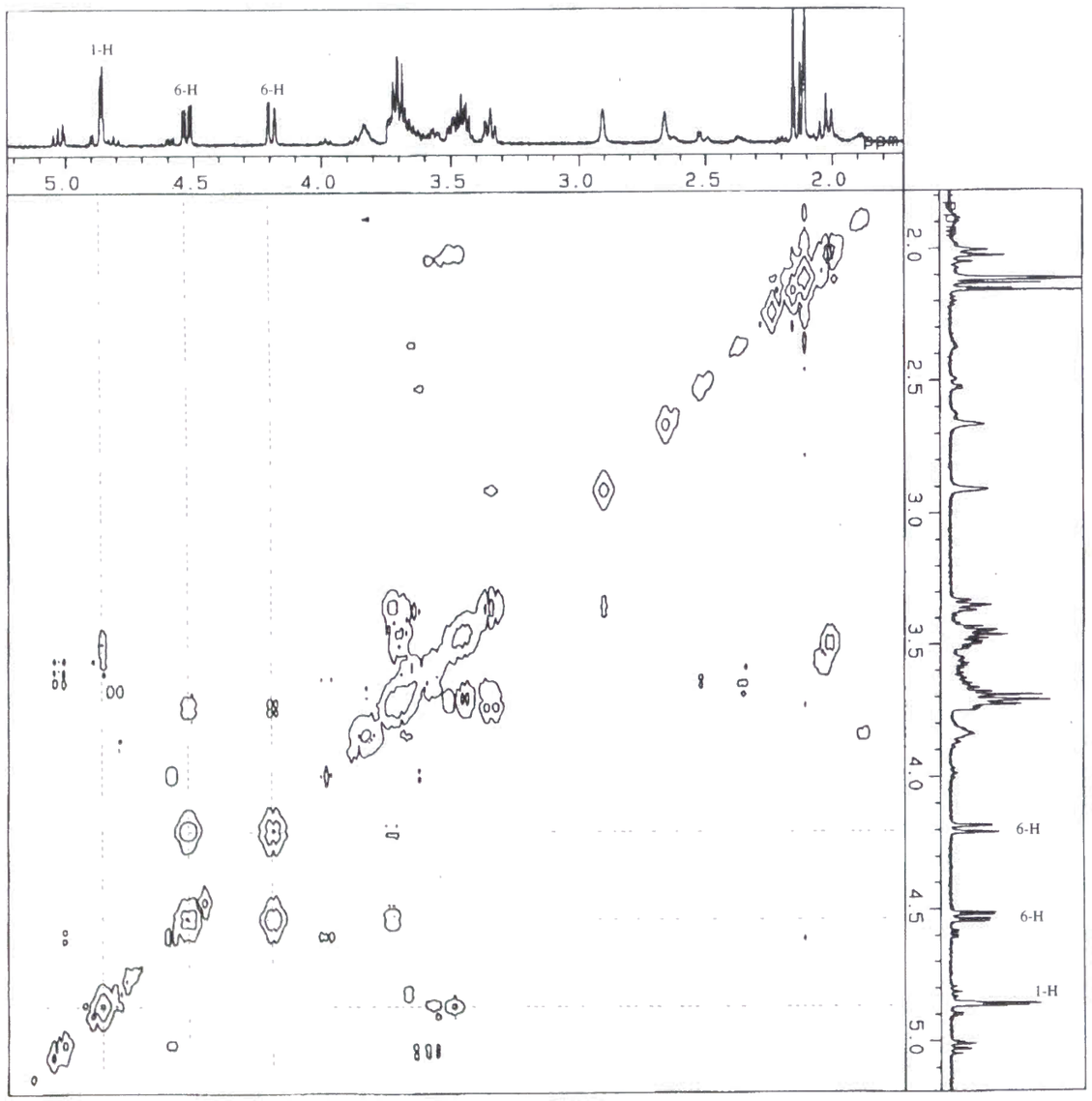

Figure 10. The COSY spectrum of octyl 6-*O*-acetyl-α-D-glucopyranoside in $CDCl_3$.

Structural Characterization of 3-, and 4-*O*-Acetyl-β-D-galactopyranosides

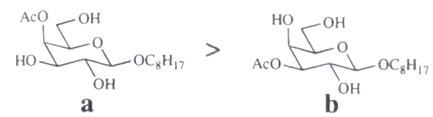

Figire. 11 The DQF-COSY spectrum of the mixture of 3-, and 4-*O*-acetyl-β-D-galactopyranosides in $CDCl_3$.

Structural Characterization of Octyl 6-*O*-Acetyl-β-D-galactopyranoside

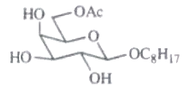

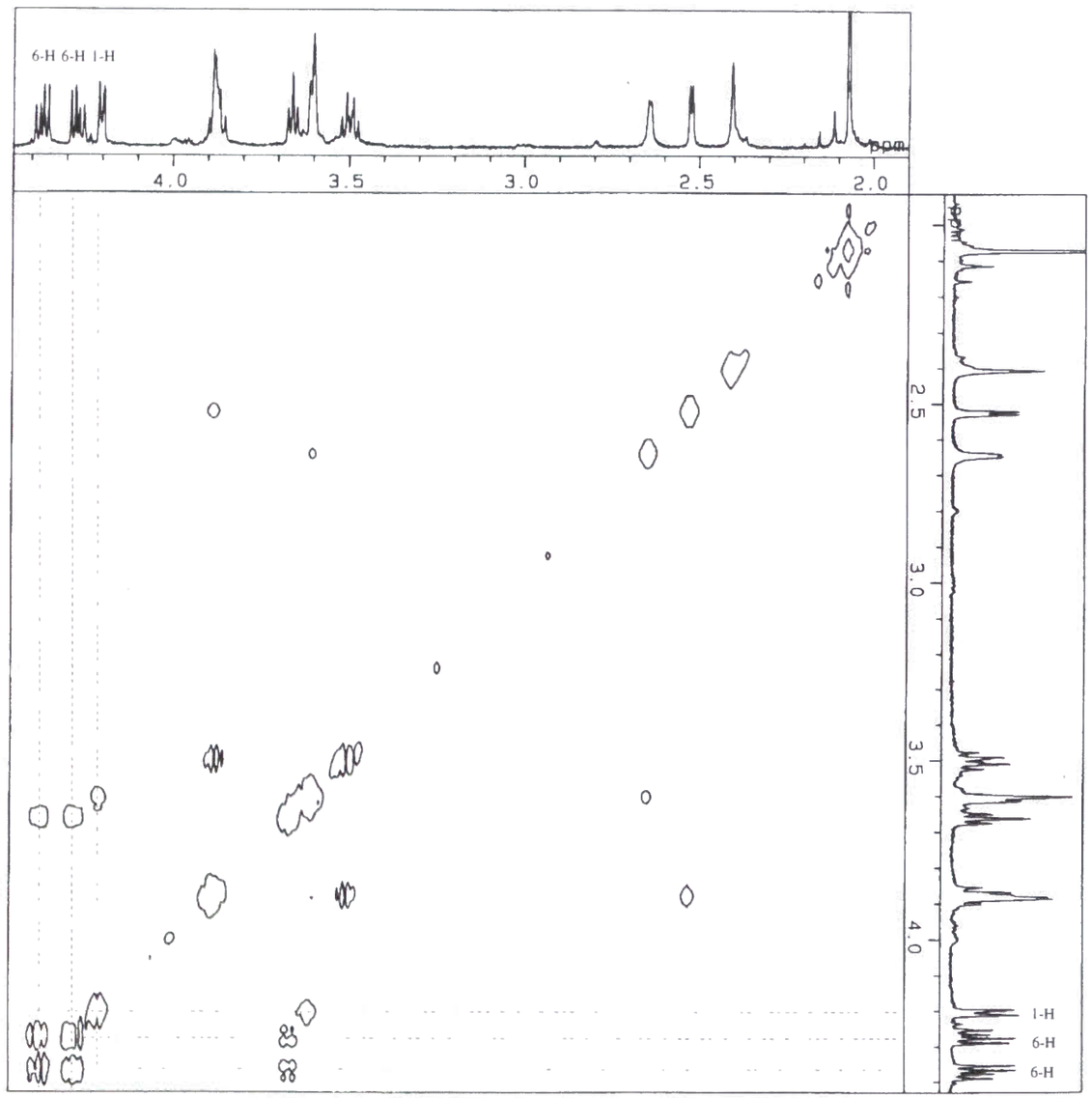

Figure 12. The COSY spectrum of octyl 6-*O*-acetyl-β-D-galactopyranoside in $CDCl_3$.

Structural Characterization of Octyl 3- and 4-*O*-Acetyl-α-D-galactopyranosides

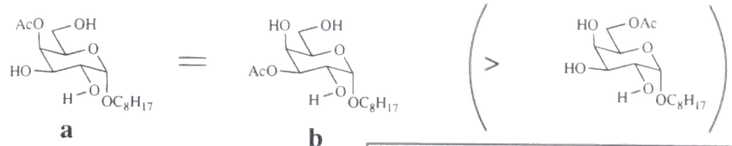

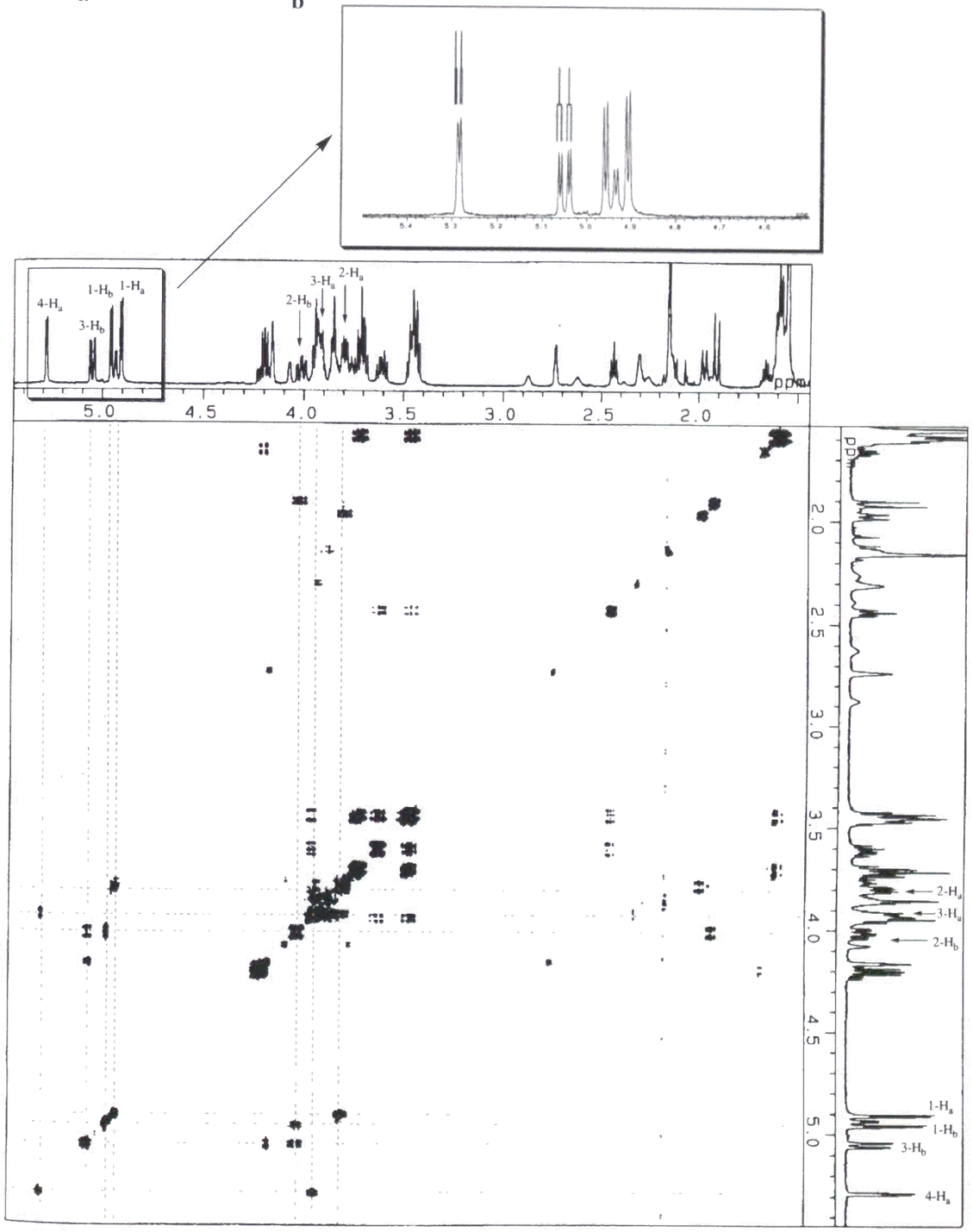

Figure 13. The DQF-COSY spectrum of the mixture of octyl 3-, 4-, and 6-*O*-acetyl-α-D-galactopyranosides in $CDCl_3$.

Structural Characterization of Octyl 6-*O*-Acetyl-α-D-galactopyranoside

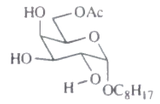

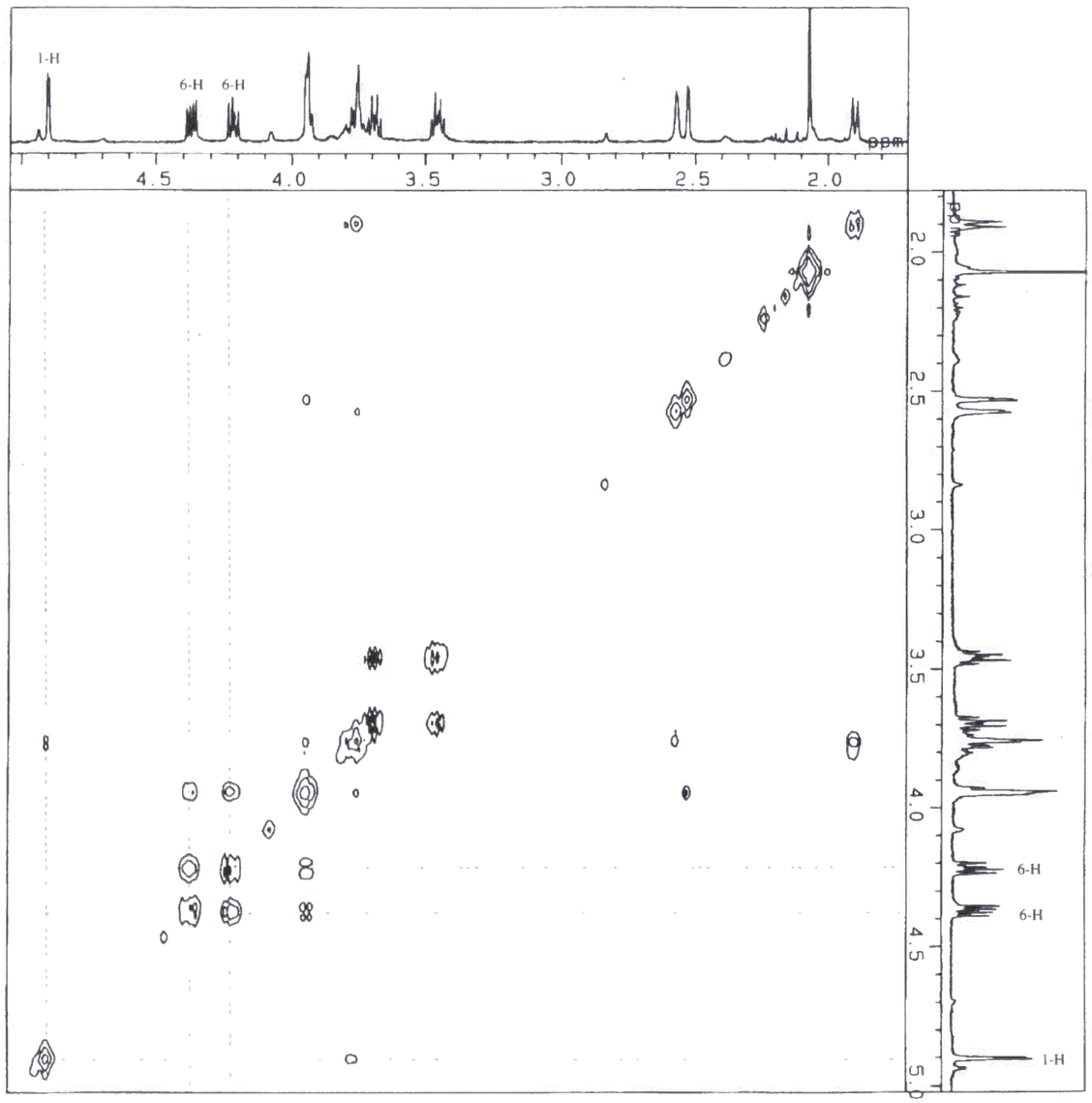

Figure 14. The COSY spectrum of octyl 6-*O*-acetyl-α-D-galactopyranoside in $CDCl_3$.

Structural Characterization of Octyl 3- and 4-*O*-Acetyl-β-D-mannopyranosides

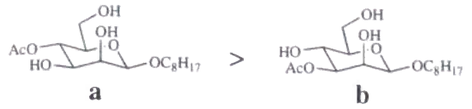

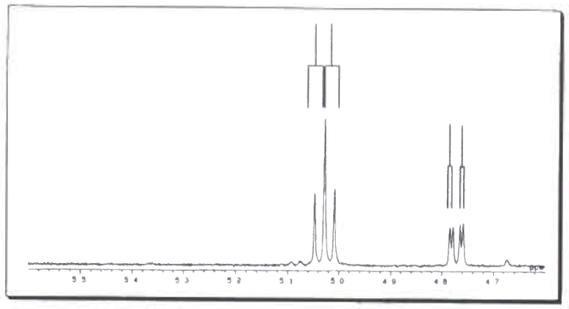

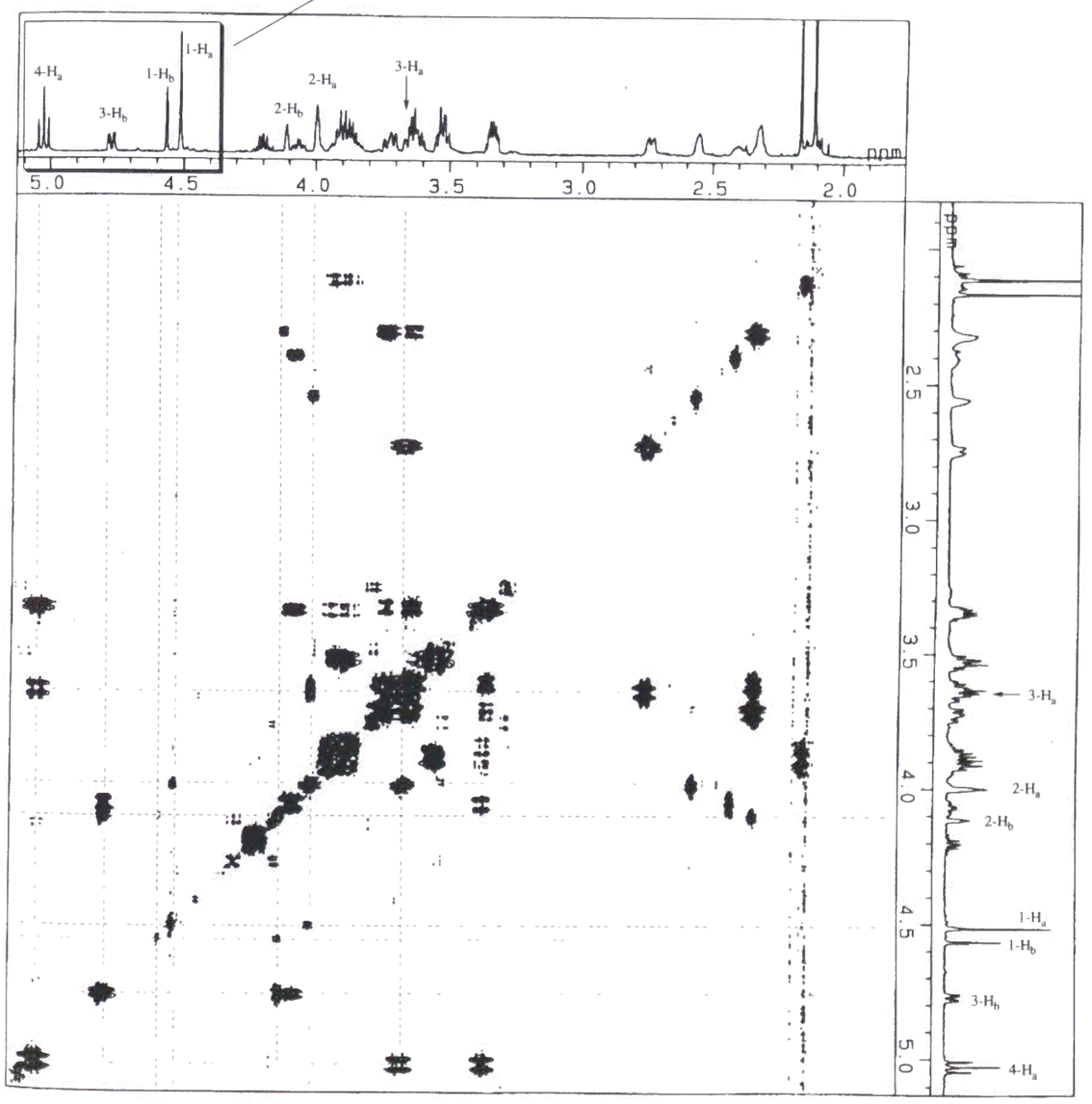

Figure 15. The DQF-COSY spectrum of the mixture of octyl 3- and 4-*O*-acetyl-β-D-mannopyranosides in $CDCl_3$.

Structural Characterization of Octyl 6-*O*-Acetyl-β-D-mannopyranoside

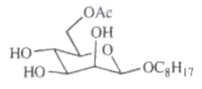

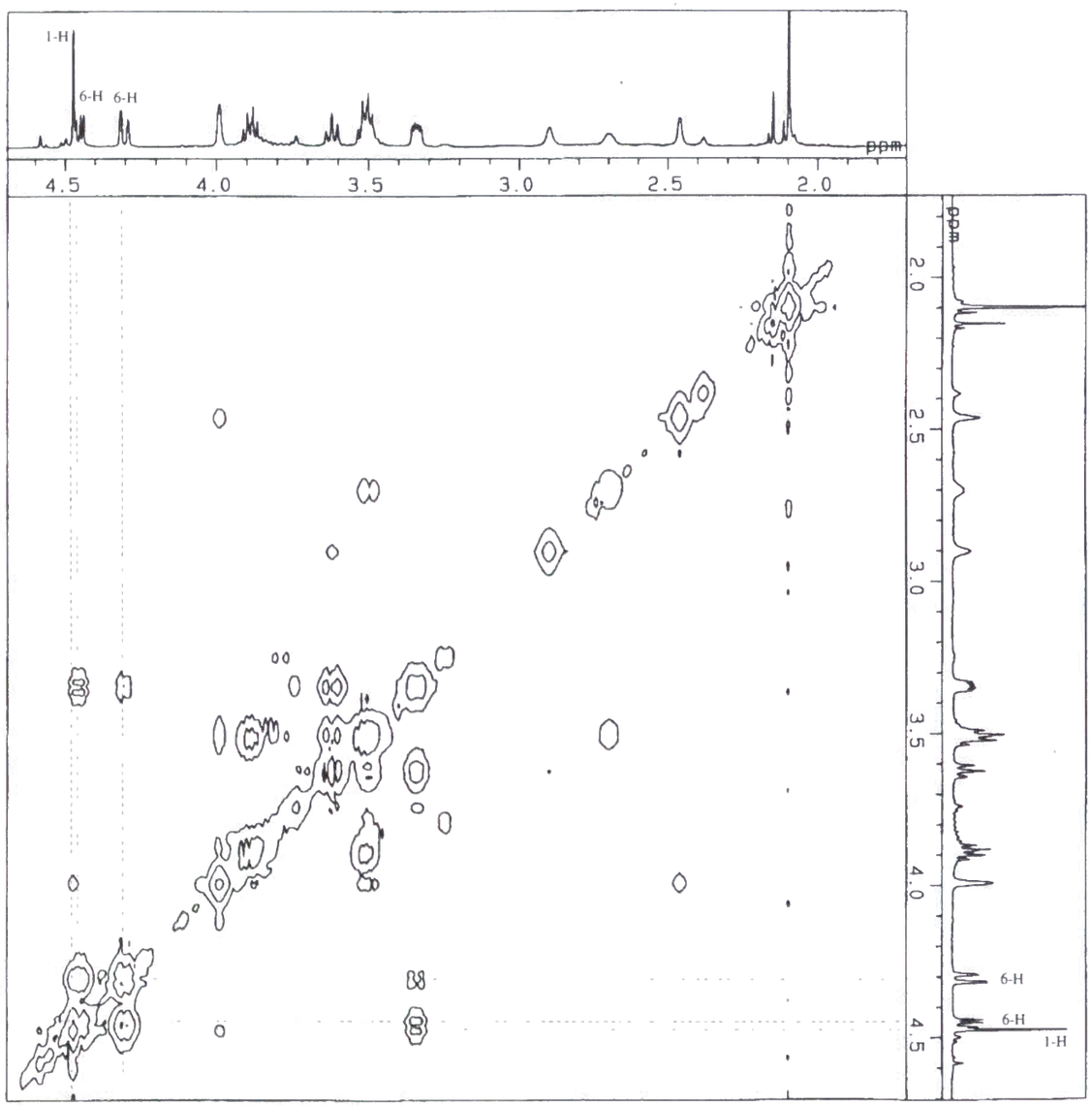

Figure 16. The COSY spectrum of octyl 6-*O*-acetyl-β-D-mannopyranoside in $CDCl_3$.

Structural Characterization of Octyl 2-, 3-, and 4-*O*-Acetyl-α-D-mannopyranosides

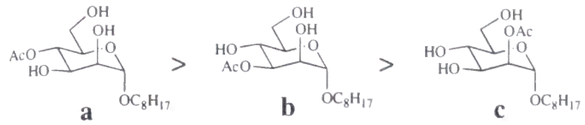

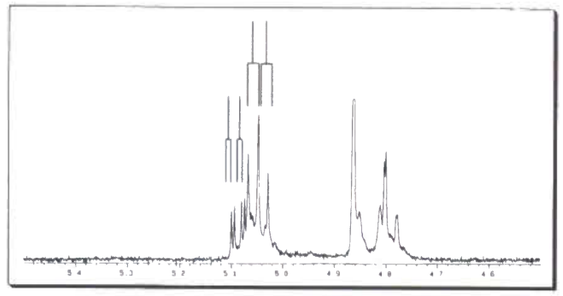

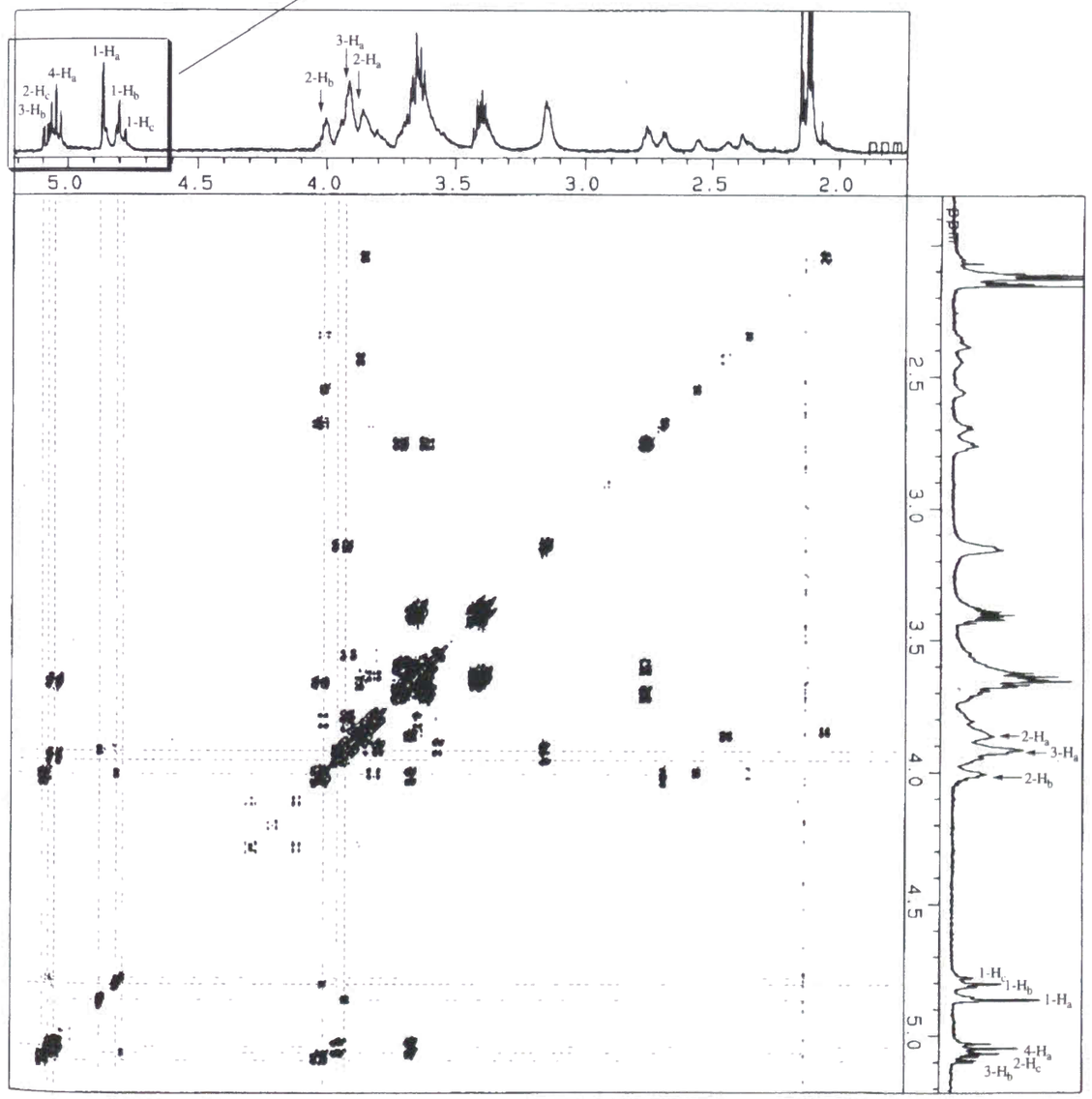

Figure 17. The DQF-COSY spectrum of the mixture of octyl 2-, 3-, and 4-*O*-acetyl-α-D-mannopyranosides in $CDCl_3$.

Structural Characterization of Octyl 6-*O*-Acetyl-α-D-mannopyranoside

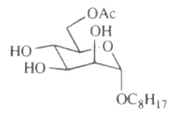

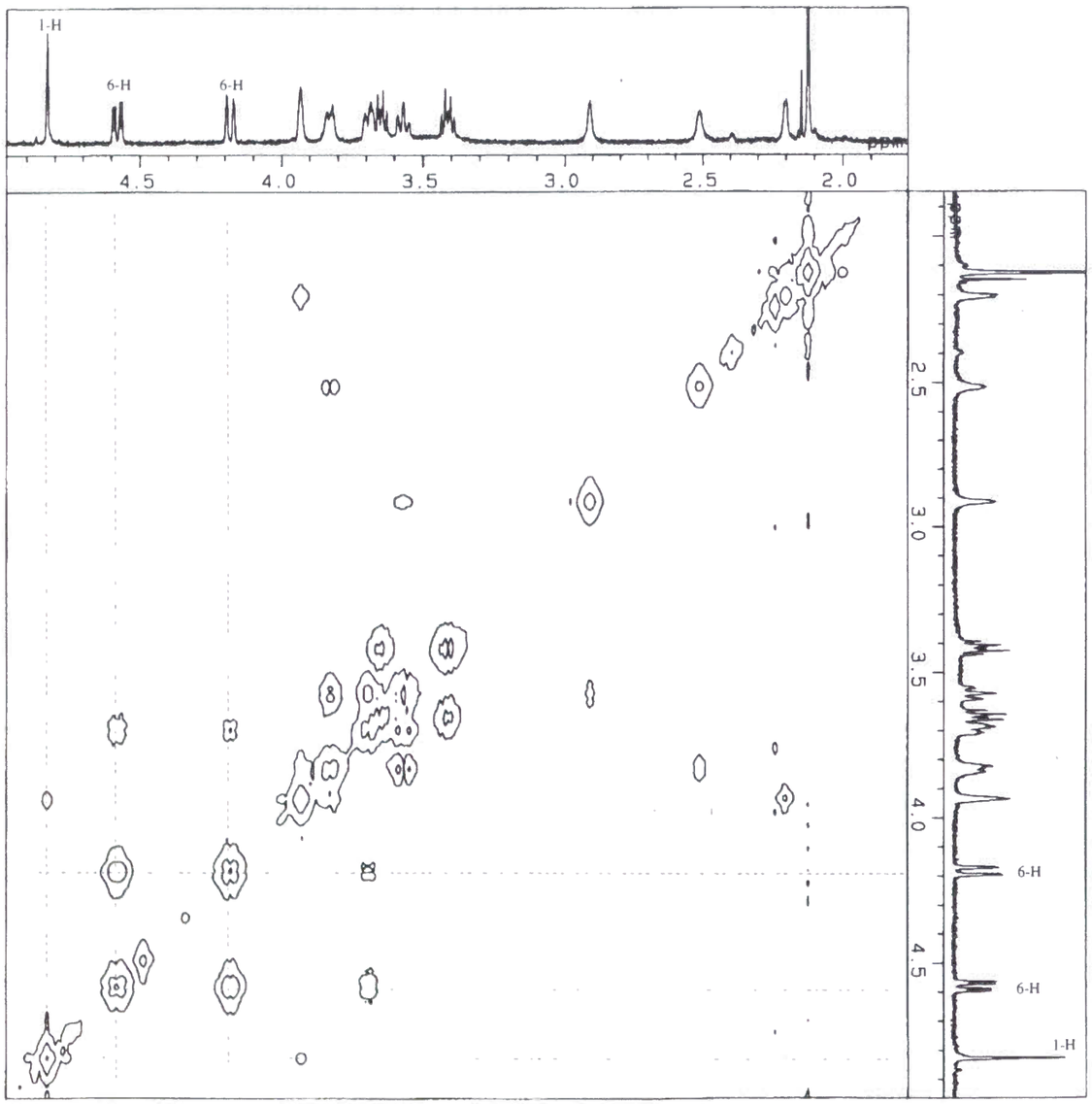

Figure 18. The COSY spectrum of octyl 6-*O*-acetyl-α-D-mannopyranoside in $CDCl_3$.

Structural Characterization of Octyl 3,6-di-*O*-Acetyl-β-D-glucopyranoside

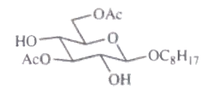

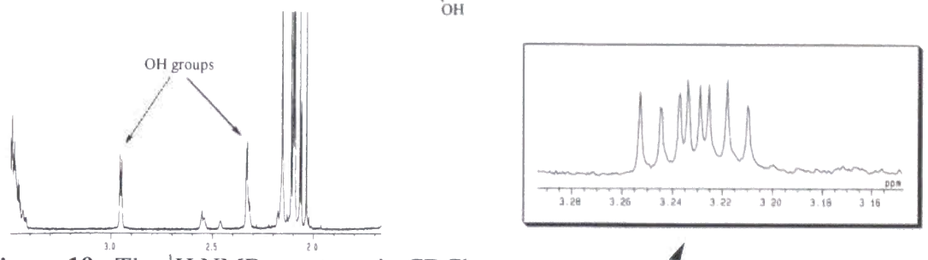

Figure 19. The ^1H NMR spectrum in $CDCl_3$.

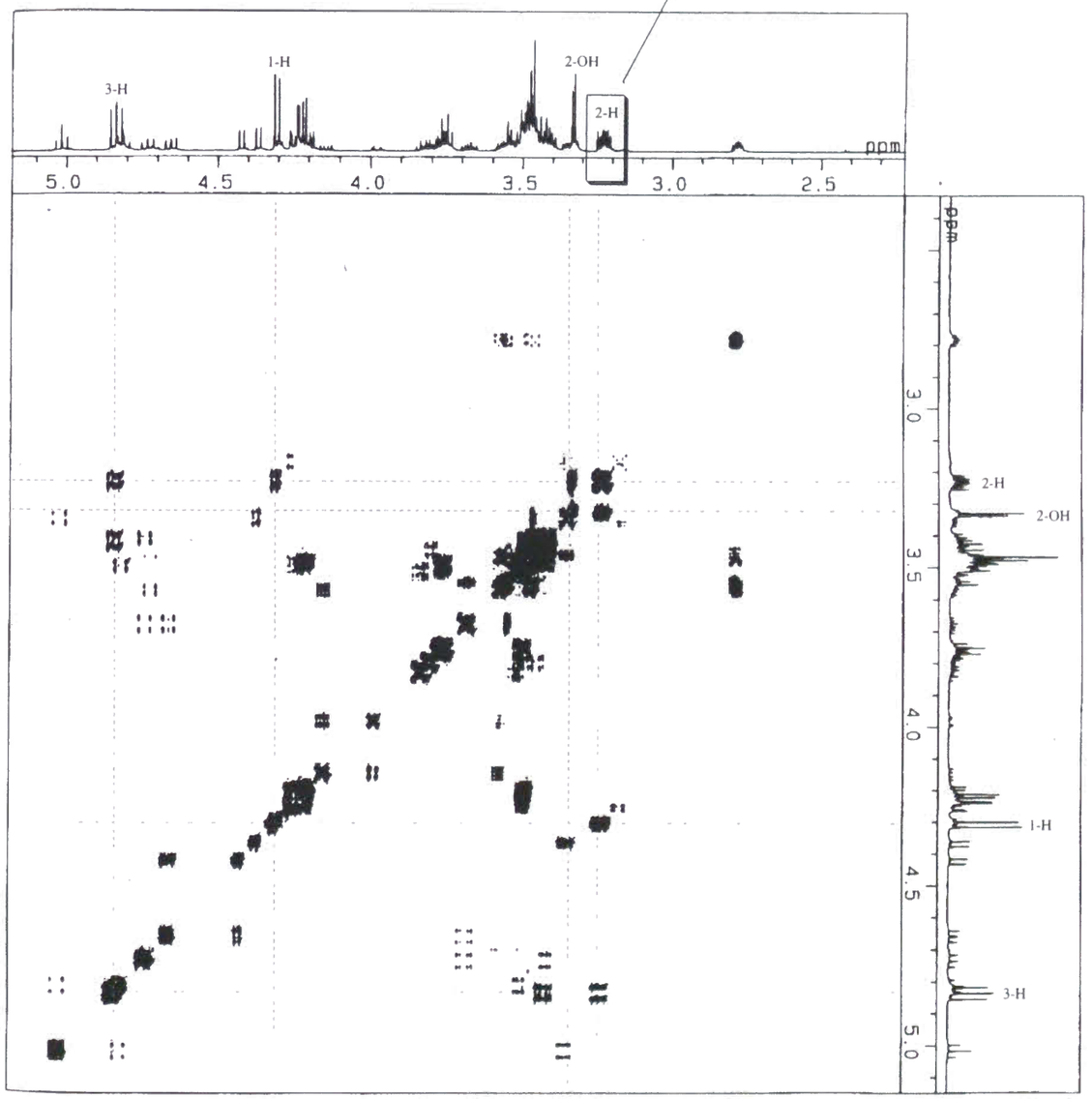

Figure 20. The DQF-COSY spectrum ot the mixture of octyl 3,6-di-*O*-acetyl-β-D-glucopyranoside and other di-*O*-acetyl-β-D-glucopyranosides in CD_3CN.

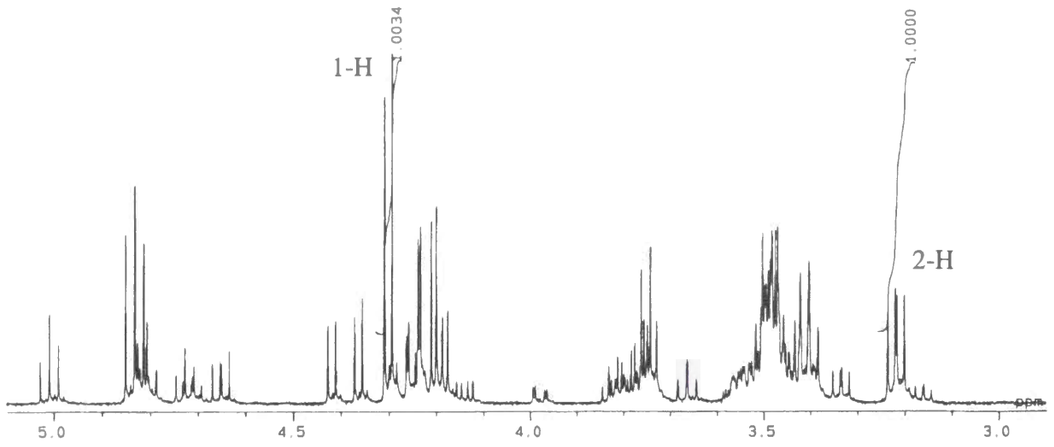

Figure 21. The ^{1}H NMR spectrum of the mixture of octyl 3,6-di-*O*-acetyl-β-D-glucopyranoside and other di-*O*-acetyl-β-D-glucopyranosides in CD_3CN-D_2O.

References and Notes

1 See, for example: *Carbohydrate Recognition in Cellular Function*; Bock, G.; Harnett, S. Ed.; Ciba Foundation Symposium 145, Wiley, New York, 1989.

2 Takayama, S.; McGarvey, G., J.; Wong, C.-H.; *Chem. Soc. Rev.* **1997**, *26*, 407.

3 See, for example: *Preparative Carbohydrate Chemistry*; Hanessian, S., Ed.; Dekker: New York, 1996.

4 Wong, C.-H.; Ye, X.-S.; Zhang, Z. *J. Am. Chem. Soc.* **1998**, *120*, 7137.

5 (a) David, S.; Hanessian, S. *Tetrahedron* **1985**, *41*, 643. (b) Oshima, K.; Kitazono, E.; Aoyama, Y. *Tetrahedron Lett.* **1997**, *38*, 5001.

6 (a) Sugihara, J. M. *Adv. Carbohydr. Chem. Biochem.* **1953**, *8*, 1. (b) Haines, A. H. *Adv. Carbohydr. Chem. Biochem.* **1976**, *33*, 11. (c) Tsuda, Y.; Yoshimoto, K. *J. Synth. Org. Chem. Jpn.* **1984**, *42*, 479.

7 Guibourdenche, C.; Podlech, J.; Seebach, D. *Liebigs Ann.* **1996**, 1121.

8 (a) Tang, T.-H.; Whitfield, D. M.; Douglas, S. P.; Krepinsky, J. J.; Csizmadia, I. G. *Can. J. Chem.* **1992**, *70*, 2434. (b) Whitfield, D. M.; Douglas, S. P.; Tang, T.-H.; Csizmadia, I. G.; Pang, H. Y. S.; Moolten, F. L.; Krepinsky, J. J. *Can. J. Chem.* **1994**, *72*, 2225. (c) Tang, T.-H.; Whitfield, D. M.; Douglas, S. P.; Krepinsky, J. J.; Csizmadia, I. G. *Can. J. Chem.* **1994**, *72*, 1803.

9 (a) Brewster, M. E.; Huang, M.; Pop, E.; Pitha, J.; Dewar, M. J. S.; Kaminski, J. J.; Bodor, N. *Carbohydr. Res.* **1993**, *242*, 53. (b) Houdier, S.; Pérez, S. *J. Carbohydr. Chem.* **1995**, *14*, 1117.

10 (a) Vedejs, E.; Daugulis, O.; Diver, S. T. *J. Org. Chem.* **1996**, *61*, 430. See, also: Vedejs, E; Chen, X. *J. Am. Chem. Soc.* **1996**, *118*, 1809. (b) Oriyama, T.; Hori, Y.; Imai, K.; Sasaki, R. *Tetrahedron Lett.* **1996**, *37*, 8543. (c) Ruble, J. C.; Latham, H. A.; Fu, G. C. *J. Am. Chem. Soc.* **1997**, *119*, 1492. (d) Kawabata, T.; Nagato, M.; Takasu, K.; Fuji, K. *J. Am. Chem. Soc.* **1997**, *119*, 3169. (e) Miller, S. J.; Copeland, G. T.; Papaioannou, N.; Horstmann, T. E.; Ruel, E. M. *J. Am. Chem. Soc.* **1998**, *120*, 1629.

11 (a) Baczko, K.; Plusquellec, D. *Tetrahedron* **1991**, *47*,3817. (b) Liguori, A.; Procopio, A.; Romeo, G.; Sindona, G.; Uccella, N. *J. Chem. Soc., Perkin Trans. 1* **1993**, 1783. (c) Ishihara, K.; Kurihara, H.; Yamamoto, H. *J. Org. Chem.* **1993**, *58*, 3791. (d) Xia, J.; Hui, Y. *Synth. Commun.* **1996**, *26*, 269. (e) Bianco A.; Brufani, M.; Melchioni, C.; Romagnoli, P. *Tetrahedron*

Lett. **1997**, *38*, 651.

12 Bonar-Law, R. P.; Sanders, J. K. M. *J. Am. Chem. Soc.* **1995**, *117*, 259.

13 *Modern Carbohydrate Chemistry*; Binkley, R. W.; Marcel Dekker, New York, 1988, p. 143.

14 Yamabe, S.; Minato, T.; Kawabata, Y. *Can. J. Chem.* **1984**, *62*, 235.

15 Hubbard and Brittain recently reported a detailed mechanistic survey of amine-catalyzed ester formation from an acid chloride and alcohol in dichloromethane. Their aim was to determine whether amine catalysis operated by a nucleophilic-, specific-base-catalyzed-, or general-base-catalyzed mechanism. They examined these mechanistic pathways based on rate information for the amine-catalyzed reactions of benzoyl chloride with alcohols, obtained by using stopped-flow FT-IR spectroscopy. Although they ruled out specific-base catalysis, they failed to draw a decisive conclusion due to several inconsistent results: Hubbard, P.; Brittain, W. J. *J. Org. Chem.* **1998**, *63*, 677.

16 In the case of mannose possessing an axial 2-OH group, the ring oxygen occupies a good position as a hydrogen acceptor, which is not shown in Figure 5 for clarity.

17 Dewar, M. J. S.; Dieter, K. M. *J. Am. Chem. Soc.* **1986**, *108*, 8075.

18 Mohamadi, F.; Richards, N. G. J.; Guida, W. C.; Liskamp, R.; Lipton, M.; Caufield, C.; Chang, G.; Hendrickson, T.; Still, W. C. *J. Comput. Chem.*, **1990**, *11*, 440.

19 Stewart, J. J. P. *J. Comput. Chem.*, **1989**, *10*, 209, and 221.

20 Mizutani, T.; Kurahashi, T.; Murakami, T.; Matsumi, N.; Ogoshi, H. *J. Am. Chem. Soc.*, **1997**, *119*, 8991.

Chapter 4

New Nucleophilic Catalysts for Regioselective Acylation of Unprotected Carbohydrates

Abstract

New nucleophilic catalysts having carboxylic acid functionality were developed for regioselective acylation of unprotected carbohydrates. One of these catalysts was found to acetylate 1-*O*-octyl glucopyranosides and 1-*O*-octyl galactopyranosides regioselectively at position 6 in $CHCl_3$, although it gave nearly 1:1 mixtures of 4- and 6-monoacetates in the case of mannopyranosides. These catalysts were proposed to regulate the proton transfer of esterification reactions and strictly recognize the primary over secondary OH groups without loss of catalytic activity.

Introduction

Highly diverse biological functions of carbohydrates stem from structural diversity of carbohydrate molecules. Due to multiple hydroxy groups appended on chiral five or six-membered rings, relatively a small number of monosaccharides are derivatized to a wide array of complex oligosaccharides, which involve in various important biological phenomena such as cell–cell communication.[1] However, synthetic organic chemistry is not sufficiently mature to handle such diversity. Efficient stereocontrolled glycosidation continues to be under active investigation.[2] Along with this, regioselective transformation of carbohydrates has also been a fundamental problem in carbohydrate chemistry.[3] Discrimination of many OH groups in carbohydrate molecules can be achieved by use of protecting groups. Excellent protecting groups developed so far have enabled the recent development of a designed monosaccharide unit by C.-H. Wong *et. al.* for an efficient orthogonal protection–deprotection sequences.[4] Four different protecting groups introduced to each OH group in galactoside can be deprotected independently in high yield.

Too much dependence on protecting groups, however, is not desirable from economical and operational point of view. But direct functionalization of unprotected carbohydrates is a difficult task and even selective modification of the primary over secondary OH groups in carbohydrates continues to be an important research topic.[5] Large substituents are reliably incorporated to the primary OH group highly regioselectively. But smaller substituents are extremely prone to the nature of carbohydrate substrates. For example, D. Plusquellec *et. al.* reported regioselective incorporation of fatty acid derivatives to the primary 6-OH groups in totally-unprotected glucose, galactose by use of 3-acylthiazolidine-2-thiones (Scheme 1).[5a] Utilization of the same acylating agent and similar reaction conditions to sucrose, on the other hand, results in highly selective acylation of the secondary 2-OH group in the presence of three primary OH groups (Scheme 2).[6] Unusually high reactivity of the 2-OH group in sucrose was ascribed to the high acidity of that hydroxy group due to intramolecular hydrogen bonds.[6, 7] Other than this extreme case, anomalous reactivity of OH groups in unprotected carbohydrates, especially oligosaccharides and nucleosides, has been repeatedly encountered.[3b, 8] These experimental results indicate that attempts to introduce even relatively large substituents to unprotected carbohydrates could possibly lead to disastrous complex mixtures or selectively modified products at utterly unexpected positions. Detailed insight on effect of hydrogen bonds on substitution reaction is

required to correctly understand these phenomena and control regioselectivity in modification of carbohydrates. Reaction of glycosylidene carbenes with diols and triols are closely discussed in terms of intramolecular hydrogen bonding in the recently-published textbook.[9]

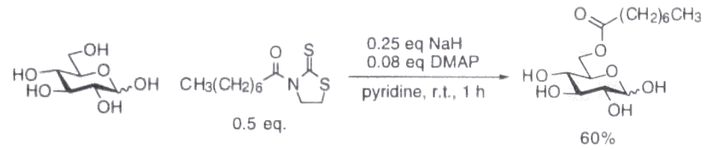

Scheme 1

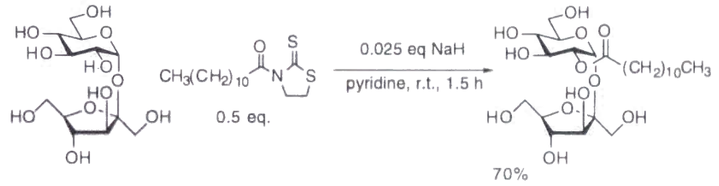

Scheme 2

Enzymes involved in the biosynthesis of oligosaccharides, on contrary, seem to successfully utilize these complex hydrogen bonds to regulate regiochemistry of substitution reactions and assemble monosaccharide units to an immense variety of complex glycoconjugates. These enzymes such as glycosyltransferases have been valuable reagents for the synthesis of saccharides.[10] It is no doubt that effective molecular catalysts for regioselective functionalization of carbohydrates will tremendously contribute to the development of carbohydrate chemistry. But there is no report on small molecular catalysts that rival biological counterparts.[11]

Recently, several groups reported well-designed chiral acylation catalysts for kinetic resolution of secondary alcohols,[12] which has traditionally been achieved by using esterases. Among these catalysts shown in Figure 1, the pioneering example reported by E. Vedejs was highly effective for kinetic resolution of benzylic secondary alcohols, but unfortunately not catalytic probably due to steric hindrance near the nuleophilic site.[12a] G. C. Fu and K. Fuji, on the other hand, developed unique catalyst designs for nucleophilic catalysts and achieved catalytic kinetic resolution of secondary alcohols. G. C. Fu successfully created an effective asymmetric environment around planar nucleophilic catalysts utilizing π-complexation.[12c] K. Fuji devised an enzyme-like induced fit process as shown in Figure 1.[12d] S. J. Miller reported peptide-based catalysts using intermolecular hydrogen-bonding for kinetic resolution.[12e]

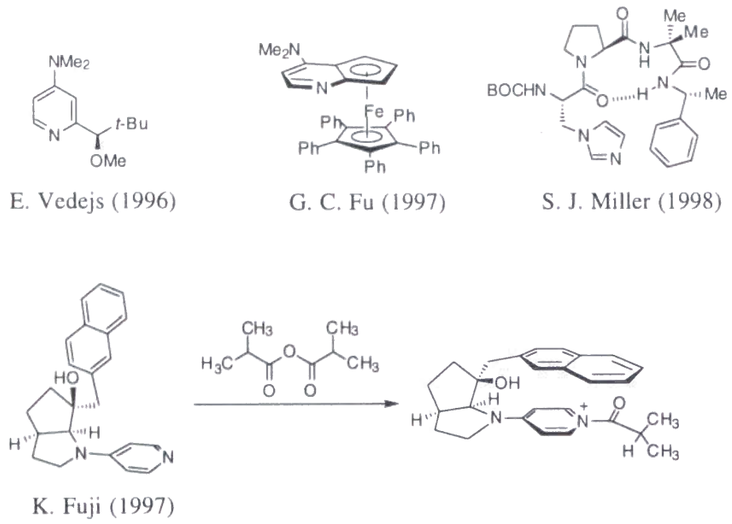

Figure 1. Nucleophilic catalysts for kinetic resolution of secondary alcohols.

Stimulated by these examples, the author applied the same strategy to regioselective acylation of carbohydrates through noncovalent bonding by providing a carbohydrate-recognition site for the nucleophilic catalysts. In this context, the author started investigation of DMAP-catalyzed acetylation of glycosides as described in Chapter 3. The ultimate goal of our work is to construct enzyme-like catalysts effectively utilizing hydrogen bonding with carbohydrate substrates to control substitution reactions. Therefore, DMAP-catalyzed acetylation of glycosides was conducted, keeping the following points in mind.

(1) A small acetyl group was introduced to glycosides to minimize steric influence.

(2) Chloroform, a non-hydrogen-bonding and non-polar solvent, was used in which hydrogen bonding is effective.

(3) Reaction conditions were well-controlled to suppress introduction of more than two acetyl groups.

(4) Neutral, mild reaction conditions and a short reaction period was employed to avoid acetyl-group migration that gives thermodynamically stable regioisomers.

Under the reaction conditions employed in Chapter 3, secondary OH groups of glucoside and mannoside were found to be preferentially acetylated in the presence of the primary OH group at position 6. After control experiments and mechanistic considerations, the author found the importance of catalysis mechanism (nucleophilic- or base-catalyzed-mechanism) and intramolecular hydrogen-bonding network of carbohydrates in

regioselection.

In this Chapter, the author developed new nucleophilic catalysts and attempted regioselective acetylation of the 6-OH group in glycosides under the reaction conditions in which unfavorable hydrogen bonding is operative, as a first step toward successful handling of sugar hydrogen bonds. In order to achieve high regioselectivity together with high catalytic activity, the author proposed a new concept on regiocontrol by regulated proton transfer catalysis and demonstrated a highly regioselective acetylation of unprotected monosaccharides catalyzed by functionalized DMAP.

Results

Catalyst Design. Catalyst design for regioselective acylation of unprotected carbohydrates is based on the regulation of the proton transfer of the esterification reaction as schematically shown in Figure 2. Carboxylic acid functionality is introduced to nucleophilic catalysts in the expectation that (1) acetic anhydride will be readily activated by proton-donating acid catalysis and (2) strict regiocontrol will be achieved through the resulting rigid zwitterionic structure and general base catalysis of the carboxylate ion.

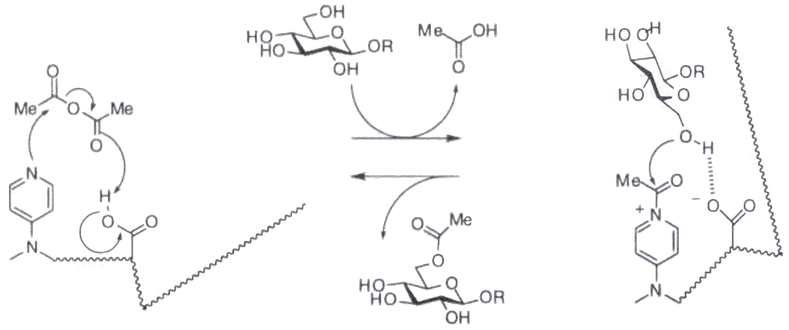

Figure 2. Nucleophilic catalysts for regioselective acylation of carbohydrates by regulating the proton transfer of the esterification reaction.

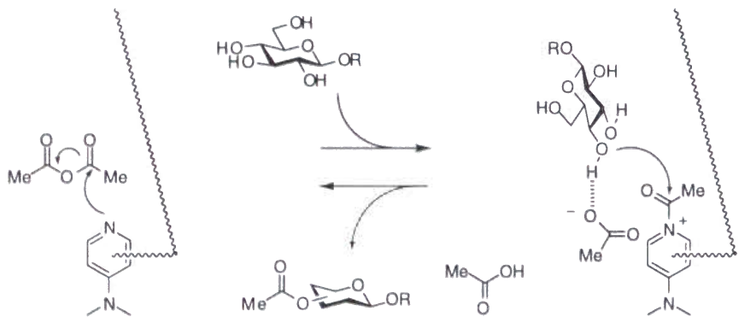

Figure 3. A schematic representation of a nucleophilic catalyst without hydrogen-donating functionality.

Importance of the regulation of the proton transfer catalysis can be readily understood through comparison with the non-regulated system. In Figure 3 is shown a schematic representation of a nucleophilic catalyst without hydrogen-donating

functionality. In this case, the incoming substrate could avoid the constructed steric hindrance, because an acetate counter anion with general base catalysis is not fixed in the catalyst. Any attempt to achieve higher regioselectivity by increasing steric hindrance around the nucleophilic site will result in considerably decreased catalytic activity.

Acetylation of Octyl β-Glc Catalyzed by New Nucleophilic Catalysts. We prepared a series of nuleophilic catalysts **1**, **3**, **4**, and **5**, which have carboxylic acid or sulfate functionality with different methylene spacers to examine the above concept. Catalysts **1** – **4** were synthesized in an analogous way to the reported method.[13] Catalyst **5** was obtained by reaction of the precursory alcohol with chlorosulfonic acid.[14] All compounds were purified by gel-permeation chromatography and characterized by ^{1}H NMR, ^{13}C NMR and high-resolution mass spectroscopy. The DMAP-catalyzed acetylation reaction of unprotected glucopyranoside was conducted under simple reaction conditions, *i.e.* substrates, acetylating agents, and catalysts in chloroform as shown in eq 1. The yield of each regioisomer was readily determined by ^{1}H NMR as already reported[15] and the results are listed in Table 1.

It is noteworthy that the parent DMAP preferentially acetylated 3- and 4-OH groups of octyl β-D-glucopyranoside in the presence of the primary 6-OH group under these reaction conditions.[15] Utilizing **1**, **3**, or **4** as a catalyst, we observed 2.5 – 2.8 times increase in regioselectivity for the primary 6-OH group compared to DMAP. Importance of carboxylic acid functionality is obvious from the observation that catalyst **2**, the methyl ester of **1**, brought no increase in regioselectivity. It should be noted that the length of methylene spacers of catalysts did not affect regioselectivity significantly. The incomplete proton transfer from catalysts to acetic anhydride seems to limit the regioselection. Indeed, catalyst **5** having far more acidic functionality exhibited much higher regioselectivity under exactly the same reaction conditions (eq 1).

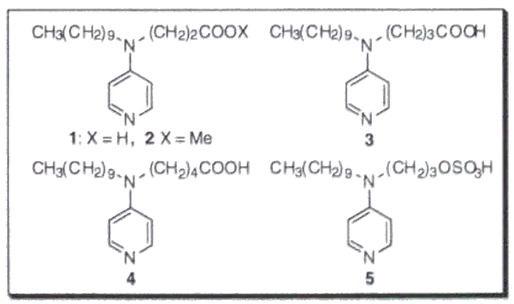

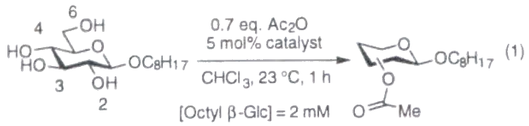

Table 1. Acetylation of Octyl β-D-glucopyranoside Catalyzed by DMAP, **1**, **2**, **3**, **4**, and **5** under Reaction Conditions Shown in Eq 1.

	Product Ratio (Yield of One Regioisomer/Total Yield)				
Catalyst	2-*O*-Acetate	3-*O*-Acetate	4-*O*-Acetate	6-*O*-Acetate	Total Yield (%)[a]
DMAP	0.06	0.42	0.36	0.16	95
1	0.03	0.24	0.28	0.45	92
2	0.06	0.38	0.34	0.22	76
3	0.04	0.32	0.24	0.40	quant.
4	0.02	0.31	0.25	0.42	quant.
5	0.05	0.10	0.14	0.71	92

a. NMR yield of monoacetates relative to Ac_2O.

Regioselective Acetylation of Monosaccharides Catalyzed by 1. Representative monosaccharides were subjected to **1**-catalyzed acetylation reaction under the reaction conditions optimized for octyl β-Glc[16] as shown in eq 2 and the results were listed in Table 2. Both anomers of D-glucose and D-galactose were all catalytically acetylated in a regioselective manner. In the case of galactosides, an excellent regioselection was achieved. On the other hand, the secondary 4-OH group in mannopyranosides exhibited reactivity comparable to that of the primary 6-OH group. Upon replacement of the axial 2-OH group of octyl α-Man by a methoxy group, exactly the same tendency was observed. Surprisingly, the catalyst **1** tolerates anomer stereochemistry of D-glucose and D-galactose and regioselectively acetylates both anomers as anticipated but is extraordinarily sensitive to the stereochemistry of the neighboring 2-position. Although regioselective acetylation of mannosides still remains to be investigated, we would like to point out that no loss of catalytic activity was observed in spite of high regioselectivity, because our catalysts do not have a bulky substituent in the vicinity of a nucleophilic site at all.

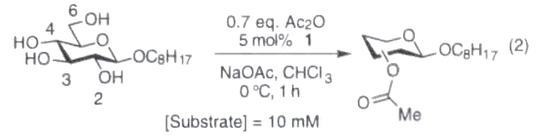

Table 2. Acetylation of Monosaccharides Catalyzed by **1** under Reaction Conditions Shown in Eq 2.

	Product Ratio (Yield of One Regioisomer/Total Yield)				
Substrate	2-*O*-Acetate	3-*O*-Acetate	4-*O*-Acetate	6-*O*-Acetate	Total Yield (%)[a]
β-Glc	b	0.02	0.09	0.89	quant.
α-Glc	b	b	0.12	0.88	95
β-Man	b	0.05	0.42	0.53	88[c]
α-Man	b	0.05	0.43	0.52	83[c]
2-*O*-Me-α-Man	b	b	0.50	0.50	quant.
β-Gal[d]	b	b	b	1.0	95
α-Gal	b	b	b	1.0	quant.

a. NMR yield of monoacetates relative to Ac_2O. b. Not detected. c. Diacetylated octyl α-Man and β-Man were formed in less than 10 %. d. [β-Gal] = 5 mM.

Effect of Added Bases on Regioselectivity. The effect of several basic additives were explored to facilitate the proton transfer from the carboxyl group of the catalyst **1** and improve regioselectivity. As shown in Table 3, addition of soluble bases such as 2,6-lutidine had negligible effect on regioselectivity. Addition of considerable amount of 2,6-lutidine (26 mol%) slightly increased regioselectivity at the cost of catalytic activity.

In contrast, added solid bases, which are insoluble in chloroform, dramatically increased regioselectivity without loss of catalytic activity. Among the insoluble bases listed in Table 3, NaOAc gave the best result and regioselectivity for the primary 6-OH group reached 75%. It is interesting to note that not only inorganic bases but also basic ion exchange resin exhibited similar regioselectivity enhancement. Although the effect of insoluble bases is dramatic, a correlation between regioselectivity and physical

properties of insoluble bases is not clear.

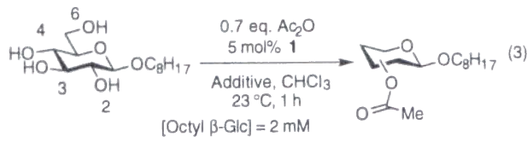

Table 3. Effect of Basic Additives on **1**-Catalyzed Acetylation of Octyl β-D-glucopyranoside as Shown in Eq 3.

	Product Ratio (Yield of One Regioisomer/Total Yield)				
Additive	2-*O*-Acetate	3-*O*-Acetate	4-*O*-Acetate	6-*O*-Acetate	Total Yield (%)[a]
2,6-lutidine (1.8 mol%)	0.06	0.21	0.25	0.47	quant.
2,6-lutidine (6.8 mol%)	0.06	0.26	0.25	0.43	53
2,6-lutidine (26 mol%)	0.06	0.20	0.10	0.64	13
Na_2CO_3	b	0.16	0.19	0.65	quant.
K_2CO_3	0.08	0.09	0.15	0.68	62
LiOAc	b	0.25	0.25	0.50	quant.
NaOAc	b	0.09	0.16	0.75	quant.
$Ca(OH)_2$	0.02	0.32	0.11	0.55	quant.
Amberlyst A21	b	0.24	0.21	0.55	66[c]
Amberlyst A26[d]	b	0.15	0.13	0.72	34[c]
Amberlyst A26[e]	b	0.26	0.18	0.56	55[c]
Amberlyst A26[f]	b	0.28	0.19	0.53	79[c]

a. NMR yield of monoacetates relative to Ac_2O. b. Not detected. c. Diacetylated β-Glc was formed in less than 10 %. d. The OH^- form. e. The CO_3^{2-} form. f. The HCO_3^- form.

In Table 4 are listed the results of other catalysts. The following two points are noteworthy. (1) Catalyst **1** having the shortest methylene spacer almost always gave the best result upon addition of each insoluble base. (2) Catalyst **5** having far more acidic sulfate functionality did not improve its performance upon addition of insoluble bases.

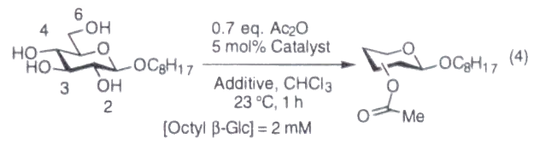

Table 4. Effect of Added bases on **3**-, **4**-, **5**-Catalyzed Acetylation of Octyl β-D-glucopyranoside under Reaction Conditions Shown in Eq 4.

		Product Ratio (Yield of One Regioisomer/Total Yield)				
Additive	Catalyst	2-*O*-Acetate	3-*O*-Acetate	4-*O*-Acetate	6-*O*-Acetate	Total Yield (%)[a]
Na_2CO_3	**3**	0.03	0.24	0.19	0.54	quant.
Na_2CO_3	**4**	0.02	0.22	0.20	0.56	quant.
K_2CO_3	**3**	0.04	0.15	0.12	0.69	quant.
K_2CO_3	**4**	0.03	0.16	0.14	0.67	97
K_2CO_3	**5**	0.08	0.10	0.11	0.71	quant.
NaOAc	**3**	0.03	0.19	0.16	0.62	quant.
NaOAc	**4**	0.02	0.16	0.16	0.66	quant.
NaOAc	**5**	0.07	0.07	0.13	0.73	quant.
$Ca(OH)_2$	**3**	0.03	0.33	0.12	0.52	quant.
$Ca(OH)_2$	**4**	0.04	0.22	0.10	0.64	quant.
Amberlyst A21	**3**	b	0.35	0.23	0.42	78
Amberlyst A21	**4**	0.02	0.31	0.23	0.44	73

a. NMR yield of monoacetates relative to Ac_2O. b. Not detected. c. Diacetylated octyl β-Glc was formed in less than 10 %.

Effect of the Reaction Temperature on Regioselectivity. Temperature effect was remarkably different between catalyst **1** and the parent DMAP. As shown in Table 5, lowering the reaction temperature to 0 °C raised the selectivity to 85% without loss of catalytic activity. Regioselectivity was slightly increased by lowering the reaction temperature to –15 °C and –50 °C, but at –50 °C, the acetylation reaction was considerably suppressed.

On the other hand, lower reaction temperature did not increase product ratio of 6-*O*-acetyl glucopyranoside in the case of DMAP-catalyzed acetylation reaction (Table 6). Rather, a change to the opposite direction was observed and yields of 3- and 4-*O*-acetyl glucopyranoside were slightly increased.

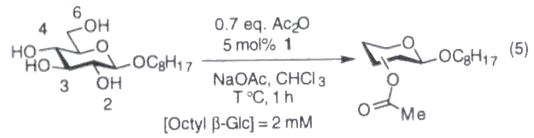

Table 5. Effect of Temperature on **1**-Catalyzed Acetylation of Octyl β-D-glucopyranoside under Reaction Conditions Shown in Eq 5.

	Product Ratio (Yield of One Regioisomer/Total Yield)				
Temperature (°C)	2-*O*-Acetate	3-*O*-Acetate	4-*O*-Acetate	6-*O*-Acetate	Total Yield (%)[a]
23	b	0.09	0.16	0.75	quant.
0	b	0.04	0.11	0.85	quant.
–15	b	0.03	0.10	0.87	98
–50	b	0.02	0.08	0.90	7

a. NMR yield of monoacetates relative to Ac_2O. b. Not detected.

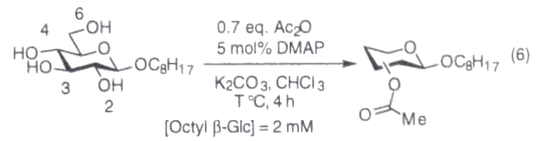

Table 6. Effect of Temperature on DMAP-Catalyzed Acetylation of Octyl β-D-glucopyranoside under Reaction Conditions Shown in Eq 6.

	Product Ratio (Yield of One Regioisomer/Total Yield)				
Temperature (°C)	2-*O*-Acetate	3-*O*-Acetate	4-*O*-Acetate	6-*O*-Acetate	Total Yield (%)[a]
23	0.02	0.42	0.37	0.19	quant.
0	b	0.39	0.38	0.23	83
–23	b	0.41	0.43	0.16	80
–50	0.04	0.39	0.52	0.05	59

a. NMR yield of monoacetates relative to Ac_2O. b. Not detected. c. Not determined.

Effect of Added Tertiary Alcohol on Regioselectivity. In order to probe the nature of the regioselection, effect of added *tert*-amyl alcohol on regioselectivity was investigated (Figure 4). In the case of glucoside and galactoside, no change of regioselectivity was observed in a wide range of the alcohol concentration. Regioselection by **1** is not inhibited by added alcohol, suggesting that sugar hydroxy groups do not participate in intermolecular hydrogen-bonding with the catalyst for regioselection.[17] Regioselectivity for the 6-OH group of mannoside, on the other hand, was gradually increased upon addition of *tert*-amyl alcohol. The observed change was not sensitive enough to be attributed to some kind of *intermolecular* hydrogen bonding. The gradual increase in regioselectivity probably stems from *intramolecular* hydrogen bonding of mannoside.

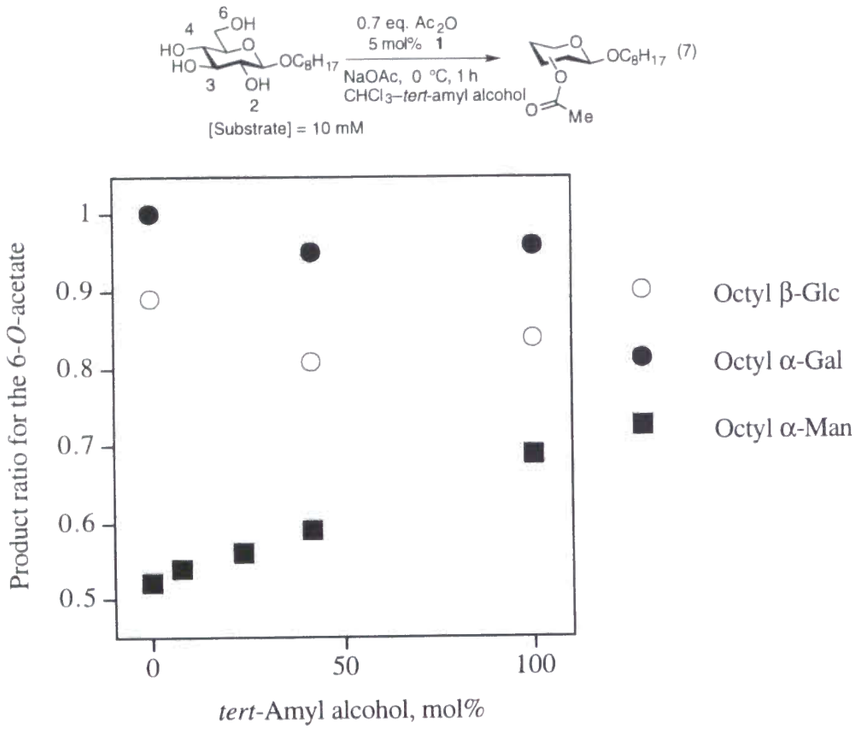

Figure 4. Effect of added *tert*-amyl alcohol on **1**-catalyzed acetylation of octyl β-D-glucopyranoside, octyl α-D-galactopyranoside, and octyl α-D-mannopyranoside under reaction conditions as shown in eq 7.

Acetylation of Monosaccharides Catalyzed by 5. Catalyst **1** exhibited characteristic substrate specificity toward typical monosaccharides. Catalyst **1** acetylated 6-OH groups of glucosides and galactosides in a regioselective manner but failed to introduce an acetyl group regioselectively to 6-OH groups of mannosides as shown in Table 2. To get a detailed insight, **5**-catalyzed acetylation of unprotected monosaccharides was investigated. As already mentioned in Table 1, catalyst **5** acetylated the 6-OH group of octyl β-D-glucopyranoside in moderate regioselectivity (71%) at room temperature without any additives (eq 1). Octyl β-D-galactopyranoside and octyl α-D-mannopyranoside was subjected to the **5**-catalyzed acetylation reaction under the same simple reaction conditions (Table 7).

Table 7. Acetylation of Octyl β-D-galactopyranoside and Octyl α-D-mannopyranoside Catalyzed by **5** under Reaction Conditions Shown in Eq 1.

	Product Ratio (Yield of One Regioisomer/Total Yield)				
Substrate	2-*O*-Acetate	3-*O*-Acetate	4-*O*-Acetate	6-*O*-Acetate	Total Yield (%)[a]
β-Gal	b	c	c	0.88	74
α-Man	b	b	0.48	0.52	32

a. NMR yield of monoacetates relative to Ac_2O. b. Not detected. c. Total product ratio of 3-*O*-acetate and 4-*O*-acetate is 0.12.

Exactly the same tendency was observed for **5**-catalyzed acetylation reactions and catalyst **5** acetylated glucose and galactose preferentially at position 6, but give nearly 1:1 mixture of 4- and 6-monoacetates in the case of mannose. It should be noted that 5-catalyzed acetylation of octyl α-D-mannopyranoside proceeds considerably slowly compared with regioselective acetylation of octyl β-D-glucopyranoside and octyl β-D-galactopyranoside. This means that the 6-OH groups of mannosides are deactivated toward the present acetylating reagent and compete with the acetylation of the 4-OH group.

Possibility of Acetyl Migration Catalyzed by New Nucleophilic Catalyst. Acyl groups introduced to carbohydrates could be readily migrated to the neighboring OH groups under certain reaction conditions. Thus, it is important to ascertain that new nucleophilic catalysts do catalyze regioselective acetylation reaction, not catalyze acetyl migration to the 6-OH group.

Control experiments shown in eq 8 and 9 were conducted. Regioisomeric mixtures containing 3- and 4-*O*-monoacetates as major regioisomers were generated by DMAP-catalyzed acetylation of octyl β-D-glucopyranoside. Catalyst **1** or **5** was then added to the solution to evaluate the acetyl migration catalyzed by **1** or **5**. As shown in Table 8 and 9, **1** or **5**-catalyzed acetyl migration was not observed.

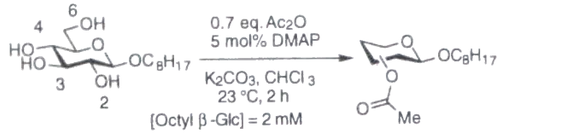

Table 8. The Product Distribution Before (8a) and After (8b) Addition of Catalyst **1**.

	Product Ratio (Yield of One Regioisomer/Total Yield)				
	2-*O*-Acetate	3-*O*-Acetate	4-*O*-Acetate	6-*O*-Acetate	Total Yield (%)[a]
8a	0.02	0.42	0.37	0.19	quant.
8b	b	0.50	0.39	0.11	quant.

a. NMR yield of monoacetates relative to Ac_2O. b. Not detected.

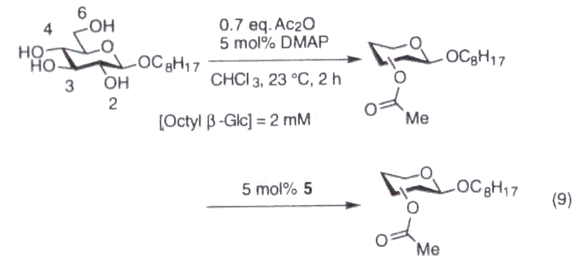

Table 9. The Product Distribution Before (9a) and After (9b) Addition of Catalyst **5**.

	Product Ratio (Yield of One Regioisomer/Total Yield)				
	2-*O*-Acetate	3-*O*-Acetate	4-*O*-Acetate	6-*O*-Acetate	Total Yield (%)[a]
9a	0.06	0.42	0.36	0.16	95
9b	b	0.48	0.41	0.11	quant.

a. NMR yield of monoacetates relative to Ac_2O. b. Not detected.

Effect of the Substrate Concentration on Regioselectivity. Unprotected carbohydrates tend to be self-aggregated especially in non-polar solvent. Self-aggregation of carbohydrates might influence the course of the acetylation reaction. Thus, **1**-catalyzed acetylation reactions at different concentrations were conducted (Table 10). Although regioselectivity was slightly reduced to 72% at an extremely low concentration (0.5 mM), octyl β-D-glucopyranoside was regioselectively acetylated when acetylaion reaction was run at 2, 10, and 20 mM of octyl β-D-glucopyranoside.

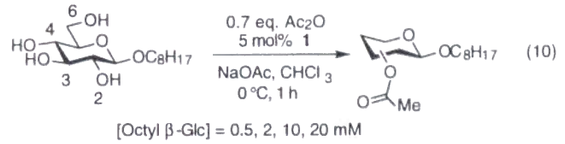

Table 10. Dependence of the Product Distribution on the Concentration of Octyl β-D-Glucopyranoside in the **1**-Catalyzed Acetylation of Octyl β-D-Glucopyranoside.

	Product Ratio (Yield of One Regioisomer/Total Yield)				
[β-Glc] (mmol / L)	2-*O*-Acetate	3-*O*-Acetate	4-*O*-Acetate	6-*O*-Acetate	Total Yield (%)[a]
0.5	b	0.14	0.14	0.72	quant.
2	b	0.04	0.11	0.85	quant.
10	b	0.02	0.10	0.88	quant.
20	b	0.02	0.09	0.89	quant.

a. NMR yield of monoacetates relative to Ac_2O. b. Not detected.

Discussion

Mechanism of Regiocontrol. As shown in Table 1, proton-donating functionalities in new nucleophilic catalysts are clearly important for regioselective acetylation of the primary 6-OH group of octyl β-D-glucopyranoside from the comparison of the observed regioselectivity by the parent DMAP, carboxylic-acid-appended DMAPs (**1**, **3**, and **4**), the methyl ester of **1** (**2**), and the sulfate-appended DMAP (**5**). Regioselectivity is determined in a kinetic sense, because acetyl migration catalyzed by these catalysts was not observed at all.

As for the mechanism of regioselective acylation catalyzed by these simple molecular catalysts, three possibilities are considered.

(1) Regiocontrol by regulated proton transfer catalysis as anticipated.

(2) Regiocontrol by hydrogen bonding between acid functionality of catalysts and sugar hydroxy groups.

(3) Regiocontrol by absorbed catalysts on the surface of basic solids or glass due to acid/base dual functionalities of these catalysts.

The possibility (2) is ruled out because regiocontrol was enhanced by addition of insoluble bases (Table 3 and 4), which disturb hydrogen bondings. In addition, regioselectivity was not reduced by addition of alcohol (Figure 5). The possibility (3) is also denied because addition of insoluble bases considerably increased regioselectivity in **1**-, **3**-, and **4**-catalyzed acetylation reactions but had almost no effect in the case of sulfate-appended DMAP, which is more tightly bound on the base surface via highly acidic sulfate functionality (Table 3 and 4).

Regiocontrol by regulated proton transfer catalysis, on the other hand, is consistently supported by several experimental results. As shown in Table 1, introduction of carboxylic acid or sulfate functionality to DMAP increased regioselectivity at 2.5 – 2.8 times, 4.4 times, respectively. Linear correlation between proton-donating ability and regioselectivity strongly supports the mechanism (1). Addition of insoluble bases improve the performance of carboxylic-acid-appended DMAPs to a extent comparable to catalyst **5**, indicating that the proton transfer from catalysts to acetic anhydride is facilitated in the case of catalyst **1**, **3**, and **4** by added bases.

Highly regioselective acetylation reactions without loss of catalytic activity demonstrated herein are based on the directionally-restricted deprotonation, which is concerted with the attack of the alcohol oxygen to the carbonyl group. As shown in Figure 5, the *fixed* carboxylate ion functioning as a general base catalyst forced substrates

to attack the carbonyl group from the direction of the pyridine ring, causing the severe steric repulsion between acetylating agents and incoming substrates to prevent the 2°OH acetylation. In contrast, an unmodified DMAP and catalyst **2**, both having a *free* acetate ion as a general base catalyst, comparably or even preferentially acetylate secondary OH groups in unprotected monosaccharides in the presence of the primary 6-OH group due to the intramolecular hydrogen bonding network.[15]

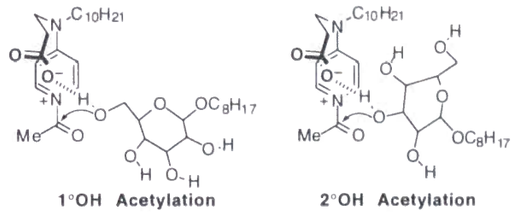

Figure 5. Proposed mechanism for regioselective acylation of carbohydrates catalyzed by **1**.

Function of Added Insoluble Bases. The performance of catalyst **1** is remarkably improved by addition of solid bases which are insoluble in chloroform. Addition of a small amount of rather weakly basic NaOAc dramatically increased regioselectivity. In contrast, a soluble organic base has practically no effect on regioselectivity, irrespective of its amount. Insolubility in reaction medium seems important for regioselectivity enhancement in **1**-catalyzed acetylation reaction.

The most rational explanation is that added insoluble bases suppress non-selective acetylation pathway by removing an acetyl pyridinium agent with *free* acetate (B) from the solution phase (Figure 6). Deprotonation liberates an acetyl pyridinium agent with *intramolecularly-bound* counter anion (C), which regioselectively acetylates unprotected carbohydrates via regulated proton transfer catalysis. Regioselectivity enhancement is varied depending on added insoluble bases, which probably reflect the reactivity of the absorbed acetyl pyridinium salt on different solid surfaces.[18]

Substrate Specificity of Catalyst 1. Mannoside, a hexose with an axial 2-OH group, is not a good substrate for acetylation reaction catalyzed by newly-developed nucleophilic catalysts. **1**- and **5**-catalyzed acetylation of mannosides gives nearly 1:1 mixtures of 4- and 6-*O*-monoacetates, probably due to the reduced reactivity of 6-OH groups of mannosides. **1**-catalyzed acetylation of 2-*O*-methyl α-mannoside also gives 1:1 mixtures of 4- and 6-*O*-monoacetates, suggesting that proton accepting nature of an axial substituent at position 2 is responsible. Addition of *tert*-amyl alcohol gradually

increased regioselectivity for the 6-OH group of mannoside.

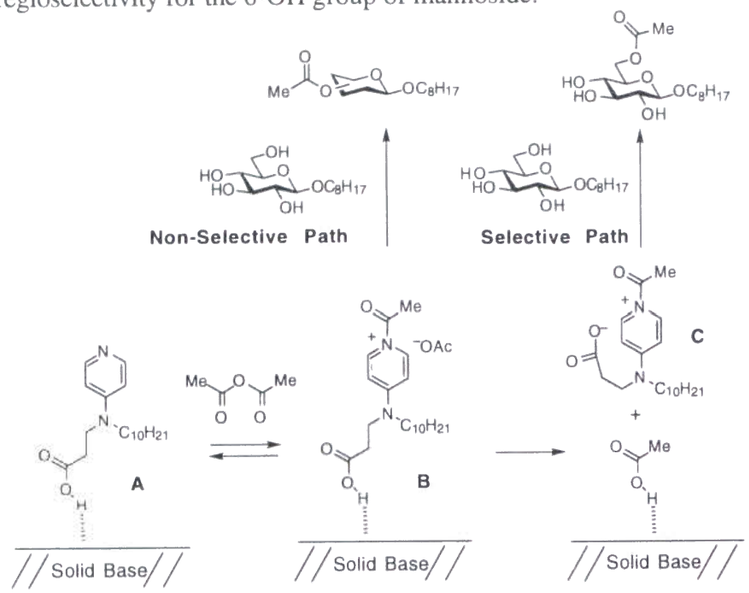

Figure 6. Proposed mechanism for improved regioselectivity by addition of insoluble bases.

From these experimental observations, the decrease of the selectivity to mannosides seems to be attributed to the intramolecular hydrogen bonding between the 6-OH group and the 2-OH group of mannosides (Figure 7). Catalyst **1** recognizes steric differences of each OH group in mannosides and tends to preferentially acetylate the primary 6-OH group from a viewpoint of steric requirements. However, intramolecular hydrogen-bonding network is a dominant factor in DMAP-catalyzed acetylation reaction of unprotected carbohydrates as already reported. From a viewpoint of intramolecular hydrogen-bonding network, the 4-OH group of mannoside is more reactive than the 6-OH group which is intramolecularly hydrogen-bonded to the axial 2-OH or 2-OMe group.[19]

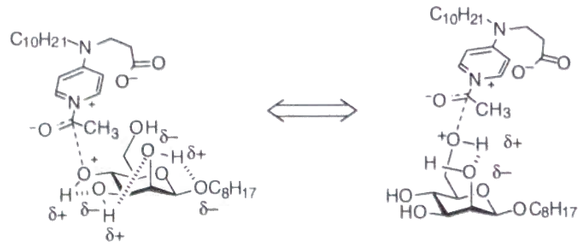

Figure 7. Effect of intramolecular hydrogen-bonding network on the **1**-catalyzed acetylation of mannosides.

Conclusions

New nucleophilic catalysts having proton-donating functionality have been developed for regioselective acylation of unprotected carbohydrates. These catalysts were expected to regulate proton transfer catalysis and introduce an acyl group to the primary 6-OH group in unprotected monosaccharides without loss of catalytic activity. As anticipated, one of these catalysts regioselectively acetylated both anomers of D-glucose and D-galactose. It should be stressed out that the high regioselectivity does not sacrifice catalytic activity. Along with the demonstrated performance of these catalysts, several control experiments consistently support the proposed mechanism for regiocontrol by regulated proton transfer catalysis.

Although presented here are simple acetylation reactions of unprotected monosaccharides, the new concept which is proposed and clearly demonstrated in this chapter will surely give a solid foundation for catalyst designs for other important regioselective transformations of polyfunctional biomolecules.

Experimental Section

Instrumentation. ^{1}H and ^{13}C NMR spectra were recorded using a JEOL A-500 spectrometer. ^{1}H and ^{13}C NMR chemical shifts in $CDCl_3$ or CD_3OD were referenced to $CHCl_3$ (7.24 ppm and 77.0 ppm, respectively) or CH_3OH (3.30 ppm and 49 ppm, respectively). NMR data were collected at 30 °C. Gel permeation chromatography (CPC) was performed on Recycling Preparative HPLC (LC-908 or LC-918) equipped with a JAIGEL-2H column (Japan Analytical Industry) and a refractive index detector; flow rate, 3.8 mL min^{-1}; mobile phase, chloroform containing 1% of triethylamine.

Materials. Octyl β-D-glucopyranoside and octyl α-D-glucopyranoside were purchased from Wako Pure Chemical Industries and SIGMA, respectively and used as received. Preparations of other octyl glycopyranosides were already reported.[20] Chloroform stabilized with 2-methyl-2-butene was purchased from Tokyo Chemical Industry and dried over molecular sieves, 3Å. Acetic anhydride was purified by distillation after azeotropic removal of acetic acid with toluene. 4-Dimethylaminopyridine (DMAP) was recrystallized from benzene and dried in vacuo. Na_2CO_3, K_2CO_3, LiOAc, NaOAc, and KOAc were dried in vacuo over P_2O_5. Column chromatography was carried out with Silica Gel 60N (spherical, neutral, 40−100 μm) from Kanto Chemicals. $CDCl_3$ was completely deacidified by passing through activated alumina just before use.

General Procedure for the DMAP-Catalyzed Acetylation. In every experiment, it was confirmed that water content of chloroform was less than 5 ppm. Stock solutions of catalyst **1** and acetic anhydride were prepared beforehand by dissolving **1** (5.2 mg, 17 μmol) in chloroform (1 mL) and acetic anhydride (62.2 mg, 609 μmol) in chloroform (2.7 mL), respectively.

Octyl β-D-glucopyranoside (3.0 mg, 10 μmol) was dissolved in chloroform (1 mL) under Ar. NaOAc (200 mg) was added to the solution. Then the catalyst stock solution (31 μL, 0.53 μmol) was added to the solution via microsyringe. The solution was stirred well with a magnetic stirrer. The temperature was kept at 0 °C during the acetylation reaction. Finally, the acetic anhydride stock solution (32 μL, 7.2 μmol) was added to initiate the acetylation reaction. After being stirred for 1 h, the reaction was quenched with methanol (0.2 mL). After 5 min at 0 °C, the reaction mixture was passed through a silica gel short column (1 g) to remove the catalyst. The reaction flask was washed well with chloroform and the washings were also put on the column.

Monoacetylated sugars, together with the remaining unprotected sugar, were eluted by ethyl acetate−methanol solvent (4:1; 15 mL). The solvent was evaporated off and the product was dried in vacuo. The product was taken up in chloroform (2 mL) and passed through a polypropylene filter to remove traces of silica gel. The chloroform was then evaporated off. The sample was completely dried in vacuo at room temperature for 4 h and subjected to NMR analysis.

Catalyst 1, 2. **1** and **2** were synthesized according to the literature.[13] **1** and **2** were purified by GPC using chloroform containing 1% of triethylamine as an eluent. Compounds were passed through a column several times to ensure purity as shown in Figure 8. Purified DMAP derivatives were dissolved in ethyl acetate and washed with distilled water three times and then saturated NaCl solution to remove a trace of triethylamine hydrochloride. Organic layer was dried over Na_2SO_4. The solvent was evaporated off and products were dried in vacuo at 60 °C for 12 h.

1: ^{1}H NMR (CD_3OD, 500 MHz) δ 8.038 (d, J = 7.5 Hz, 2H), 6.980 (d, J = 7.5 Hz, 2H), 3.806 (t, J = 7.3 Hz, 2H), 3.565 (t, J = 8 Hz, 2H), 2.479 (t, J = 7.3 Hz, 2H), 1.700-1.600 (m, 2H), 1.400-1.240 (m, 14H), 0.887 (t, J = 7 Hz, 3H)

^{13}C NMR (CD_3OD, 125.65 MHz) 178.389, 157.701, 140.822, 108.496 (signals in the methylene region are omitted.)

t_R = 44 min

HRMS calcd for $C_{18}H_{30}N_2O_2$ m/z 306.2307, found 306.2303 (EI)

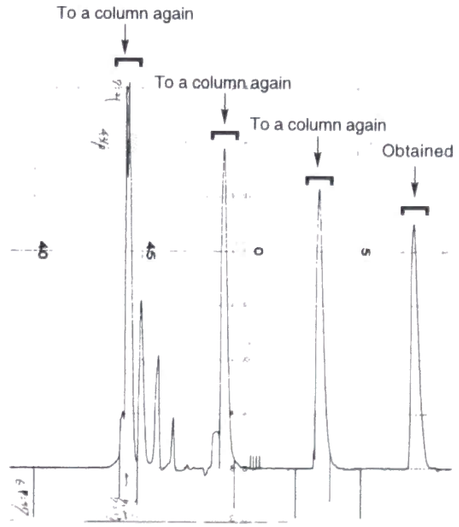

Figure 8. GPC chart of catalyst **1**.

2: ^{1}H NMR ($CDCl_3$, 500 MHz) δ 8.179 (d, J = 6.5 Hz, 2H), 6.432 (d, J = 7 Hz, 2H), 3.672 (s, 3H), 3.621 (t, J = 7.3 Hz, 2H), 3.267 (t, J = 7.8 Hz, 2H), 2.572 (t, J = 7.5 Hz, 2H), 1.600-1.500 (m, 2H), 1.300-1.190 (m, 14H), 0.858 (t, J = 6.8 Hz, 3H)

^{13}C NMR ($CDCl_3$, 125.65 MHz) 172.030, 151.985, 150.109, 106.513 (signals in the methylene region are omitted.)

t_R = 48 min

HRMS calcd for $C_{19}H_{32}N_2O_2$ *m/z* 320.2464, found 320.2462 (EI)

Catalyst 3, 4. Similar compounds which differ only in the methylene length were already synthesized.[13] So, **3** and **4** were synthesized following the reported procedure, except for the reduction of amide bonds (eq 11). Both amide and ester functionality were reduced by the literature method. To prevent reduction of ester functionality, the following method was employed.

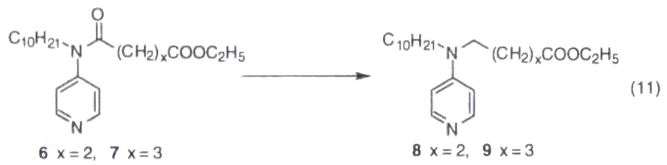

6 x = 2, **7** x = 3 → **8** x = 2, **9** x = 3 (11)

Catalyst 3. **6** (528.9 mg, 1.46 mmol) was dissolved in THF (14.6 mL). Borane-THF complex (1 M in THF, 14.6 mL, 14.6 mmol) was added at room temperature and the reaction mixture was heated at 60 °C for 5 min. Excess borane was then decomposed by the careful slow addition of 5% HCl in ethanol (40 mL) at 0 °C. The mixture was stirred at room temperature for 3 h. After evaporation of the solvent, the residue was dissolved in water (10 mL). The solution was made basic with 1M NaOH (50 mL) and then extracted with ethyl acetate (50 mL × 3). The combined organic phase was washed with saturated aqueous NaCl (20 mL × 2) and dried over Na_2SO_4. The solvent was evaporated off and the residue was purified by flash column chromatography (chloroform : hexane : triethylamine = 5 : 20 : 1) to yield **8** contaminated with **6**. Without further purification, the mixture was subjected to the hydrolysis step to yield crude **3**. Purification was performed in exactly the same way as catalyst **1** to give **3** (37.8 mg, 0.118 mmol) in 8% yield.

3: ^{1}H NMR (CD_3OD : $CDCl_3$ = 1 : 1, 500 MHz) δ 8.158 (d, J = 6.5 Hz, 2H), 7.077 (d, J = 6 Hz, 2H), 3.656 (t, J = 7.8 Hz, 2H), 3.609 (t, J = 7.8 Hz, 2H), 2.444 (t, J = 6.3 Hz, 2H), 2.08-2.00 (m, 2H), 1.80-1.70 (m, 2H), 1.55-1.35 (m, 14H), 1.015 (t, J = 7 Hz, 3H)

^{13}C NMR (CD_3OD : $CDCl_3$ = 1 : 1, 125.65 MHz) 180.000, 156.516, 141.422, 107.813

(signals in the methylene region are omitted.)

t_R = 42 min

HRMS calcd for $C_{19}H_{32}N_2O_2$ *m/z* 320.2464, found 320.2457 (EI)

Catalyst 4. **7** (313.1 mg, 0.83 mmol) was dissolved in THF (29 mL). Borane-THF complex (1 M in THF, 5 mL, 5 mmol) was added at room temperature and the reaction mixture was heated at 60 °C for 30 min. Excess borane was then decomposed by the careful slow addition of 5% HCl in ethanol (18 mL) at 0 °C. The mixture was stirred at room temperature for 3 h. After the evaporation of the solvent, the residue was dissolved in water (10 mL). The solution was made basic with 1M NaOH (50 mL) and then extracted with ethyl acetate (50 mL × 3). The combined organic phase was washed with saturated aqueous NaCl (20 mL × 2) and dried over Na_2SO_4. The solvent was evaporated and the residue was purified by flash column chromatography (chloroform : hexane : triethylamine = 5 : 20 : 1) to yield **9** contaminated with **7**. Without further purification, the mixture was subjected to the hydrolysis step to yield crude **4**. Purification was performed in exactly the same way as catalyst **1** to give **4** (58.5 mg, 0.175 mmol) in 21% yield.

4: ^{1}H NMR (CD_3OD : $CDCl_3$ = 10 : 1, 500 MHz) δ 7.976 (d, J = 7 Hz, 2H), 6.833 (d, J = 7.5 Hz, 2H), 3.50-3.40 (m, 4H), 2.197 (t, J = 6.8 Hz, 2H), 1.65-1.55 (m, 6H), 1.35-1.15 (m, 14H), 0.832 (t, J = 7 Hz, 3H)

^{13}C NMR (CD_3OD : $CDCl_3$ = 10 : 1, 125.65 MHz) 181.498, 157.142, 141.793, 108.216 (signals in the methylene region are omitted.)

t_R = 45 min

HRMS calcd for $C_{20}H_{34}N_2O_2$ *m/z* 334.2620, found 334.2611 (EI)

Catalyst 5. **5** was synthesized according to eq 12 as follows. To a suspension of $LiAlH_4$ (18 mg, 0.47 mmol) in ether (0.5 mL) was added a solution of **2** (101.4 mg, 0.316 mmol) in ether (1.5 mL). The reaction mixture was stirred at room temperature for 4 h and then excess $LiAlH_4$ was decomposed by addition of ethyl acetate and then water. The aqueous solution was extracted with ethyl acetate (10 mL × 3) and the combined organic layer was dried over Na_2SO_4. After evaporation of the solvent, the residue was purified by flash column chromatography (chloroform : hexane : triethylamine = 5 : 2 : 1) to yield **10** (69.1 mg, 0.236 mmol) in 75% yield.

10: ^{1}H NMR ($CDCl_3$, 300 MHz) δ 8.060 (d, J = 6 Hz, 2H), 6.444 (d, J = 6.6 Hz, 2H), 4.200 (br s, 1H), 3.664 (t, J = 5.7 Hz, 2H), 3.419 (t, J = 7.2 Hz, 2H), 3.245 (t, J = 7.7 Hz, 2H), 1.84-1.74 (m, 2H), 1.59-1.45 (m, 2H), 1.35-1.10 (m, 14H), 0.840 (t, J = 6.6 Hz, 3H)

^{13}C NMR ($CDCl_3$, 75 MHz) 152.847, 149.234, 106.498 (signals in the methylene region

were omitted.)

HRMS calcd for $C_{18}H_{32}N_2O$ *m/z* 292.2515, found 292.2520 (EI)

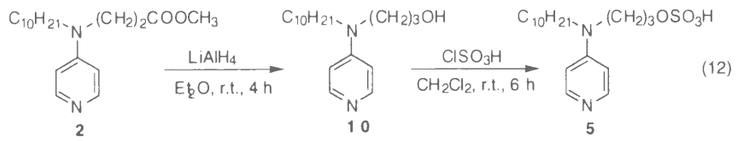

(12)

10 (69.1 mg, 0.236 mmol) was converted to **5** in exactly the same manner as the reported method[14] for the preparation of 10-[N-butyl-N-(4-pyridinyl)amino] decyl sulfate. Purification was performed in exactly the same way as catalyst **1** to give **5** (7.7 mg, 0.02 mmol) in 9% yield. The ^{1}H NMR spectrum showed that at least two species were present in $CDCl_3$ / CD_3OD (1 : 1), although the product was confirmed to be pure enough to be a single peak with the repeated GPC purification. We assigned signals from the minor species to the equilibrated zwitterion as shown in Figure 9. Observed four non-equivalent pyridine protons support the above assignment.

t_R = 41 min

HRMS calcd for $C_{18}H_{32}N_2O_4S \cdot H^+$ *m/z* 373.2161, found 373.2159 (FAB)

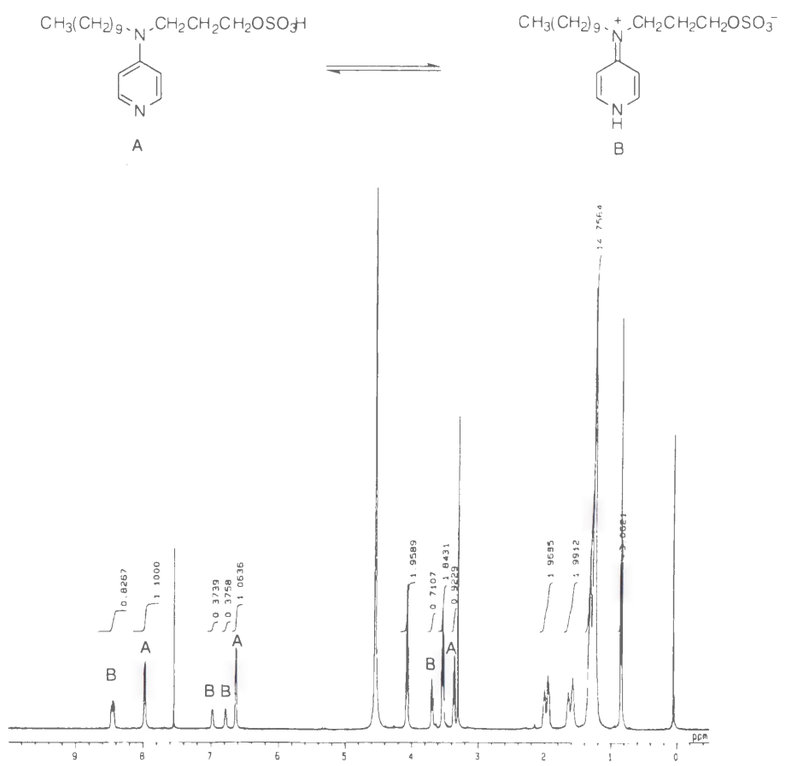

Figure 9. ^{1}H NMR spectrum of catalyst **5** in $CDCl_3$ / CD_3OD (1 : 1).

Structural Characterization of Partially Acetylated Octyl 2-*O*-Me-α-Man. The structural characterization relied on analysis of coupling constants and the phase-sensitive DQF-COSY spectrum as follows (Figure 10).

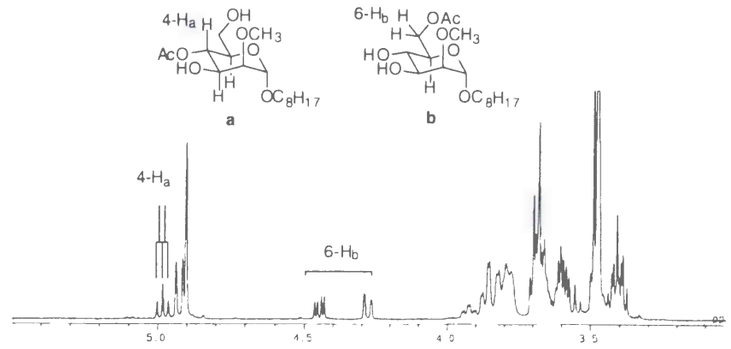

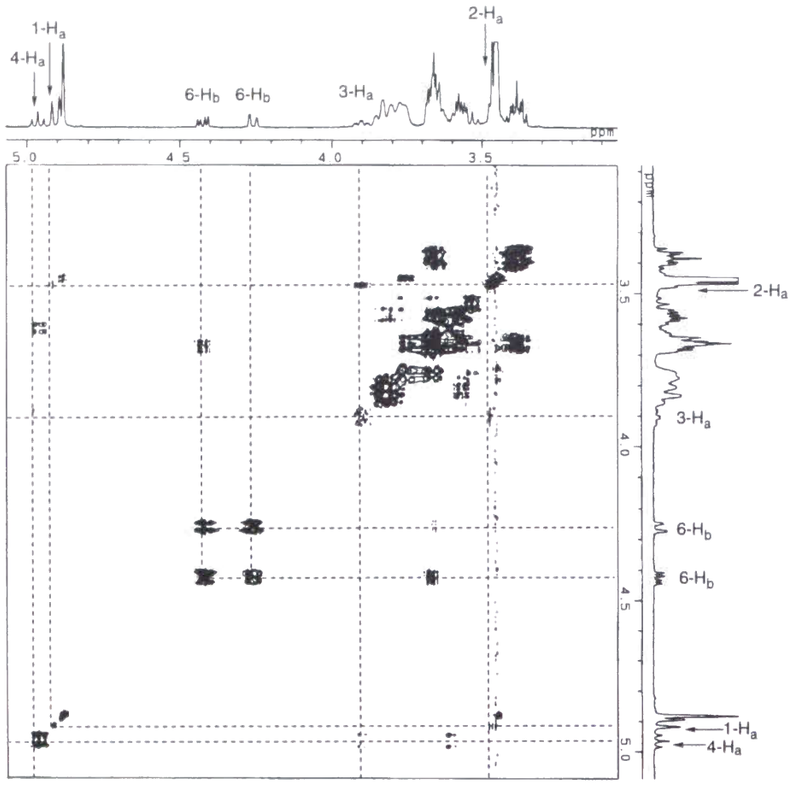

Figure 10. ^{1}H NMR and DQF-COSY spectra of the mixture of octyl 2-*O*-methyl-α-D-mannopyranoside and 4-, or 6-*O*-acetyl-2-*O*-methyl-α-D-mannopyranosides.

References and Notes

1 See, for example: *Carbohydrate Recognition in Cellular Function*; Bock, G.; Harnett, S. Ed.; Ciba Foundation Symposium 145, Wiley, New York, 1989.

2 Reviews: Toshima, K.; Tatsuta, K. *Chem. Rev.* **1993**, *93*, 1503.

3 Reviews: (a) Sugihara, J. M. *Adv. Carbohydr. Chem. Biochem.* **1953**, *8*, 1. (b) Haines, A. H. *Adv. Carbohydr. Chem. Biochem.* **1976**, *33*, 11. (c) Haines, A. H. *Adv. Carbohydr. Chem. Biochem.* **1981**, *39*, 13. See, also: *Preparative Carbohydrate Chemistry*; Hanessian, S., Ed.; Dekker: New York, 1996.

4 Wong, C.-H.; Ye X.-S.; Zhang, Z *J. Am. Chem. Soc.* **1998**, *120,* 7137.

5 (a) Baczko, K.; Plusquellec, D. *Tetrahedron* **1991**, *47*,3817. (b) Liguori, A.; Procopio, A.; Romeo, G.; Sindona, G.; Uccella, N. *J. Chem. Soc., Perkin Trans. 1* **1993**, 1783. (c) Ishihara, K.; Kurihara, H.; Yamamoto, H. *J. Org. Chem.* **1993**, *58*, 3791. (d) Xia, J.; Hui, Y. *Synth. Commun.* **1996**, *26*, 269. (e) Bianco A.; Brufani, M.; Melchioni, C.; Romagnoli, P. *Tetrahedron Lett.* **1997**, *38*, 651.

6 Chauvin, C.; Baczko, K.; Plusquellec, D. *J. Org. Chem.* **1993**, *58*, 2291.

7 Houdier, S.; Pérez, S. *J. Carbohydr. Chem.* **1995**, *14*, 1117.

8 Guibourdenche, C.; Podlech, J.; Seebach, D. *Liebigs Ann.* **1996**, 1121.

9 Vasella, A. In *Bioorganic Chemistry: Carbohydrates*; Hecht, S. M. Ed.; Oxford University Press: New York, 1999; p 56.

10 See, for example: Wong, C.-H.; Halcomb, R., L.; Ichikawa, Y.; Kajimoto, T. *Angew. Chem., Int. Ed. Engl.* **1995**, *34*, 412. For a review of enzymatic transformation in carbohydrate chemistry including regioselective acylation, see: Drueckhammer, D. G.; Hennen, W. J.; Pederson, R. L.; Barbas, C. F., III; Gautheron, C. M.; Krach, T.; Wong, C.-H. *Synthesis* **1991**, 499.

11 U. Lüning *et. al.* recently reported selective acylation of diols including a carbohydrate derivative catalyzed by bimacrocyclic pyridines: Lüning, U.; Petersen, S.; Schyja, W.; Hacker, W.; Marquardt, T.; Wagner, K.; Bolte, M. *Eur. J. Org. Chem.* **1998**, 1077.

12 (a) Vedejs, E.; Daugulis, O.; Diver, S. T. *J. Org. Chem.* **1996**, *61*, 430. See, also: Vedejs, E; Chen, X. *J. Am. Chem. Soc.* **1996**, *118*, 1809. (b) Oriyama, T.; Hori, Y.; Imai, K.; Sasaki, R. *Tetrahedron Lett.* **1996**, *37*, 8543. (c) Ruble, J. C.; Latham, H. A.; Fu, G. C. *J. Am. Chem. Soc.* **1997**, *119*,

1492. (d) Kawabata, T.; Nagato, M.; Takasu, K.; Fuji, K. *J. Am. Chem. Soc.* **1997**, *119*, 3169. (e) Miller, S. J.; Copeland, G. T.; Papaioannou, N.; Horstmann, T. E.; Ruel, E. M. *J. Am. Chem. Soc.* **1998**, *120*, 1629.

13 Delaney, E. J.; Wood, L. E.; Klotz, I. M. *J. Am. Chem. Soc.* **1982**, *104*, 799.

14 Katritzky, A. R.; Duell, B. L.; Seiders, R. P.; Durst, H. D. *Langmuir* **1987**, *3*, 976.

15 Kurahashi, T.; Mizutani, T.; Yoshida, J. *J. Chem. Soc., Perkin Trans. 1* **1999**, 465.

16 Among new nucleophilic catalysts, catalyst **1** gave the best result in the acetylation reaction of octyl β-D-glucopyranoside in the presence of basic additives. As a basic additive to facilitate the proton transfer, NaOAc was selected among the basic additives examined. Finally, lowering the reaction temperature to 0 °C and increasing the glucoside concentration to 10 mM gave rise to the selectivity (89%) without loss of catalytic activity. For the details, see the following sections.

17 S. J. Miller *et. al.* reported peptide-based asymmetric catalysts for kinetic resolution of secondary alcohols having amide functionality, in which transition state hydrogen bonding was claimed to play a role in differentiation. They observed completely nonselective reaction when the reaction was run in a chloroform–*t*-BuOH medium. See, ref. 12e.

18 Several groups reported polymer-bound (dialkylamino)pyridine catalysts. They observed that activities (per mole of heterocycle) of these polymeric acylation catalysts generally did not exceed, but were sometimes comparable to those of their low molecular weight analogues. (a) Tomoi, M.; Akada, Y.; Kakiuchi, H. *Makromol. Chem., Rapid Commun.* **1982**, *3*, 537. (b) Guendouz, F.; Jacquier, R.; Verducci, J. *Tetrahedron Lett.* **1984**, *25*, 4521. (c) Menger, F. M.; McCann, D. J. *J. Org. Chem.* **1985**, *50*, 3928. (d) Deratani, A.; Darling, G. D.; Horak, D.; Fréchet, J. M. J. *Macromolecules* **1987**, *20*, 767.

19 We observed that 3- and 4-OH groups of glucosides and mannosides were preferentially acetylated in the presence of the primary 6-OH group in DMAP-catalyzed acetylation reaction, and attributed extraordinary high reactivities of 3- and 4-OH groups to delocalized positive charge through hydrogen-bonding network in the transition state. In Figure 7, acetylation of the 4-OH group is more favorable in terms of intramolecular hydrogen-bonding network than acetylaion of the 6-OH group. See, ref. 15 or Chapter 3.

20 Mizutani, T.; Kurahashi, T.; Murakami, T.; Matsumi, N.; Ogoshi, H. *J. Am. Chem. Soc.*, **1997**, *119*, 8991.

Chapter 5

Regioselective Acylation of Polyhydroxy Compounds Catalyzed by Functionalized DMAP in Polar Solvent

Abstract

New nucleophilic catalysts described in Chapter 4 were applied for regioselective acylation of polyhydroxy compounds in polar solvent. Polyhydroxy compounds of natural origin such as oligosaccharides are notoriously insoluble in most organic solvents. Thus, polar solvents which dissolve unprotected monosaccharides were explored as a reaction medium for the new nucleophilic catalysts. Among polar solvents tested, *tert*-amyl alcohol was found to be suitable solvent for our catalytic system. Several polyhydroxy compounds were regioselectively acetylated in relatively high yield.

Introduction

Polyhydroxy biomolecules such as saccharides and sterols, abundant in Nature, are attractive for combinatorial drug discoveries, construction of artificial supramolecular assemblies and so on. Due to multiple OH groups appended on enantiomerically-pure and conformationally-rigid platforms, a wide array of spationally-well-defined derivatives could be produced through regiospecific introduction of various substituents.

Regioselective transformation of these polyhydroxy compounds, however, poses a challenging problem for synthetic organic chemistry.[1] This usually requires multi-step protection-deprotection procedures and even selective acylaiton of the primary OH groups in the presence of other secondary OH groups has suffered from unexpectedly low yield. Until now, several methodologies for regioselective acylation of polyhydroxy compounds have been reported.

Several groups reported enzymatic procedures for regioselective acylation of sugars.[2] For example, A. M. Klibanov *et. al.* utilized porcine pancreatic lipase as a catalyst for transesterifications between various sugars and trichloroethyl carboxylates in pyridine.[2a] They obtained 6-*O*-acetyl glucose in 33% yield according to their procedure (eq 1).

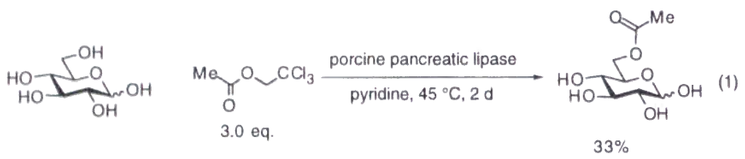

Several chemical methodologies for regioselective acylation have also been reported.[3] D. Plusquellec[3a] and S. Yamada[3b] utilized 3-acylthiazolidine-2-thiones as acylating agents for regioselective acylation of monosaccharides (eq 2) and sterols (eq3), respectively. H. Yamamoto[3d] reported an extremely simple method by running the acetylation reaction at controlled low temperature using acetyl chloride in collidine (eq 4). A. Bianco[3f] recently reported a new method of regioselective acetylation in exceptionally high yield by using methyl orthoacetate and the chloride of rare earths, dispersed on silica, as catalysts (eq 5). Very recently, M. J. Whitcombe reported imprinted polymers for regioselective modification of sterols.[3g]

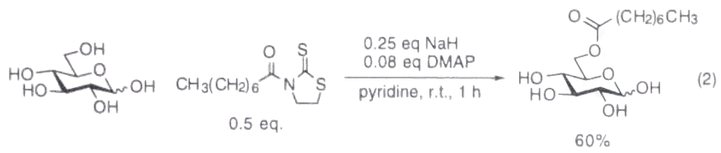

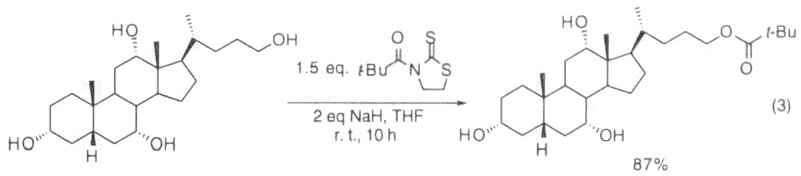

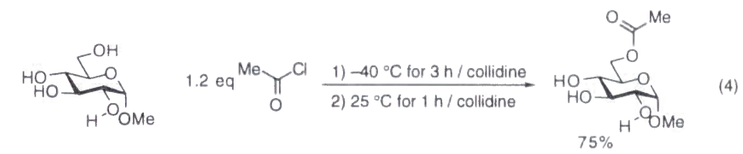

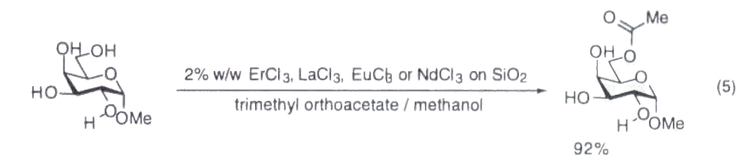

In the previous chapter, the author reported new nucleophilic catalysts which acetylate the primary 6-OH group of unprotected monosaccharides using acetic anhydride in chloroform. However, polyhydroxy compounds in general are insoluble in such nonpolar solvent. Thus, several polar solvents which dissolve polyhydroxy compound relatively well were explored as a reaction medium for the new catalyst. Herein, the author reports catalytic acetylation reaction in polar solvent. Several polyhydroxy compounds are regioselectively acetylated in relatively high yield by using acetic anhydride and **1** as a catalyst in *tert*-amyl alcohol.

Results and Discussion

Acetylation of Octyl β-D-glucopyranoside in Polar Solvent. Polyhydroxy compounds such as oligosaccharides are notoriously insoluble in most organic solvents. Among polar aprotic solvents, DMF, pyridine, and DMSO have often been used as reaction medium which dissolves carbohydrates quite well. Thus, the possibility of regioselective acylation in those solvents were explored.

As shown in Table 1, catalyst **1** exhibited both high regioselectivity and high catalytic activity in DMF or pyridine compared with catalyst **2**. These results suggest that in polar solvent such as DMF or pyridine, catalyst **1** operates in exactly the same manner as in chloroform. Again, effectiveness of proton transfer catalysis was confirmed. Although the effects of several insoluble basic additives were explored using DMF as solvent, regioselectivity was not further improved.

Recently, G. C. Fu demonstrated that *tert*-amyl alcohol can be used as solvent for kinetic resolution of secondary alcohols catalyzed by their chiral nucleophilic catalyst, without acylation of the protic solvent itself to any significant extent.[4] Then, the same solvent was applied for our catalytic regioselective acylation of unprotected carbohydrates. As shown in Table 1, high regioselectivity was achieved (84%) when the acetylation reaction was run in *tert*-amyl alcohol. The effects of insoluble basic additives were also explored. NaOAc and K_2CO_3 exhibited remarkable enhancement.

As already mentioned in Chapter 4, regioselectivity in catalytic acetylation of octyl α-D-mannopyranoside was gradually increased upon addition of *tert*-amyl alcohol, which was attributed to unfavorable intramolecular hydrogen bonding. Therefore, utilization of *tert*-amyl alcohol as solvent would be advantageous when one encounters unexpectedly low regioselectivity in our catalytic system, although catalytic activity is slightly reduced.

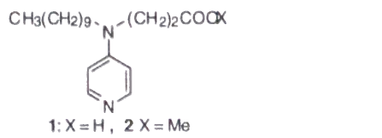

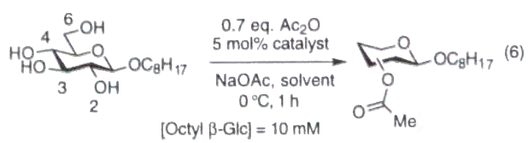

(6)

Table 1 Acetylation of Octyl β-D-glucopyranoside Catalyzed by **1** or **2** in polar solvents as shown in Eq 6.

Solvent	Product Ratio (Yield of One Regioisomer/Total Yield)				
	2-*O*-Acetate	3-*O*-Acetate	4-*O*-Acetate	6-*O*-Acetate	Total Yield (%)[a]
$CHCl_3$[d]	b	0.02	0.09	0.89	quant.
$CHCl_3$[e]	b	0.49	0.30	0.21	52
DMF[d]	b	0.24	0.11	0.65	43
DMF[e]	b	0.41	0.18	0.41	15
pyridine[d]	b	0.17	0.18	0.65	18
pyridine[e]	b	0.24	0.24	0.52	6
t-amyl alcohol[d]	b	0.11	0.05	0.84	56[c]
t-amyl alcohol[e]	b	0.34	0.10	0.56	28

a. NMR yield of monoacetates relative to Ac_2O. b. Not detected. c. Diacetylated glucosides were formed in less than 5 %. d. Catalyst **1** was utilized. e. Catalyst **2** was utilized.

Regioselective Acetylation of Octyl β-D-glucopyranoside in a *tert*-Amyl Alcohol–DMF Medium. *tert*-Amyl alcohol is a better solvent than THF or acetonitrile to dissolve unprotected carbohydrates. For example, 10 mL of *tert*-amyl alcohol dissolves 18 mg of totally-unprotected glucose, while glucose is practically insoluble in THF or acetonitrile even when refluxed for a few hours. However, solubility is considerably limited even in *tert*-amyl alcohol. Then, addition of DMF as cosolvent was examined.

As shown in Figure 1, added DMF slightly reduced regioselectivity, but not thoroughly. Catalytic acetylation reaction could be performed in 1:1 mixture of *tert*-amyl alcohol and DMF at the cost of slightly reduced regioselectivity.

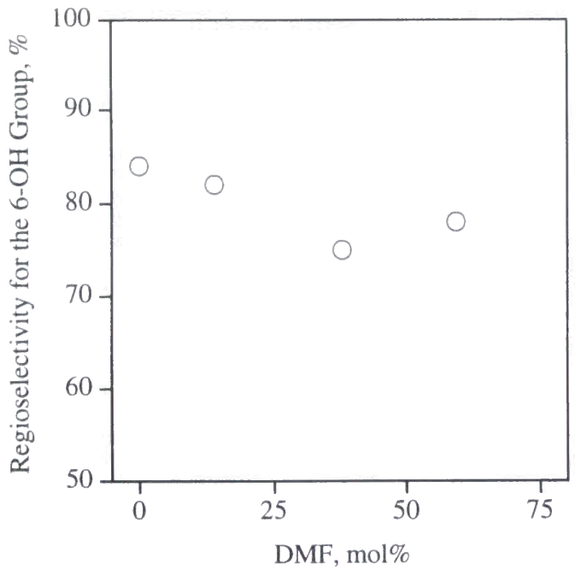

Figure 1. Plot of regioselectivity in **1**-catalyzed acetylation of octyl β-D-glucopyranoside in tert-amyl alcohol against DMF concentrations.

Regioselective Acetylation of Polyhydroxy Compounds. Commercially-available methyl α-D-glucopyranoside and methyl α-D-galactopyranoside were subjected to **1**-catalyzed acetylation reaction in *tert*-amyl alcohol. As shown in eq 7 and 8, 6-*O*-acetyl-glucoside and 6-*O*-acetyl-galactoside were obtained in 60% and 69% yield, respectively, after chromatographic purification.

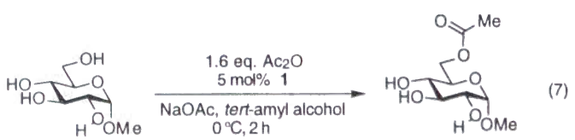

(7)

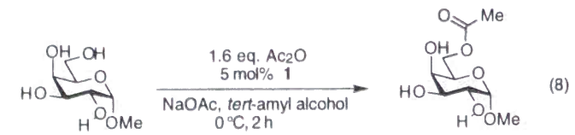

(8)

Conclusions

The catalytic acylation reaction presented in Chapter 5 offers a new access to selectively esterificated polyhydroxy compounds in relatively high yield. The author would like to point out the following advantages compared with reported methodologies.

(1) Relatively cheap reagents were used for selective acetylation of polyhydroxy compounds.

(2) No complicated operations such as strict control of reaction temperature are required to achieve high regioselectivity.

(3) New nucleophilic catalysts could be applied for wide varieties of selective reactions, because DMAP has been widely utilized as a catalyst so far.

Experimental Section

Instrumentation. ^{1}H and ^{13}C NMR spectra were recorded using a JEOL A-500 spectrometer. ^{1}H and ^{13}C NMR chemical shifts in $CDCl_3$ or CD_3OD were referenced to $CHCl_3$ (7.24 ppm and 77.0 ppm, respectively) or CH_3OH (3.30 ppm and 49 ppm, respectively). NMR data were collected at 30 °C.

Materials. Octyl β-D-glucopyranoside were purchased from Wako Pure Chemical Industries and used as received. Chloroform stabilized with 2-methyl-2-butene was purchased from Tokyo Chemical Industry and dried over molecular sieves, 3Å. DMF and pyridine were distilled over P_2O_5 and CaH_2, respectively. Acetic anhydride was purified by distillation after azeotropic removal of acetic acid with toluene. Na_2CO_3, K_2CO_3, LiOAc, NaOAc, and KOAc were dried in vacuo over P_2O_5. Column chromatography was carried out with Silica Gel 60N (spherical, neutral, 40−100 μm) from Kanto Chemicals. $CDCl_3$ was completely deacidified by passing through activated alumina just before use. Catalyst **1** and **2** were prepared according to the reported procedure in Chapter 4.

General Procedure for the DMAP-Catalyzed Acetylation. Stock solutions of catalyst **1** and acetic anhydride were prepared beforehand by dissolving **1** (5.2 mg, 17 μmol) in the designated solvent (1 mL) and acetic anhydride (62.2 mg, 609 μmol) in that solvent (2.7 mL), respectively.

Octyl β-D-glucopyranoside (3.0 mg, 10 μmol) was dissolved in the designated solvent (1 mL) under Ar. NaOAc (200 mg) was added to the solution. Then the catalyst stock solution (31 μL, 0.53 μmol) was added to the solution via microsyringe. The solution was stirred well with a magnetic stirrer. The temperature was kept at 0 °C during the acetylation reaction. Finally, the acetic anhydride stock solution (32 μL, 7.2 μmol) was added to initiate the acetylation reaction. After being stirred for 1 h, the reaction was quenched with methanol (0.2 mL). After 5 min at 0 °C, the reaction mixture was passed through a silica gel short column (1 g) to remove the catalyst. The reaction flask was washed well with the solvent and the washings were also put on the column. Monoacetylated sugars, together with the remaining unprotected sugar, were eluted by ethyl acetate−methanol solvent (4:1; 15 mL). The solvent was evaporated off and the product was dried in vacuo. The product was taken up in chloroform (2 mL) and passed through a polypropylene filter to remove traces of silica gel. The chloroform

was then evaporated off. The sample was completely dried *in vacuo* at room temperature for 4 h and subjected to NMR analysis.

Regioselective Acetylation of Methyl α-D-glucopyranoside. Methyl α-D-glucopyranoside (100.6 mg, 0.518 mmol) was completely dissolved in *tert*-amyl alcohol (104 mL) by stirring for several hours. Catalyst **1** (7.9 mg, 2.58×10^{-2}) was then added to the solution. After dissolving the sugar and the catalyst, NaOAc (20 g) was added to the solution. The solution was stirred under Ar at 0 °C for half an hour and then acetic anhydride (84 mg, 0.825 mmol) was added to the solution. After being stirred for 2 h, the reaction was quenched with methanol (1 mL). After 10 min at 0 °C, NaOAc was removed by filtration and the solvent was evaporated. The crude product was dissolved in a small amount of chloroform–methanol (20 : 1) and subjected to the flash column chromatography (toluene : acetone = 1 : 1) to give methyl 6-*O*-acetyl-α-D-glucopyranoside (73.4 mg, 0.31 mmol) in 60% yield.

^{1}H NMR (CD_3OD, 500 MHz) δ 4.621 (d, J = 3.5 Hz, 1H), 4.324 (dd, J = 12, 2.5 Hz, 1H), 4.163 (dd, J = 12, 6 Hz, 1H), 3.673 (ddd, J = 8.5, 6, 2.5 Hz, 1H), 3.577 (dd, J = 9, 9 Hz, 1H), 3.365 (dd, J = 9.5, 4 Hz, 1H), 3.366 (s, 3H), 3.247 (dd, J = 10, 9 Hz, 1H), 2.028 (s, 3H).

^{13}C NMR (CD_3OD, 125.65 MHz) δ 172.828, 101.274, 75.009, 73.438, 71.826, 70.962, 64.925, 55.572, 20.687.

HRMS calcd for $C_9H_{16}O_7 \cdot H^+$ m/z 237.0974 , found 237.0964 (FAB)

Regioselective Acetylation of Methyl α-D-galactopyranoside. Methyl α-D-galactopyranoside monohydrate (101.6 mg, 0.479 mmol) was selectively acetylated in exactly the same way to give methyl 6-*O*-acetyl-α-D-galactopyranoside (77.4 mg, 0.328 mmol) in 68% yield.

^{1}H NMR (CD_3OD, 500 MHz) δ 4.693 (d, J = 3.5 Hz, 1H), 4.242 (dd, J = 11.5, 7.5 Hz, 1H), 4.191 (dd, J = 11.5, 4.5 Hz, 1H), 3.939 (ddd, J = 7.5, 4.5, 1 Hz, 1H), 3.848 (dd, J = 3.5, 1 Hz, 1H), 3.758 (dd, J = 10, 3.5 Hz, 1H), 3.706 (dd, J = 10, 3.5 Hz, 1H), 3.380 (s, 3H), 2.044 (s, 3H).

^{13}C NMR (CD_3OD, 125.65 MHz) δ 172.664, 101.488, 71.234, 70.880, 70.058, 69.622, 65.130, 55.580, 20.687.

HRMS calcd for $C_9H_{16}O_7 \cdot H^+$ m/z 237.0974 , found 237.0977 (FAB)

References and Notes

1 Reviews on selective modification of carbohydrates: (a) Sugihara, J. M. *Adv. Carbohydr. Chem. Biochem.* **1953**, *8*, 1. (b) Haines, A. H. *Adv. Carbohydr. Chem. Biochem.* **1976**, *33*, 11. (c) Haines, A. H. *Adv. Carbohydr. Chem. Biochem.* **1981**, *39*, 13. See, also: *Preparative Carbohydrate Chemistry*; Hanessian, S., Ed.; Dekker: New York, 1996.

2 (a) Therisod, M.; Klibanov, A. M. *J. Am. Chem. Soc.* **1986**, *108*, 5638 and **1987**, *109*, 3977. (b) Riva, S.; Chopineau, J.; Kieboom, A. P. G.; Klibanov, A. M. *J. Am. Chem. Soc.* **1988**, *110*, 584. (c) Wang, Y.-F.; Lalonde, J. J.; Momongan, M.; Bergbreiter, D. E.; Wong, C.-H. *J. Am. Chem. Soc.* **1988**, *110*, 7200. (d) Hennen, W. J.; Sweers, H. M.; Wang, Y.-F.; Wong, C.-H. *J. Org. Chem.* **1988**, *53*, 4939. (e) Zhong, Z.; Liu, J. L.-C.; Dinterman, L. M.; Finkelman, M. A. J.; Mueller, W. T.; Rollence, M. L.; Whitlow, M.; Wong, C.-H. *J. Am. Chem. Soc.* **1991**, *113*, 683. (f) Holla, E. W. *Angew. Chem. Int. Ed. Engl.* **1989**, *28*, 220. (g) Björkling, F.; Gotfredsen, S. E.; Kirk, O. J. *J. Chem. Soc., Chem. Commun.* **1989**, 934. (h) Carrea, G.; Riva, S.; Secundo, F.; Danieli, B. *J. Chem. Soc., Perkin Trans. 1* **1989**, 1057. (i) Nicotra, F.; Riva, S.; Secundo, F.; Zucchelli, L. *Tetrahedron Lett.* **1989**, *30*, 1703. (j) Uemura, A.; Nozaki, K.; Yamashita, J.; Yasumoto, M. *Tetrahedron Lett.* **1989**, *30*, 3817. (j) Adelhorst, K.; Björkling, F.; Gotfredsen, S. E.; Kirk, O. J. *Synthesis* **1990**, 112. (k) Ciuffreda, P.; Colombo, D.; Ronchetti, F.; Toma, L. *J. Org. Chem.* **1990**, *55*, 4187.

3 (a) Baczko, K.; Plusquellec, D. *Tetrahedron* **1991**, *47*,3817. (b) Yamada, S. *J. Org. Chem.* **1992**, *57*, 1591. (c) Liguori, A.; Procopio, A.; Romeo, G.; Sindona, G.; Uccella, N. *J. Chem. Soc., Perkin Trans. 1* **1993**, 1783. (d) Ishihara, K.; Kurihara, H.; Yamamoto, H. *J. Org. Chem.* **1993**, *58*, 3791. (e) Xia, J.; Hui, Y. *Synth. Commun.* **1996**, *26*, 269. (f) Bianco A.; Brufani, M.; Melchioni, C.; Romagnoli, P. *Tetrahedron Lett.* **1997**, *38*, 651. (g) Alexander, C.; Smith, C. R.; Whitcombe, M. J.; Vulfson, E. N. *J. Am. Chem. Soc.* **1999**, *121*, 6640.

4 Ruble, J. C.; Tweddell, J.; Fu, G. C. *J. Org. Chem.* **1998**, *63*, 2794.

List of Publications

Chapter 1 — Molecular Recognition of Carbohydrates by Functionalized Zinc Porphyrins
Mizutani, T; Murakami, T.; Matsumi, N.; Kurahashi, T.; Ogoshi, H.
J. Chem. Soc., Chem. Commun. **1995**, 1257–1258.

Chapter 2 — Molecular Recognition of Carbohydrates by Zinc Porphyrins: Lewis Acid/Lewis Base Combinations as a Dominant Factor for Their Selectivity
Mizutani, T; Kurahashi, T.; Murakami, T.; Matsumi, N.; Ogoshi, H.
J. Am. Chem. Soc. **1997**, *119*, 8991–9001.

Chapter 3 — Effect of Intramolecular Hydrogen-Bonding Network on the Relative Reactivities of Carbohydrate OH Groups
Kurahashi, T.; Mizutani, T.; Yoshida, J.
J. Chem. Soc., Perkin Trans. 1 **1999**, 465–473.

Chapter 4 — Regioselective Acylation of Carbohydrates Catalyzed by Functionalized DMAP: Regiocontrol by Regulated Proton Transfer Catalysis
Kurahashi, T.; Mizutani, T.; Yoshida, J.
to be submitted.

Chapter 5 — Regioselective Acylation of Polyhydroxy Compounds Catalyzed by Functionalized DMAP in Polar Solvent
Kurahashi, T.; Mizutani, T.; Yoshida, J.
to be submitted.

Other Publications

An Artificial Receptor for Dimethyl Aspartate
Mizutani, T; Murakami, T.; Kurahashi, T.; Ogoshi, H.
J. Org. Chem. **1996**, *61*, 539–548.